Ground-Water Chemical Evolution and Diagenetic Processes in the Upper Floridan Aquifer, Southern South Carolina and Northeastern Georgia

United States Geological Survey Water-Supply Paper 2392

Prepared in cooperation with the South Carolina Water Resources Commission

AVAILABILITY OF BOOKS AND MAPS OF THE U.S. GEOLOGICAL SURVEY

Instructions on ordering publications of the U.S. Geological Survey, along with prices of the last offerings, are given in the current-year issues of the monthly catalog "New Publications of the U.S. Geological Survey." Prices of available U.S. Geological Survey publications released prior to the current year are listed in the most recent annual "Price and Availability List." Publications that may be listed in various U.S. Geological Survey catalogs (**see back inside cover**) but not listed in the most recent annual "Price and Availability List" may be no longer available.

Reports released through the NTIS may be obtained by writing to the National Technical Information Service, U.S. Department of Commerce, Springfield, VA 22161; please include NTIS report number with inquiry.

Order U.S. Geological Survey publications **by mail** or **over the counter** from the offices given below.

BY MAIL

Books

Professional Papers, Bulletins, Water-Supply Papers, Techniques of Water-Resources Investigations, Circulars, publications of general interest (such as leaflets, pamphlets, booklets), single copies of Earthquakes & Volcanoes, Preliminary Determination of Epicenters, and some miscellaneous reports, including some of the foregoing series that have gone out of print at the Superintendent of Documents, are obtainable by mail from

U.S. Geological Survey, Map Distribution
Box 25286, MS 306, Federal Center
Denver, CO 80225

Subscriptions to periodicals (Earthquakes & Volcanoes and Preliminary Determination of Epicenters) can be obtained ONLY from the

Superintendent of Documents
Government Printing Office
Washington, D.C. 20402

(Check or money order must be payable to Superintendent of Documents.)

Maps

For maps, address mail orders to

U.S. Geological Survey, Map Distribution
Box 25286, Bldg. 810, Federal Center
Denver, CO 80225

Residents of Alaska may order maps from

U.S. Geological Survey, Earth Science Information Center
101 Twelfth Ave. - Box 12
Fairbanks, AK 99701

OVER THE COUNTER

Books and Maps

Books and maps of the U.S. Geological Survey are available over the counter at the following U.S. Geological Survey offices, all of which are authorized agents of the Superintendent of Documents:

- **ANCHORAGE, Alaska**—Rm. 101, 4230 University Dr.
- **LAKEWOOD, Colorado**—Federal Center, Bldg. 810
- **MENLO PARK, California**—Bldg. 3, Rm. 3128, 345 Middlefield Rd.
- **RESTON, Virginia**—USGS National Center, Rm. 1C402, 12201 Sunrise Valley Dr.
- **SALT LAKE CITY, Utah**—Federal Bldg., Rm. 8105, 125 South State St.
- **SPOKANE, Washington**—U.S. Post Office Bldg., Rm. 135, West 904 Riverside Ave.
- **WASHINGTON, D.C.**—Main Interior Bldg., Rm. 2650, 18th and C Sts., NW.

Maps Only

Maps may be purchased over the counter at the following U.S. Geological Survey offices:

- **FAIRBANKS, Alaska**—New Federal Bldg., 101 Twelfth Ave.
- **ROLLA, Missouri**—1400 Independence Rd.
- **STENNIS SPACE CENTER, Mississippi**—Bldg. 3101

Ground-Water Chemical Evolution and Diagenetic Processes in the Upper Floridan Aquifer, Southern South Carolina and Northeastern Georgia

By RONALD ALLEN BURT

Prepared in cooperation with the South Carolina Water Resources Commission

U.S. GEOLOGICAL SURVEY WATER-SUPPLY PAPER 2392

U.S. DEPARTMENT OF THE INTERIOR
BRUCE BABBITT, Secretary

U.S. GEOLOGICAL SURVEY
Robert M. Hirsch, Acting Director

UNITED STATES GOVERNMENT PRINTING OFFICE: 1993

For sale by
U.S. Geological Survey, Map Distribution
Box 25286, MS 306, Federal Center
Denver, CO 80225

Library of Congress Cataloging in Publication Data

Burt, Ronald Allen
Ground-water chemical evolution and diagenetic processes in the upper Floridan aquifer, southern South Carolina and northeastern Georgia / Ronald Allen Burt ; prepared in cooperation with the South Carolina Water Resources Commission.
p. cm. — (U.S. Geological Survey water-supply paper : 2392)
1. Water, Underground—South Carolina. 2. Water, Underground—Georgia. 3. Water chemistry. 4. Floridan Aquifer. I. South Carolina Water Resources Commission. II. Series.
GB1025.S6B87 1993
551.49'09757—dc20 92–13596

CONTENTS

FIGURES

TABLES

CONVERSION FACTORS AND VERTICAL DATUM

Multiply	By	To obtain
inch (in.)	25.4	millimeter
foot (ft)	0.3048	meter
foot per day (ft/d)	0.3048	meter per day
mile (mi)	1.609	kilometer
million gallons per day (Mgal/d)	0.04381	cubic meter per second
square mile (mi^2)	2.590	square kilometer

Temperature in degrees (°C) can be converted to degrees Fahrenheit (°F) as follows:

$$°F = 1.8 \times °C + 32$$

Concentrations of chemical constituents in water are reported here in terms of molality as millimoles per kilogram (mmol/kg) rather than the more commonly used weight per volume units, milligrams per liter (mg/l), to facilitate the mass balance and equilibrium calculations. To convert mmol/kg to mg/L for a compound or element, multiply mmol/kg by:

$$\left[\frac{(\text{molecular weight of compound})(\text{solution density})(\text{solution weight} - \text{total solute weight})}{(\text{solution weight})}\right]$$

Sea level: In this report "sea level" refers to the National Geodetic Vertical Datum of 1929 (NGVD of 1929)—a geodetic datum derived from a general adjustment of the first-order level nets of both the United States and Canada, formerly called "Sea Level Datum of 1929."

Ground-Water Chemical Evolution and Diagenetic Processes in the Upper Floridan Aquifer, Southern South Carolina and Northeastern Georgia

By Ronald Allen Burt

Abstract

The bulk of the Upper Floridan aquifer in southern South Carolina and northeastern Georgia is composed of low-magnesium calcite (1–6 percent magnesium carbonate), silicates that are primarily quartz, and minor to trace amounts of alkali feldspar, oligoclase, and clay minerals. Trace amounts of gypsum, pyrite, and apatite are also present. If classified by ground-water chemistry, the aquifer can be subdivided into two zones: (1) a low-salinity zone, where chloride concentration in ground water is less than 0.20 millimoles per kilogram (7.09 milligrams per liter), and (2) a mixing zone, where seawater mixed with fresh ground water is indicated by chloride concentrations as much as 430 millimoles per kilogram (15,200 milligrams per liter).

The ground-water composition changes along flow paths in the low-salinity zone and is characterized by decreases in calcium and bicarbonate concentrations and increases in magnesium, sodium, potassium, sulfate, silica, and fluoride. Similarly, pH values increase. Chloride concentrations do not change significantly. Along one 40-mile flow path, $\delta^{13}C$ values increase from -10.5 to -3.3 per mil by Chicago PDB standard (belemnitella americana from the Cretaceous Peedee Formation, South Carolina). Calculations of chemical mass balance and isotope mass transfer in ground water, coupled with saturation calculations for aquifer minerals, show that the differences in ground-water composition in the low-salinity zone can be attributed primarily to a net precipitation of stable low-magnesium calcite accompanied by dissolution of unstable high-magnesium calcite, and incongruent dissolution of oligoclase. The stability of the low-magnesium calcite is probably a function of its magnesium content. Oligoclase dissolution appears to drive the precipitation of calcite by increasing the pH and contributing calcium ions to the solution. Other reactions, such as cation exchange, anion exchange, gypsum dissolution, and incongruent dissolution of alkali feldspar, appear to play a less significant role. Input to the ground water of nonmethanogenic carbon dioxide ($\delta^{13}C \sim$ -25 to -10 per mil) may be significant but is limited to less than 22 percent of the total dissolved inorganic carbon (DIC) input. Methanogenic carbon dioxide ($\delta^{13}C$ unknown, but probably much greater than -10 per mil) is limited to less than 67 percent of the total inorganic carbon input.

In the mixing zone, the observed concentrations of most ground-water constituents deviate from the values expected for conservative mixing of freshwater with seawater. While bromide and silica appear conservative, calcium, DIC, ammonia, sulfide, phosphate, magnesium, sodium, potassium, fluoride, and sulfate are all nonconservative. Mineral saturation and mass balance calculations show that the nonconservative behavior can be explained by dissolution of carbonate minerals in response to carbon dioxide influx along with other reactions such as ion exchange, gypsum dissolution, ammonification, and sulfate reduction. The total dissolution of carbonate minerals is only half that expected from the calculated amount of carbon dioxide influx, indicating that the net effect of the other reactions has been to neutralize part of the carbonic acid introduced by the carbon dioxide influx.

A spatial correlation between DIC, carbon-14 activity, and chloride indicates that the carbon dioxide flux to the aquifer in the mixing zone is primarily related to recharge by surface seawater. The distribution of hydraulic conductivity (K) in the aquifer is consistent with the hypothesis that dissolution of carbonate minerals in the mixing zone (K>500 feet per day) and precipitation of calcite in the low-salinity zone (K<500 feet per day) have had a significant influence on the diagenesis of the aquifer.

INTRODUCTION

Background, Purpose, and Scope

The Upper Floridan aquifer in the southern part of coastal South Carolina and part of northeastern Georgia is an upper Eocene limestone aquifer that contains both fresh ground water and high-salinity, diluted seawater. The diluted seawater occurs as a wedge lying beneath the freshwater, and the two are separated by a zone of diffuse

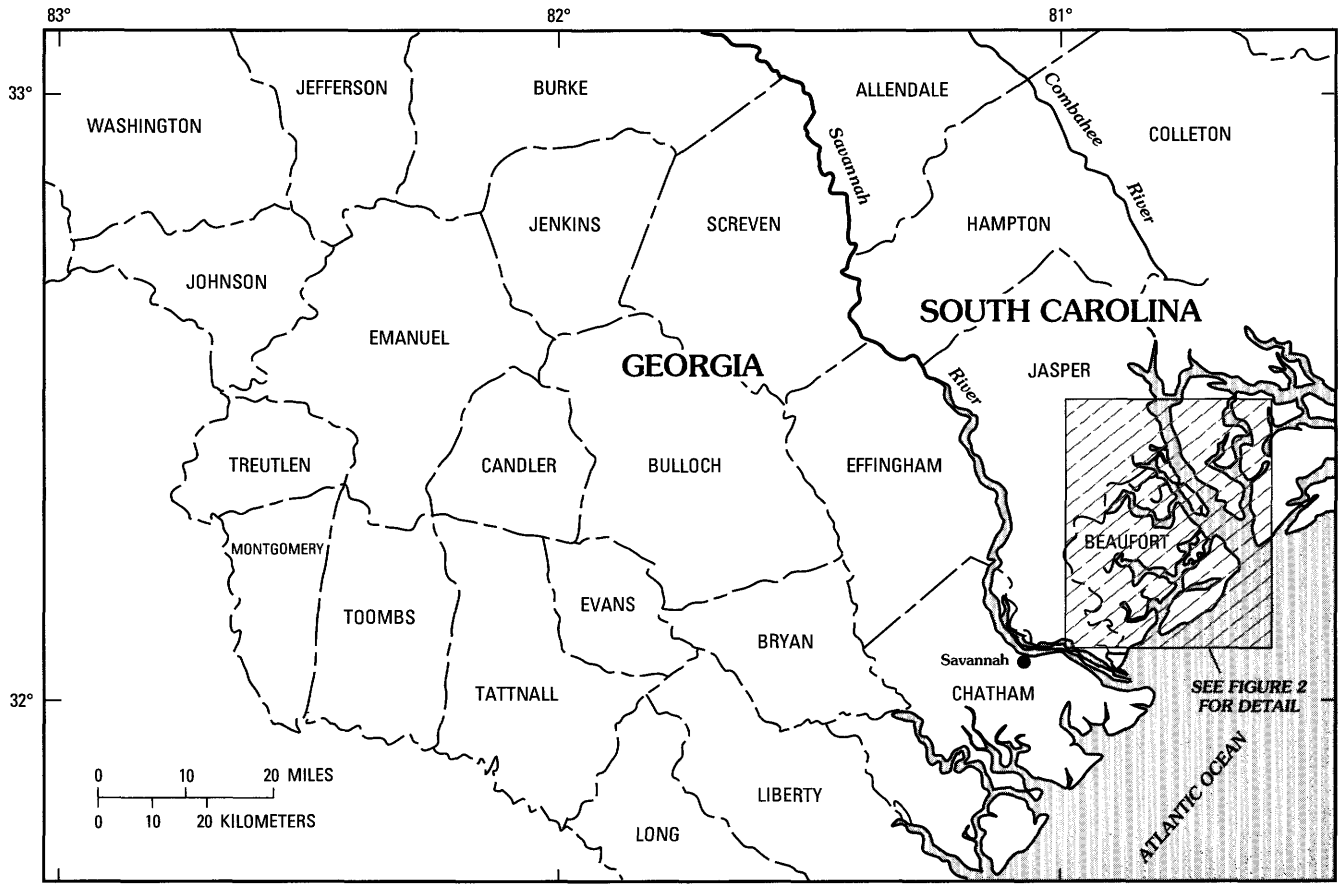

Figure 1. Study area.

mixing. Water in the aquifer is derived from several sources, including recharge by freshwater in upgradient areas distant from the coast, and recharge by freshwater and seawater in areas near the coast. Ancient seawater extending from the offshore part of the aquifer may also exist. This report shows that the chemical composition of the ground water in the Upper Floridan aquifer cannot be fully explained on the basis of simple mixing of water from these different sources, and therefore must result from some combination of processes that may include mixing, chemical interaction of the ground water with minerals, and input of compounds resulting from organic processes.

This report describes the results of a study to formulate quantitative conceptual models of the geochemical reactions that have determined the chemical composition of the ground water, and to demonstrate the probable effect these reactions have had on diagenesis of the aquifer, particularly concerning the net dissolution or precipitation of the carbonate minerals that compose the bulk of the aquifer. The models will be constrained by analyses of the mineralogy of the aquifer and solubility of the minerals, analyses of the chemical and isotopic composition of the ground water and the calculated distribution of dissolved chemical species at equilibrium, mass balance of chemical constituents in the ground water and minerals, and mass balance and fractionation of carbon-13 between minerals and dissolved chemical species.

The study area (figs. 1 and 2) includes 3 counties in South Carolina (Beaufort, Jasper, and Hampton) and parts of 14 counties in Georgia (Johnson, Treutlen, Emanuel, Montgomery, Toombs, Tattnall, Bryan, Evans, Candler, Jenkins, Screven, Bulloch, Effingham, and Chatham). Notable landmarks include Port Royal Sound, Hilton Head Island, Parris Island Marine Corps Recruit Depot, and the city of Beaufort, all in South Carolina, and the city of Savannah in Georgia. The investigation was divided into two parts, one focused on the area in the aquifer immediately surrounding Port Royal Sound, where mixing between seawater and freshwater has occurred (zone of mixing), and the other limited to the parts of the aquifer where seawater mixing has not influenced the ground-water composition (low-salinity zone). Data used for this study were compiled from ground-water chemical and isotopic analyses of previous investigators as well as from analyses performed as part of this project. The well locations for all samples are shown in figures 3 and 4. Ground-water samples collected in the course of this study were limited to wells in South Carolina. The formulation of geochemical reaction models

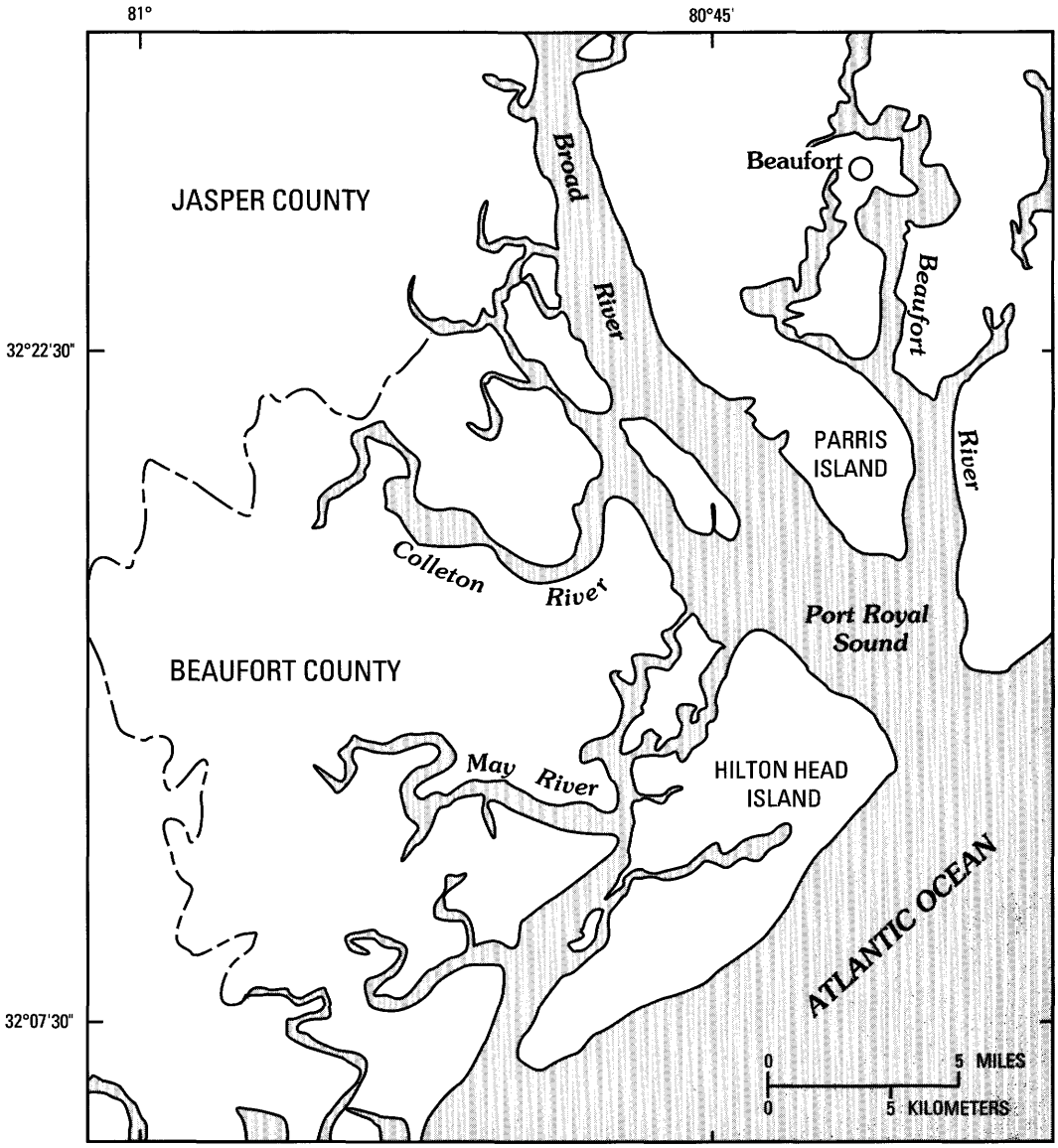

Figure 2. Port Royal Sound area.

was also restricted to areas in South Carolina. The inclusion of data from the bordering parts of Georgia was intended to provide a regional perspective within which the more areally limited models could be interpreted.

The Upper Floridan aquifer is part of the Floridan aquifer system, which extends over Florida and parts of Alabama, Georgia, and South Carolina (Stringfield, 1966). The system is divided into Upper and Lower Floridan aquifers over much of its extent (Miller, 1986). This report deals only with the upper part of the Upper Floridan aquifer that constitutes a highly permeable limestone section about 100 ft thick in South Carolina and somewhat thicker in Georgia. Because of the influence of recharge on ground water in the Upper Floridan aquifer, some consideration of the overlying sediments is also included, and interpretations of processes in these shallower units are based on several ground-water samples from these horizons.

The identification of plausible chemical processes in the aquifers is based not only on chemical and isotopic analyses of ground water, but also on the mineralogy of the aquifer as determined from analyses of drill cuttings and cores; several cores were available from the aquifer in the zone of mixing. The mineralogy of the aquifer in the low-salinity zone is based on analysis of drill cuttings.

Subsurface environments are influenced by chemical and physical processes that vary according to the prevailing hydrologic, geologic, and geochemical conditions. The effect of these processes on the chemical evolution of ground water and the chemical diagenesis of sediments is

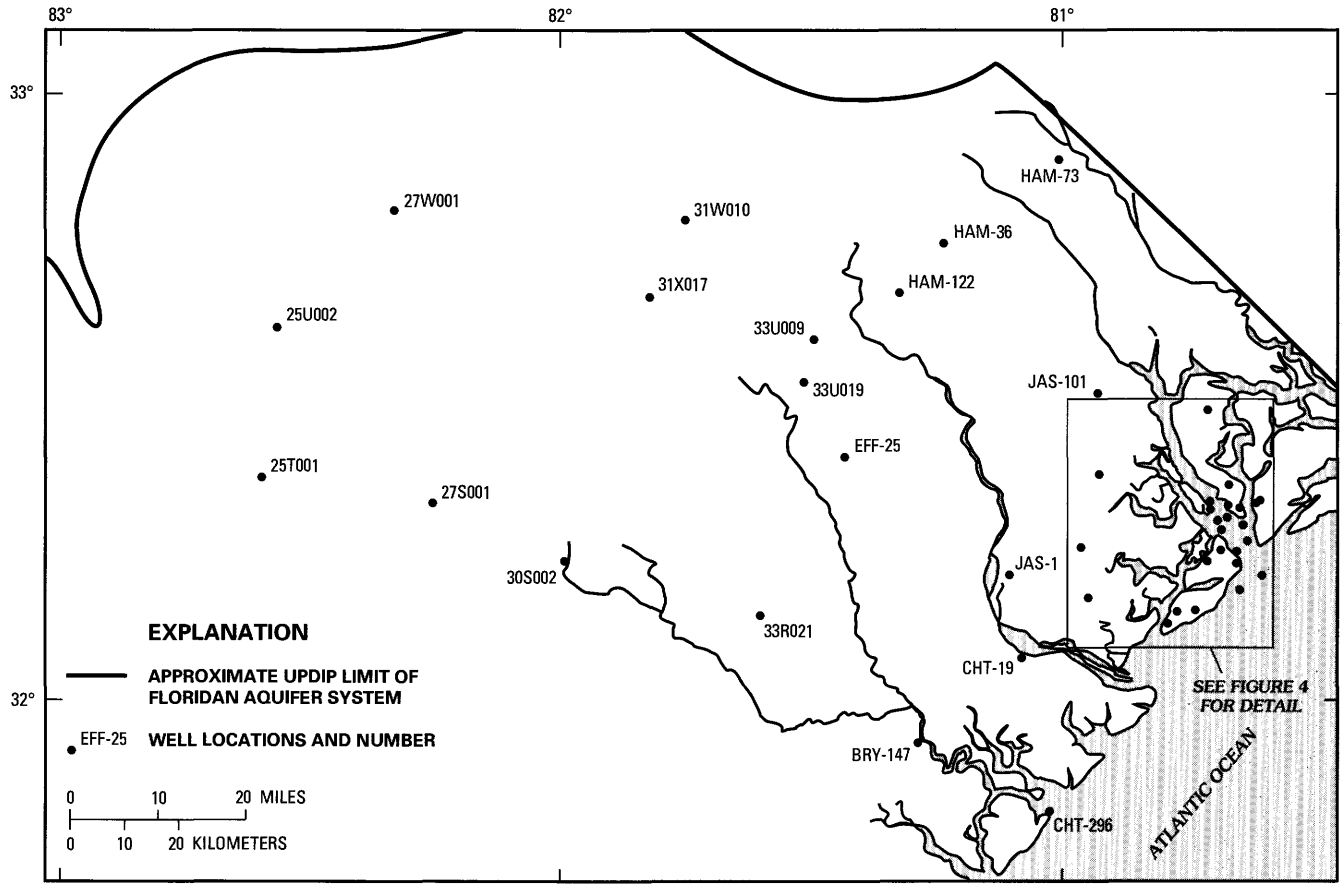

Figure 3. Ground-water sample locations and delineation of the updip limit of the Floridan aquifer system.

reflected in changes in the ground-water composition. Compositional changes may be due to simple conservative mixing of chemically different ground waters. If the end-member ground-water compositions of such a mixture are known, the degree of mixing can be determined if n-1 conservative constituents have been measured, where n is the number of end-members. If in addition to mixing of ground water, chemical reactions have occurred between the ground water, dissolved constituents, and minerals (nonconservative behavior), the compositional deviation of the ground water from that expected from conservative mixing reflects the nonconservative processes. Likewise, in the absence of ground-water mixing, compositional changes observed along a closed hydrologic flow path (no chemical flux in or out of the aquifer) reflect the chemical interaction of the ground water with its environment. On the basis of information about the hydrology and mineralogy, geochemical reaction models that explain the observed ground-water compositions can be formulated.

A practical study of chemical processes in the zone of mixing between seawater and low-salinity ground water in a limestone aquifer is of particular interest because of the variety of effects that can be theoretically predicted. Several investigators (Bogli, 1964; Thrailkill, 1968; Runnels, 1969; Plummer, 1975; Wigley and Plummer, 1976) have discussed the nonlinear properties of mixing waters of different compositions. For instance, Plummer (1975) showed how mixing seawater with calcite-equilibrated ground water can result in solutions that are either supersaturated or subsaturated with respect to calcite, depending on the degree of mixing, partial pressure of carbon dioxide, and temperature. Mixtures with a high percentage of seawater tended to be supersaturated because the seawater was significantly supersaturated. At lower percentages of seawater, the mixtures tended to fall below saturation in response to five factors (Wigley and Plummer, 1976): (1) algebraic effects, (2) redistribution of carbon species, (3) nonlinear dependence of activity coefficients on ionic strength, (4) nonlinear variation of equilibrium constants with temperature, and (5) redistribution of ion pairs. The tendency for mixed seawater and ground water to form solutions subsaturated with respect to calcite is believed to have been the process responsible for massive dissolution of carbonates along the east coast of the Yucatan Peninsula (Back and others, 1979).

The mixing zone for seawater and low-salinity water is also suspected as an environment for dolomite formation (Hanshaw and others, 1971; Land, 1973a, b; Badiozamani, 1973; Ward and Halley, 1985). Solutions of low-salinity

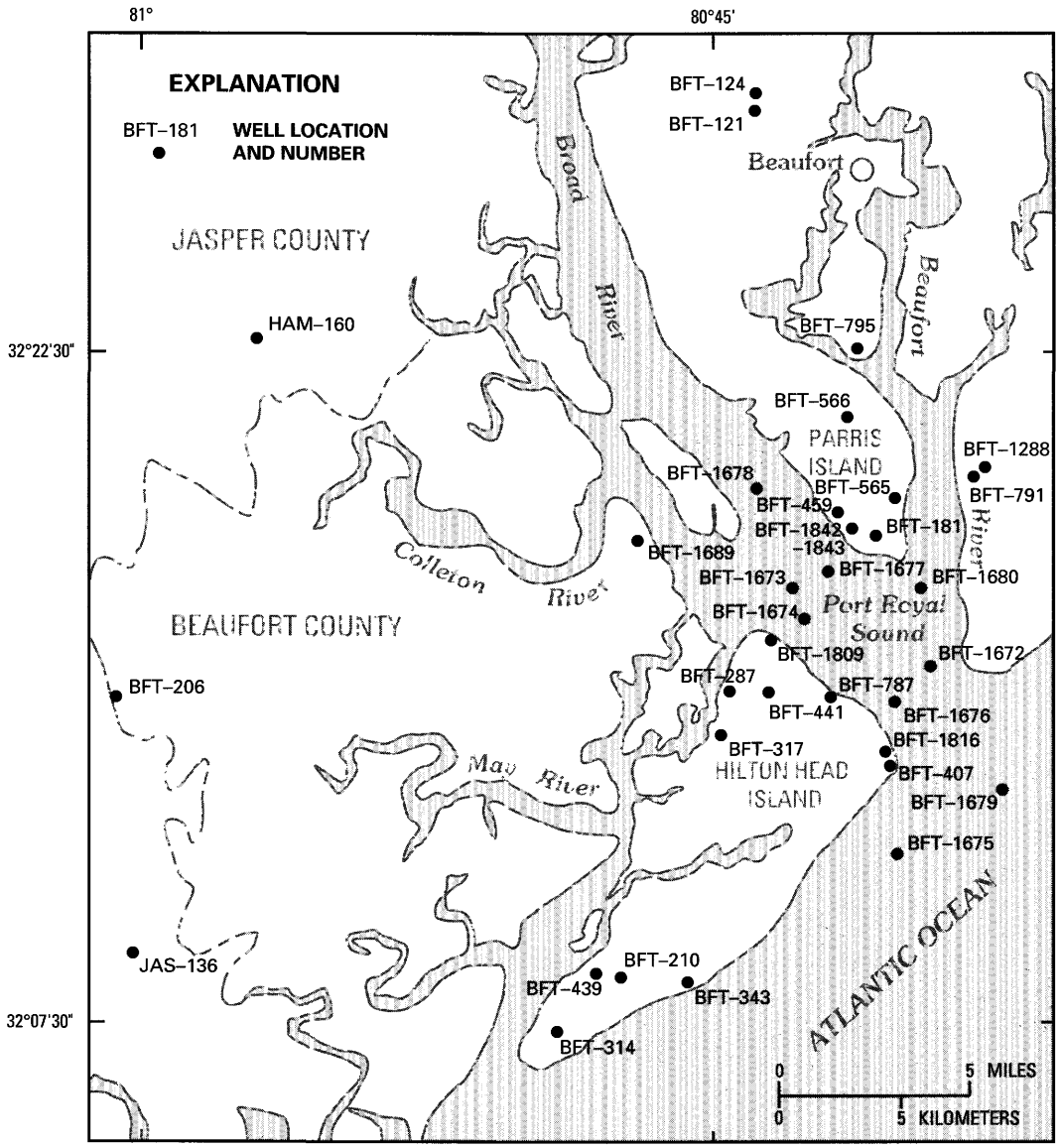

Figure 4. Well locations in the Port Royal Sound area.

ground water mixed with seawater may remain supersaturated with respect to dolomite while being subsaturated with respect to calcite. Under such conditions, dolomite may replace calcite. Badiozamani (1973) explained the origin of dolomite in the Middle Ordovician of Wisconsin using this concept. Hanshaw and others (1971) proposed that dolomite in the Tertiary limestone aquifer (Floridan aquifer system) of central Florida was formed in such a brackish water environment.

The zone of mixing is also suspected to be an area of significant ion exchange due to the large concentration changes occurring as seawater and low-salinity water mix. The significance of ion exchange is dependent on the availability of exchange sites in the subsurface environment. These may be provided by organic material, clays, and other minerals. Mercado (1985) identified compositional patterns in mixed ground water in Israel related to both cation exchange and carbonate equilibria, which differed according to whether seawater was intruding into the aquifer or being flushed out by low-salinity water.

The ground-water chemical evolution and diagenesis of carbonate minerals can also be significantly influenced by dissolution and precipitation of noncarbonate minerals, depending on their abundance and reactivity to the environment. Mineral reactions involving ions common to the carbonate minerals, or reactions that alter solution pH, are most likely to affect carbonate mineral diagenesis. For example, dedolomitization with concurrent precipitation of

calcite in the Mississippian Pahasapa Limestone of South Dakota and Wyoming is driven by the dissolution of gypsum (Back and others, 1983).

Compounds produced by organic processes in the subsurface may also affect chemical evolution and carbonate mineral diagenesis. These compounds include ammonia, phosphate, sulfide, organic acids, and, of particular importance, carbon dioxide.

Conceptual geochemical models were formulated in this study that show that the net effect of chemical processes on the diagenesis of carbonate minerals in the zone of mixing is significantly different from what has transpired in the low-salinity zone. In the low-salinity zone, calcite dissolution and precipitation have both occurred, the precipitation of more stable, lower-magnesium calcites having occurred to a greater extent than dissolution of less stable, higher magnesium calcites. This process has resulted in a net precipitation of calcite that was driven by the combined influences of feldspar incongruent dissolution, cation exchange, and gypsum dissolution. In contrast, in the zone of mixing the combined effect of several chemical processes has been a net dissolution of carbonate minerals. A significant influx of carbon dioxide has occurred in the zone of mixing that is related to local recharge of the aquifer. The quantity of carbonate minerals that has dissolved is substantially less than would have been expected in response to the carbon dioxide influx, indicating that other chemical processes have buffered the effects of carbon dioxide. The diagenetic processes described by the geochemical models appear to be reflected in the distribution of hydraulic conductivity in the Upper Floridan aquifer. Within the approximate boundaries of the zone of mixing, hydraulic conductivity values are greater than 500 feet per day (ft/d), whereas in the low-salinity zone the aquifer is substantially less conductive.

Previous Investigations

This investigation builds on earlier work in the study area by several investigators. Back and others (1970) originally described the various origins of the ground water in the area around Port Royal Sound based on radiocarbon analyses. Reports published in conjunction with this study include Smith (1988), which describes a numerical flow model of the Upper Floridan aquifer, and Burt and others (1987), a compilation of data from wells drilled in Port Royal Sound. Other published reports pertaining to the ground-water resources and geology of the locality are Callahan (1964), Colquhoun and others (1969), Comer (1973), Cooke (1936), Cooke and MacNeil (1952), Counts and Donsky (1963), Counts (1958), Duncan (1972), Hayes (1979), Hazen and Sawyer (1956, 1957), McCollum and Counts (1964), Mundorff (1944), Nuzman (1970, 1972), Siple (1956, 1960, 1967), Stringfield (1966), and Warren (1944).

Methods of Analysis

Techniques for formulating geochemical reaction models have been published by Plummer and others (1983), Plummer and Back (1980), and Wigley and others (1978). These papers provide the theoretical basis for the geochemical modeling studies presented in this report. The following section on methods is drawn primarily from these sources as they apply to the present study.

The conceptual models are formulated by initially compiling a set of chemical reactions that qualitatively describe the observed changes in ground-water composition using minerals and organic compounds as sources and sinks for the ground-water constituents. This set of reactions is based on chemical analyses of the ground water, chemical and mineralogical analyses of the aquifer, and an understanding of the principles of mineral and water chemistry. The plausibility of the set of reactions is evaluated, implausible reactions are eliminated, and the plausible reactions are quantified by applying a series of constraints:

1. Mineral saturation.—The ground water must be subsaturated with respect to all minerals chosen as sources for chemical constituents; the ground water must be supersaturated with respect to all minerals chosen as sinks.
2. Mass balance.—The total increase or decrease in concentration of each chemical constituent between two points on a flow line must be quantitatively accounted for by the set of reaction coefficients that quantify the magnitude of each reaction.
3. Isotope mass transfer.—Changes in the isotopic composition of chemical constituents in the ground water between two points on a flow line must be consistent with the redistribution predicted by the hypothesized chemical reactions and isotope fractionation.

When data are insufficient to evaluate a reaction based on these constraints, the hypothetical effect that the reaction would have on the ground water can often be calculated to demonstrate the possible significance of the reaction to the model. This is done using reaction path calculations.

Mineral saturation, mass balance, and isotope mass transfer constraints were all applied to formulation of the models in the low-salinity zone of this study, while only mineral saturation and mass balance were applicable in the mixing zone. Reaction path calculations were used to demonstrate the possible effects of some hypothetical reactions. The remainder of this introductory section briefly

describes the calculation methods used. Their application is demonstrated in the main body of the report.

Equilibrium Speciation Calculations

The determination of the state of saturation of a sample of ground water with respect to some specific mineral requires that equilibrium speciation calculations be done. Equilibrium speciation calculations determine the distribution of chemical species (free ions and ion pairs) in a solution based on the bulk concentrations of the elemental constituents in a ground-water sample and a thermodynamic equilibrium model. The method is based on conservation of mass and charge of each element. The algebraic unknowns are the activities of the free ions and ion pairs, and to solve for these, it is required that one independent equation be written for each unknown. The thermodynamic equilibrium model consists of a mass action equation and a corresponding equilibrium constant for each ion pair considered in the problem. A mass balance equation is written for each free ion except H^+ and OH^- (hydrogen and oxygen are excluded due to the impracticality of measuring their masses in solution). The mass action equation for the dissociation of water provides one more equation that corresponds (arbitrarily) to OH^-. If pH is measured, one of the unknowns is eliminated, and the problem can be solved; alternatively, a charge balance equation can be included, and the speciation can be accomplished with H^+ as a dependent variable. Minerals and gases can be included as additional unknowns. If a mass action equation and equilibrium constant are provided for each of these additional phases, a determination can be made of the saturation state with respect to a mineral or the partial pressure of a gas for the aqueous solution. The saturation states with respect to minerals indicate whether or not a given mineral is favored to dissolve or precipitate in the system.

Mass Balance Calculations

Mass balance calculations are used for determining the amounts of plausible reactants and products that must have reacted in order to effect a change in composition between ground water at two points in a system. The initial and final ground-water compositions are known from chemical analyses, and the plausible reactants and products are hypothesized from minerals and other compounds (gases, organic compounds) thought to exist in the system. One mass balance equation is written for each constituent. Modifying the notation of Plummer and Back (1980), the mass balance equations can be represented by

$$\sum_{j=1}^{\phi} \alpha_j b_c \, , j = \Delta m_c |_{c=1,n}$$

where ϕ total number of minerals or other reactants or products in the reaction;

n minimum number of constituents necessary to define the composition of the chosen minerals or other reactants or products;

α_j stoichiometric (reaction) coefficient of the jth mineral or other reactant or product;

b_c,j stoichiometric coefficient of the cth constituent in the jth mineral or other reactant or product; and

Δm_c change of the concentration of the cth constituent in the aqueous phase between the initial and final points in the system.

The equations are solved simultaneously for a solution to the mass balance problem. A unique solution to the problem is only possible if the sum of plausible reactant minerals, gases, and other compounds is equal to the number of constituents.

Isotope Mass Transfer Calculations

Isotope mass transfer calculations relate changes in isotope composition of ground water and minerals to changes in conventional chemistry that have occurred between two points in a system. The observed changes in isotopic composition must be consistent with the changes predicted by the mass balance solution in order for the hypothetical reaction model to be considered plausible. The isotope mass transfer constraints may help eliminate some of the mass balance solutions. Changes in the carbon isotope, carbon-13, have been applied to the problems in this study. Wigley and others (1978) have derived general equations for describing carbon isotope evolution in aqueous systems under the influence of a variable number of sources and sinks of carbon occurring in response to chemical reactions (see eq. 17). Their treatment combines mass balance calculations with calculations that describe the effects of carbon isotope fractionation that may occur between the aqueous phase, gases, and precipitating carbonate minerals. No fractionation is assumed to occur between incoming carbon and the solution. Chemical and isotopic equilibrium are assumed to exist in the aqueous phase, and isotopic equilibrium is assumed to hold between phases. The equations also only rigorously apply to situations where isotopic changes are determined by product and reactant stoichiometry, independent of the reaction path.

Reaction Path Simulations

Reaction path simulations are a modeling technique for determining the effect on water composition and mineralogy of hypothetical chemical reactions. The initial composition and reactions are assumed to be known, and the final composition is the unknown to be solved. The calculations are fundamentally the same as those for equilibrium speciation calculations except that rather than solving for an unknown mineral saturation state or gas partial pressure, an assumed value for these might be input to determine the effect on the water composition. For

example, the change in composition of a given ground water could be determined as it evolved from subsaturation to equilibration with respect to calcite. In addition, the effect of hypothetical reactions on ground water can be calculated by adding the net change in bulk constituents, due to the reactions, to the initial solution, and then performing the calculations.

Calculations of the types described above were often aided by the use of computer programs. Equilibrium speciation calculations were performed with WATEQF (Plummer and others, 1976) and PHREEQE (Parkhurst and others, 1980). Reaction path calculations were also calculated with PHREEQE.

The discussion above has outlined the constraints that have been applied in the formulation of geochemical models for this study. The fact that a model conforms to each of these constraints is not proof that the model is a unique representation of the geochemical reactions that have occurred, but the number of imaginable possibilities can often be restricted such that the resulting models provide useful interpretations of the system.

GEOHYDROLOGIC FRAMEWORK

The geologic characteristics of the study area are integrally related to the hydrology of the Upper Floridan aquifer, and both the geology and hydrology determine the geochemical interactions that may impact ground water in the aquifer. These features of the study area and the interrelationships significant to this investigation are reviewed in this section.

Geology

The Upper Floridan aquifer is part of a sequence of unconsolidated to semiconsolidated sedimentary rocks that underlie the Coastal Plain Province of the southeastern United States. The sedimentary sequence in the study area consists of Upper Cretaceous, Tertiary, and Quaternary sediments and forms a wedge that generally dips and thickens toward the coast from its terminal edge at the Fall Line to more than 3,450 ft at Parris Island (Mundorff, 1944) and approximately 4,000 ft in southern Jasper County (W.B. Hughes, South Carolina Water Resources Commission, written commun., 1987). The sediments overlie pre-Cretaceous igneous and metamorphic rocks.

The Upper Floridan aquifer is the permeable section of a thick sequence of Tertiary carbonate rocks, which generally grade updip into clastic facies (Miller, 1986) and are in contact with overlying and underlying clastic sediments. W.B. Hughes (South Carolina Water Resources Commission, written commun., 1987) compiled a detailed description of the stratigraphic relation of these sediments in the study areas. Except as noted, the following discussion is drawn from his interpretations. Within the study area, the older clastic units include in ascending order the Cretaceous Cape Fear, Middendorf, Black Creek, and Peedee Formations and the Paleocene Black Mingo Formation. The carbonate rock sequence consists of the middle Eocene (Claiborne) Santee Limestone and the upper Eocene (Jackson) Ocala Limestone. The younger clastic units, overlying the carbonate rocks, include the Miocene Hawthorn Formation; the Pleistocene Waccamaw, Talbot, and Pamlico Formations; and the undifferentiated sands of Holocene age. A generalized geologic section of the carbonate sequence is shown in figure 5.

The Santee Limestone in the carbonate rock sequence is a porous, fossiliferous, and glauconitic limestone in updip areas near its outcrop in South Carolina (Siple, 1960). However, downdip in Beaufort County the formation is much less porous, and according to Miller (1986), the Santee Limestone is probably a low-permeability zone.

The Ocala Limestone is lithologically similar to the Santee but contains more permeable zones. The limits of the Upper Floridan aquifer are coincident with the top and bottom of the Ocala in the study area. The Ocala Limestone consists of two units. The upper unit is a clean, porous, bioclastic limestone and is approximately 100 ft thick in the area near Port Royal Sound, but pinches out along the Combahee River to the north. To the south the unit thickens to approximately 300 ft near the Savannah River. The lower unit, about 300 ft thick, is a silty, clayey, glauconitic limestone. McCollum and Counts (1964) demonstrated that the Upper Floridan aquifer consisted of more than one water-bearing zone. Only two zones are significant in the area near Hilton Head Island and Port Royal Sound, and these zones are coincident with the upper unit of the Ocala Limestone. Near Savannah, Ga., five zones exist, although the same two upper zones account for more than 70 percent of the ground-water flow. Some zones of relatively high permeability exist in the lower unit of the Ocala Limestone, but the lower unit appears to be more significant as a lower confining unit, along with the Santee Limestone, of the shallower zones of the Upper Floridan aquifer. The Ocala Limestone units grade updip from the coast into sandy or argillaceous limestones, calcareous sand or clay, and finally into stratigraphically equivalent, fully clastic sediments (Miller, 1986). The approximate updip limit of the Floridan aquifer system after Miller (1986) is given in figure 3. The limit was defined as the line where the aquifer system is less than 100 ft thick and clastic rocks constitute more than 50 percent of the rock column between the uppermost and lowermost limestone beds. These units crop out updip in Georgia and South Carolina.

The Upper Floridan aquifer is confined at the top throughout much of the study area by the Hawthorn Formation, which consists of dolomitic and phosphatic sand, clayey sand, and sandy clay. The Hawthorn Formation thins in a generally northeast direction from as much as

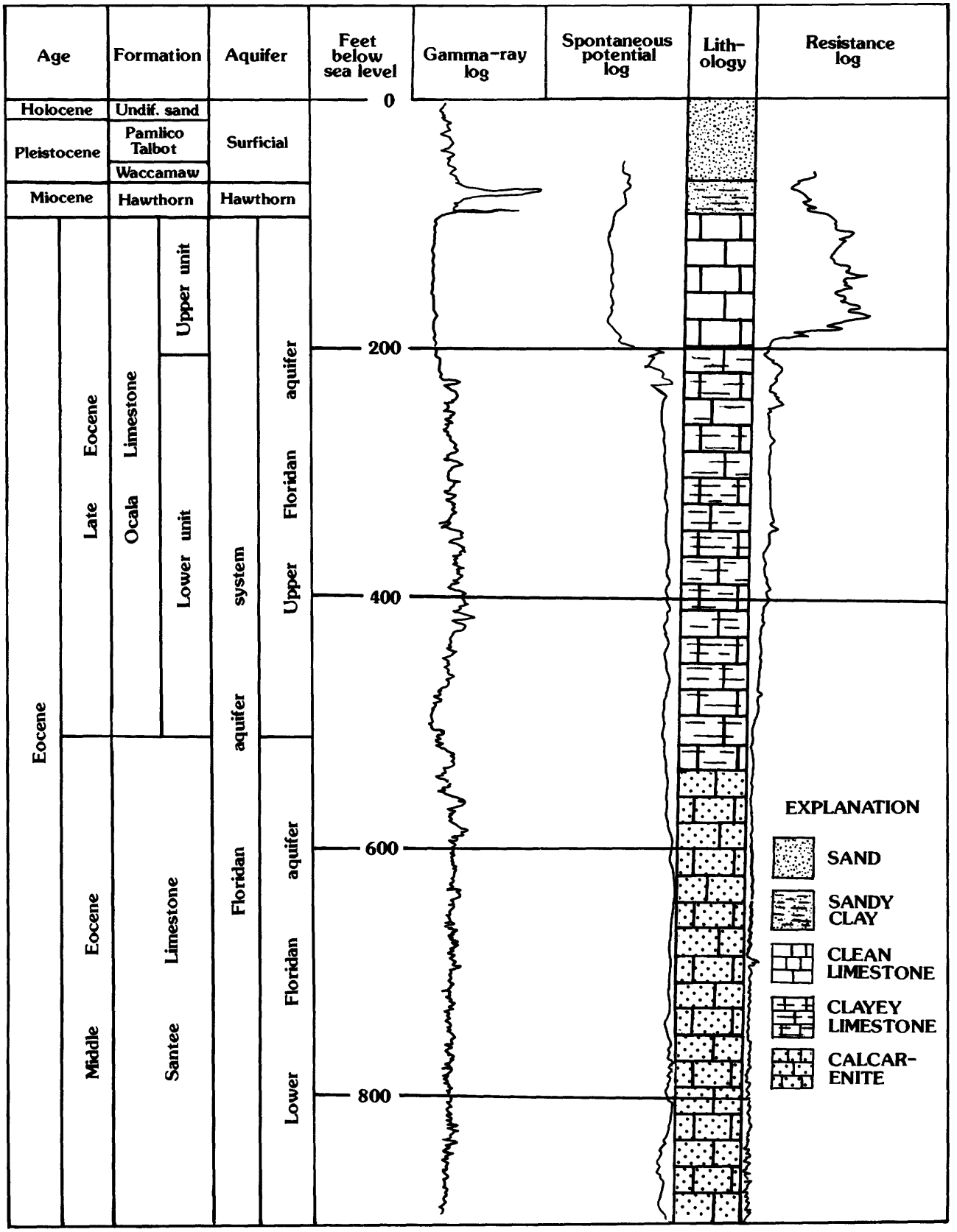

Figure 5. Generalized geologic section of formations in the Floridan aquifer system including geophysical logs.

70 ft near Savannah, Ga., to 30–50 ft beneath Port Royal Sound, and to approximately 10 feet near Beaufort, S.C. The thin zone near Beaufort corresponds to a structural feature, the Burton High (Siple, 1969), an uplift that structurally altered both the Ocala Limestone and the Hawthorn Formation. Where the Hawthorn Formation is thin, it probably provides less confinement for the Upper Floridan aquifer. The Hawthorn Formation may also be breached in some parts of the study area (M. Crouch, South Carolina Water Resources Commission, written commun., 1987), adding to the loss of confinement.

Overlying the Hawthorn Formation, the post-Miocene sands and clays constitute an unconfined surficial aquifer. The lithology is laterally and vertically variable.

The carbonate rocks that compose the Upper Floridan aquifer in the study area were sampled and examined petrographically as part of this investigation. In addition, selected samples were analyzed for mineralogy and isotopic compositions using other methods. These analyses were used to characterize the aquifer materials in terms of diagenetic features and possible chemical interaction with ground water and are discussed below.

Petrographic Analyses

Thin sections were prepared for 13 core samples collected from the Ocala Limestone at different depths in well BFT–1809, located on the north end of Hilton Head Island (see fig. 4 for well location). Examination of the sections showed that the carbonate rocks range in porosity from less than 5 percent to 48 percent, and consist primarily of skeletal fragments of bryozoans and lesser amounts of echinoderms, forams, brachiopods, mollusks, ostracods, and unidentified grains. Noncarbonate grains of quartz and glauconite are rare to common. The rocks contain varying amounts of micrite, often recrystallized and microcrystalline. A variety of both primary and secondary porosity types exists including interparticle, intraparticle, intercrystalline, moldic, and possibly vuggy. Calcite spar growth is common but makes up less than 1 percent of the rocks. The petrographic analyses and the percentage of porosity and matrix encountered at various depths are listed in table 1. The shallower part of the section is characterized by high-porosity grainstones and packstones (see Dunham (1962) for classification of carbonate rocks) typical of the upper unit of the Ocala Limestone. Deeper in the section, quartz and glauconite become more common, indicative of the transition into the lower unit of the Ocala Limestone. The rocks are characteristic of a shallow, carbonate shelf, depositional environment.

Diagenetic features vary throughout the section and include the effects of both porosity-occluding and porosity-enhancing processes. Sediment filling of primary porosity is common. Primary and secondary porosity are also often reduced by sparry calcite cements. Bryozoan zooecia rimmed with coarse calcite spar are shown in figure 6. Some of the intraparticle porosity is totally occluded by microcrystalline spar, which is probably recrystallized micrite. Rim cements in the micrite-filled pores apparently formed early, allowing subsequent sediment infilling.

Dissolution features in the rocks are generally fabric selective molds. A highly recrystallized bryozoan skeleton from which the zooecia septa have been partially dissolved, leaving casts of the filled zooecia, is shown in figure 7. A partially formed mold resulting from dissolution of an unidentified fossil fragment is shown in figure 8. A more stable calcite cast of filled intraparticle primary porosity remains. A mold that probably resulted from dissolution of a mollusk is shown in figure 9. Irregular, coarse, sparry calcite cements have reduced this porosity. Molds and possible vugs in a micrite matrix are shown in figure 10.

Features that may not affect porosity but indicate chemical alteration of the sediments are recrystallization of fossils or the matrix. The partial recrystallization of a crinoid (echinoderm) fragment is shown in figure 11. The light colored crystal is replacing the mottled crystal. The bryozoan skeleton in figure 7 is an example of complete recrystallization to a microcrystalline form.

Five thin sections were prepared from epoxy-mounted drill cuttings collected from well HAM–160, which is approximately 25 mi updip of BFT–1809 (fig. 4). The cuttings were sampled from 80 ft of section in the upper unit of the Ocala Limestone. The amounts of porosity, matrix, and cements were indeterminable on a whole-rock basis because of the use of cuttings; however, the grain composition was similar to that in BFT–1809 (see table 1), as were the diagenetic features. Quartz was more abundant in the samples from HAM–160.

Mineralogical Analyses

Samples of the upper unit of the Ocala Limestone were analyzed for mineralogical content using petrography, X-ray diffraction, scanning electron microscopy, and microprobe analysis. The analytical results for core samples from BFT–1809 and drill-cutting samples from HAM–160 are presented in tables 2 and 3, respectively. The analyses were made on samples from various depths and have been composited in the tables. The data show that the samples from both wells consist primarily of calcite; no dolomite was detected. Lesser amounts of silicate minerals that make up the remaining bulk of the rocks are quartz, alkali feldspar, kaolinite, illite, smectite, and other undifferentiated clays. Plagioclase was detected in HAM–160 but not in BFT–1809. Trace amounts of gypsum, pyrite, and apatite were found. In addition to the analyses presented in tables 2 and 3, 17 thin sections of the Ocala Limestone made from cores and cuttings (wells BFT–1672, BFT–1673, BFT–1674, BFT–1676, BFT–1677, and BFT–1680) were stained with alizarin red–S for identification of dolomite.

Table 1. Petrographic analyses of the Ocala Limestone from wells BFT–1809 and HAM–160

[C, common (>10%); R, rare (< 10%); TR, trace (<1%); and O, not detected]

Well	Sample depth (feet below land surface)	Bryozoan	Echinoderm	Foram	Mollusk	Brachiopod	Quartz	Glauconite	Unknown	Porosity (percent)	Matrix		Cements		Notes
											Type	Percent	Type	Percent	
BFT-1809	90	C	O	R	O	O	O	O	R	28	micrite	48	calcite spar	<1	
(core)	100	C	R	C	O	R	TR	O	R	26	micrite	6	calcite spar	<1	
	114	C	TR	R	R	O	TR	O	R	14	micrite	46	calcite spar	<1	
	125	C	TR	C	O	TR	O	O	C	28	—	0	calcite spar	<1	
	137	C	R	R	R	R	TR	O	R	42	micrite	12	calcite spar	<1	
	140	R	C	C	O	C	O	O	C	10	micrite	72	calcite spar	<1	highly micritized
	143	C	C	R	R	O	R	O	R	8	micrite	50	calcite spar	<1	micritized
	158.5	C	C	C	molds	O	C	O	O	20	micrite	10	calcite spar	<1	
	180	C	C	C	molds	C	C	R	C	5–10	micrite	50	calcite spar	<1	
	190	R	C	R	R	O	C	R	C	3–5	micrite	50	calcite spar	<1	intraclasts common
	195	C	C	C	molds	O	C	C	C	5–10	micrite	60	calcite spar	<1	ostracods and coral
	205	C	C	C	molds	O	R	C	C	10–15	micrite	50	calcite sapr	<1	
	209	C	C	C	molds	O	C	C	C	30	micrite	30	calcite spar	<1	recrystallized allochems
HAM-160	120–130	C	C	O	O	O	R	O	C	—	micrite	—	calcite spar	—	
(cuttings)	130–140	C	C	C	molds	O	C	O	C	—	micrite	—	calcite spar	—	
	140–150	C	C	C	molds	O	C	O	C	—	micrite	—	calcite spar	—	
	160–180	C	C	C	molds	O	C	O	C	—	micrite	—	calcite spar	—	
	200–220	C	C	C	molds	O	C	O	C	—	micrite	—	calcite spar	—	

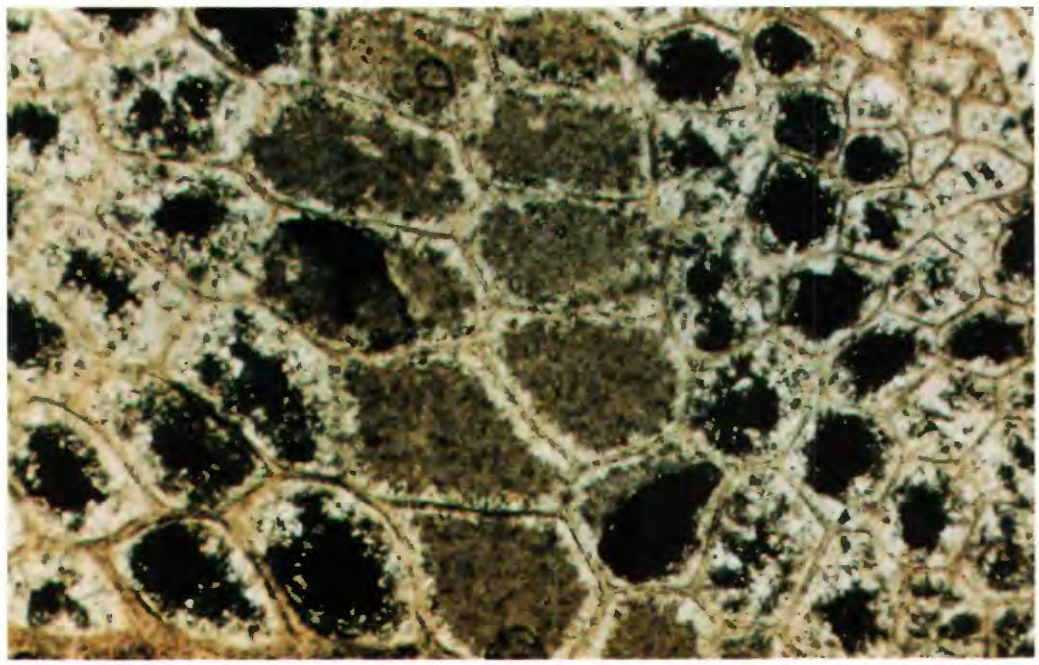

Figure 6. Bryozoan zooecia rimmed with coarse calcite spar, ×40, from well BFT–1809, 205 ft below land surface.

Table 2. Composite mineralogical analysis of core from well BFT–1809 (Ocala Limestone)

[The analyses are composite results of measurements made on core samples from depths of 94, 143, 195, and 205 ft below land surface. P, petrographic; XR, X-ray diffraction; and MP, microprobe]

Mineral	Analytical detection method	Weight percent	Compositional range
Carbonates		>90	
Calcite	P, MP, XR		$Ca_{0.99}\ Mg_{0.01}\ CO_3$ – $Ca_{0.96}\ Mg_{0.04}\ CO_3$
Dolomite	Not detected XR		
Silicates		<10	
Quartz	P, XR		
Alkali feldspar	XR		
Kaolinite	XR		
Illite	XR		
Smectite	XR		
Undifferentiated clays	XR		
Sulfate		trace	
Gypsum	XR		
Sulfide		trace	
Pyrite	XR		
Phosphate			
Apatite	Not detected		

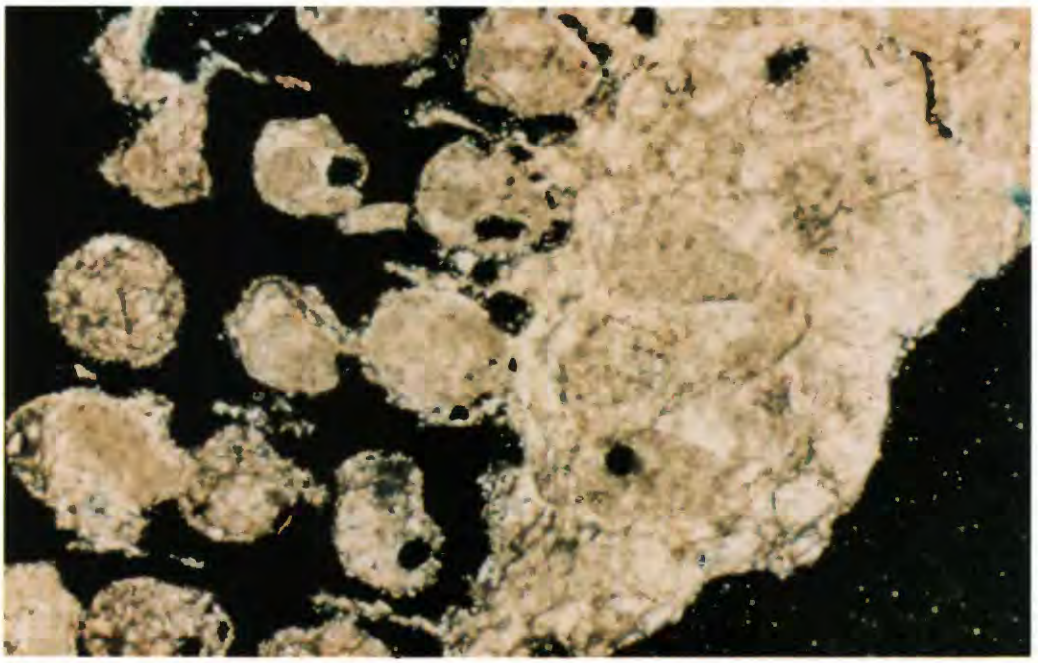

Figure 7. Recrystallized bryozoan skeleton with partially dissolved zooecia septa and casts, ×40, from well BFT–1809, 140 ft below land surface.

Table 3. Composite mineralogical analysis of drill cuttings from well HAM–160 (Ocala Limestone)

[The analyses are composite results of measurements made on drill cuttings from depth intervals at 120–130, 130–140, 160–180, and 200–220 ft below land surface. P, petrographic; XR, X-ray diffraction; MP, microprobe; and SEM, scanning electron microscope]

Mineral	Analytical detection method	Weight percent	Compositional range
Carbonates		76	
Calcite	P, MP, XR		$Ca_{0.98}\ Mg_{0.02}\ CO_3$ – $Ca_{0.94}\ Mg_{0.06}\ CO_3$
Dolomite	Not detected XR		
Silicates		24	
Quartz	P, XR		
Alkali feldspar	MP, XR, SEM		$Na_{0.31}\ K_{0.69}\ ALSi_3O_8$ – $Na_{0.23}\ K_{0.77}\ ALSi_3O_8$
Oligoclase	MP, XR, SEM		$Na_{0.70}Ca_{0.30}\ Al_{1.3}Si_{2.7}O_8$ – $Na_{0.75}Ca_{0.25}Al_{1.25}\ Si_{2.75}O_8$
Kaolinite	XR		
Illite	XR		
Smectite	XR		
Undifferentiated clays	XR		
Sulfate		trace	
Gypsum	XR		
Sulfide		trace	
Pyrite	MP, XR, SEM		
Phosphate		trace	
Apatite	MP, SEM		

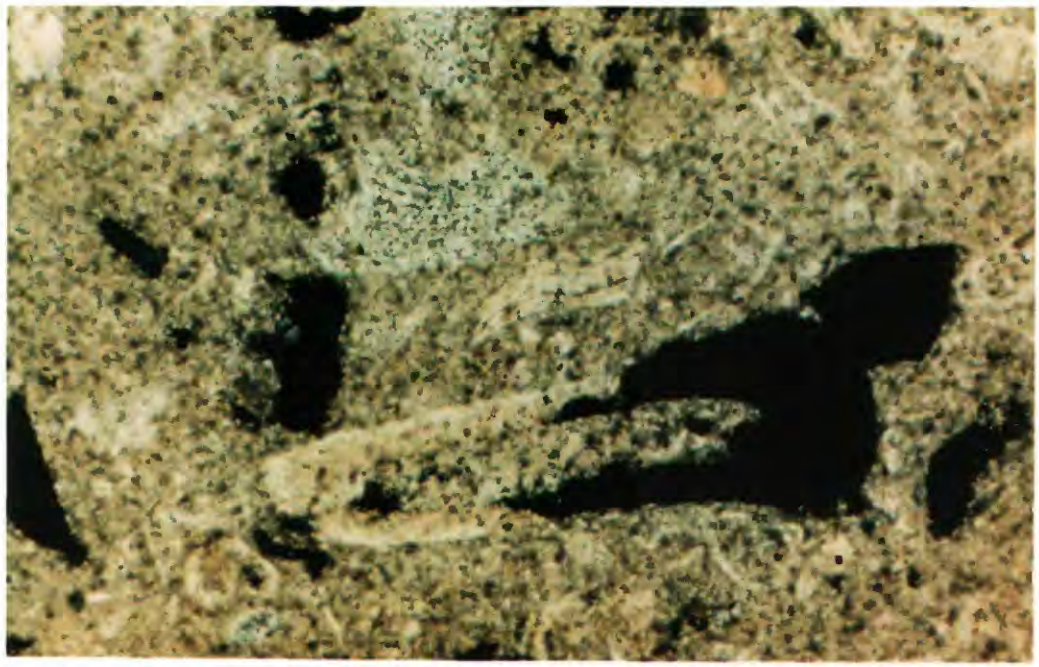

Figure 8. Mold resulting from partial dissolution of an unidentified fossil, ×40, from well BFT–1809, 140 ft below land surface.

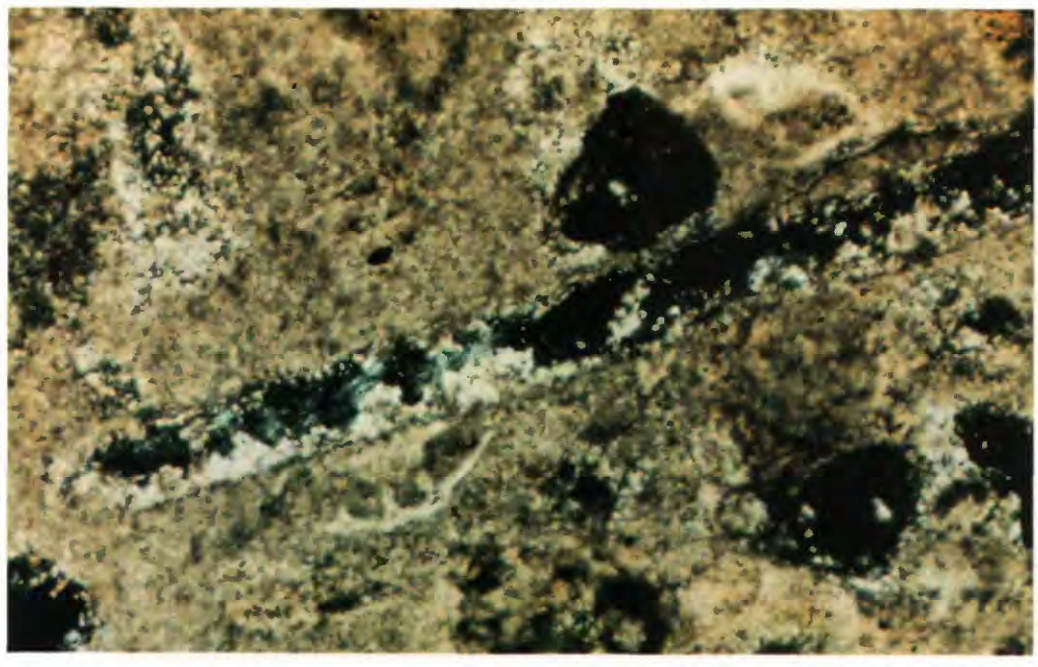

Figure 9. Mold resulting from probable dissolution of a mollusk, ×100, from well BFT–1809, 205 ft below land surface.

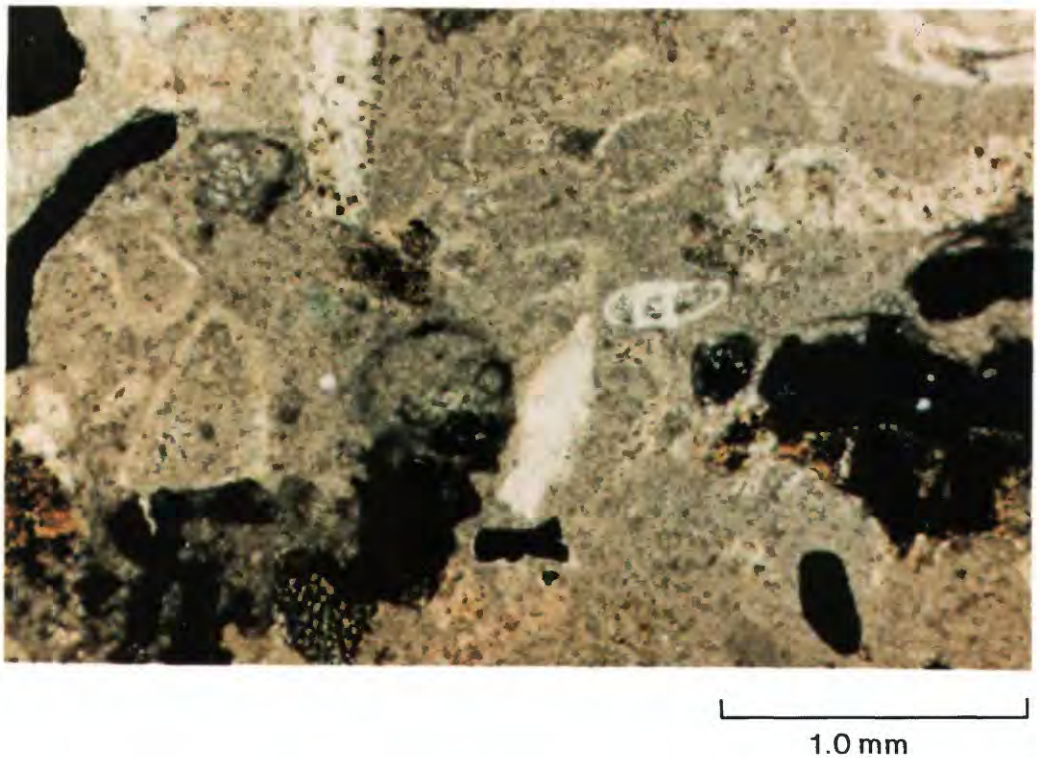

Figure 10. Molds and possible vugs in a micrite matrix, ×40, from well BFT–1809, 205 ft below land surface.

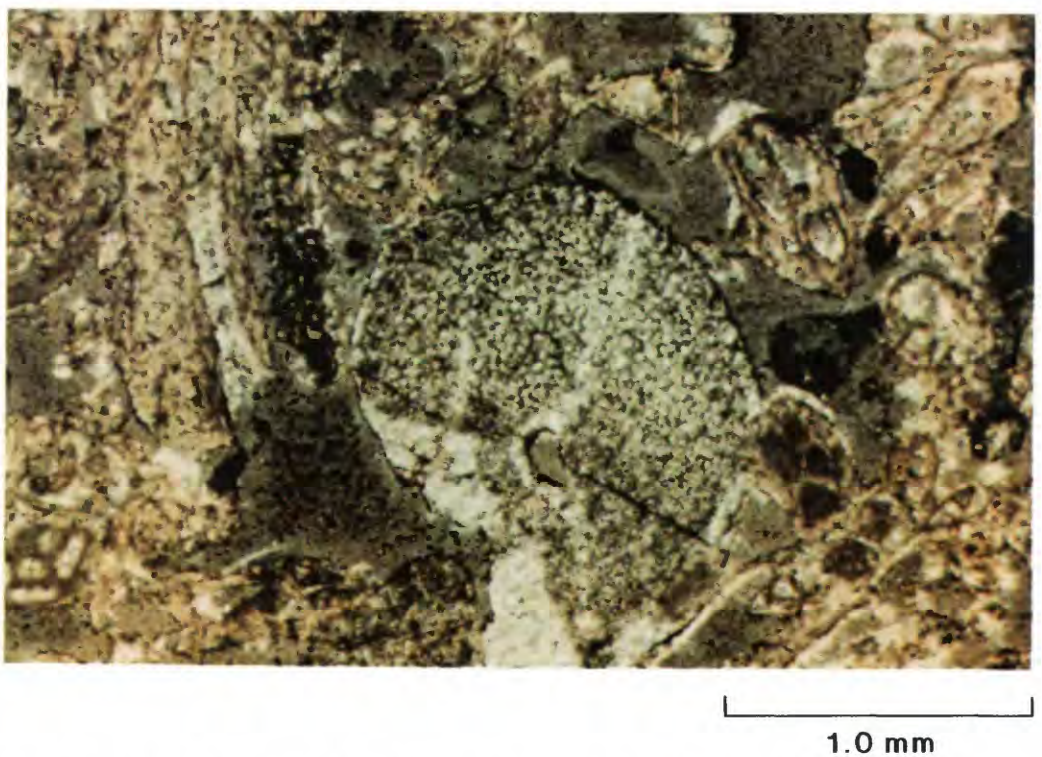

Figure 11. Partial recrystallization of a crinoid fragment, ×40, from well BFT–1809, 137 ft below land surface.

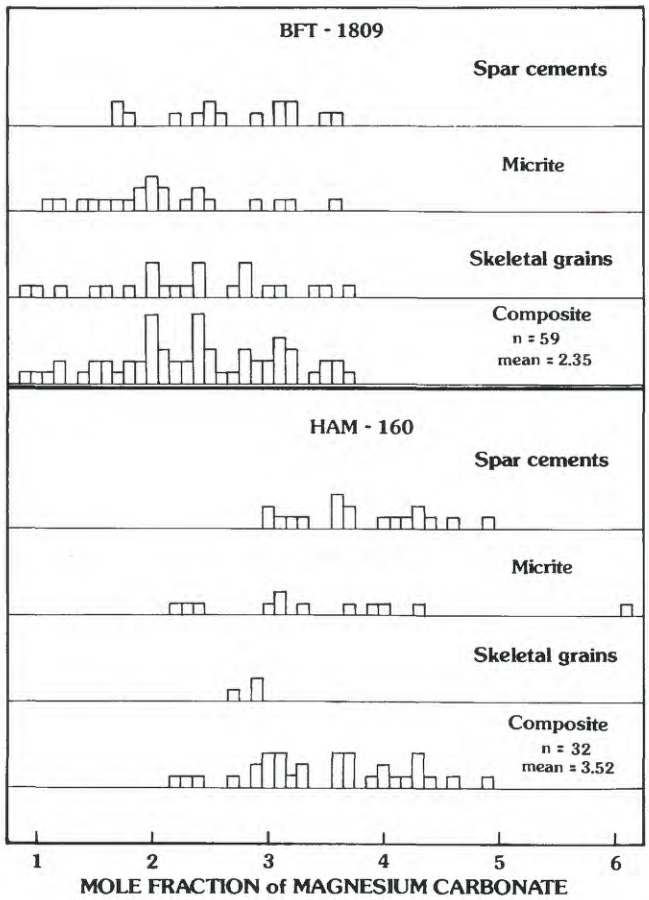

Figure 12. The distribution of mole fraction magnesium carbonate among calcite categories in the Ocala Limestone.

Consistent with the data discussed above, no dolomite was identified in any of the samples using this method (R.C. Lindholm, George Washington University, written commun., 1986).

Calcite samples from BFT–1809 and HAM–160 were analyzed with a microprobe for magnesium carbonate content. Measurements were cataloged into three categories according to the carbonate rock feature that contained the calcite, namely, micrite, spar cements, and skeletal grains. The distribution of mole fraction magnesium carbonate with respect to these categories for both wells is presented in figure 12. Within wells, there is no significant difference in magnesium carbonate concentration between categories, but a variation in mole fraction of magnesium carbonate of 2–3 percent is apparent within all categories in both wells excepting HAM–160 skeletal grains, for which only three measurements were made. A significant difference exists between the means of the composite analyses of the two wells, showing that the magnesium carbonate content of the calcite in HAM–160 averages about 2 percent higher than that in BFT–1809. The significance of this difference is unclear. Several of the skeletal fragments identified in the Ocala Limestone are types expected to initially contain higher amounts of magnesium carbonate than found here. Unaltered echinoderms generally range from approximately 3 to 16 percent magnesium carbonate in sediments; bryozoans range between 1 and 8 percent; and foraminifera range between 0 and 25 percent (Scholle, 1978). The consistently low concentrations of magnesium carbonate in the Ocala Limestone samples indicate that the calcite

Table 4. Carbon-13 in per mil (PDB)[1] of the Ocala Limestone from wells BFT–1809 and HAM–160

Well	Sample depth (feet below land surface)	Carbonate features	Carbon-13 per mil
		Spar cements	
BFT–1809	205		1.40
BFT–1809	205		−.95
HAM–160	140–150		1.04
HAM–160	140–150		1.19
HAM–160	140–150		1.04
HAM–160	140–150		−.23
		Micrite	
BFT–1809	143		0.15
BFT–1809	205		1.42
BFT–1809	205		1.14
HAM–160	120–130		.98
HAM–160	120–130		.38
HAM–160	130–140		1.46
		Skeletal grains	
BFT–1809	195	(Recrystallized bryozoan)	0.37
HAM–160	130–140	(Recrystallized bryozoan)	1.22
HAM–160	160–180	(Crinoid)	1.47
HAM–160	160–180	(Crinoid)	1.72
HAM–160	160–180	(Recrystallized bryozoan)	1.88

[1]Chicago belemnitella americana standard from the Cretaceous Peedee Formation in South Carolina.

has been altered, probably in a meteoric (nonmarine) environment.

Drill cuttings from HAM–160 were additionally analyzed by microprobe for feldspar compositions. Oligoclase, its calcium content ranging from 25 to 30 percent, was found along with alkali feldspar ranging between 23 and 31 percent sodium (see table 3).

Carbon-13 Analyses

Eighteen samples of calcite from the Ocala Limestone were analyzed for $\delta^{13}C$, relative to the Chicago belemnitella americana standard from the Cretaceous Peedee Formation in South Carolina (PDB standard), which can be related to the depositional environment of the calcite. Very small samples of calcite were drilled from pieces of cores or mounted cuttings in order to sample different rock features, such as sparry cements, micrite, and skeletal fragments. Results of the analyses are compiled in table 4 according to well name and carbonate feature. It was not possible to sample spar cements exclusively, so all samples labeled as spar cement actually represent a mixture of calcite features with a high percentage of spar. The $\delta^{13}C$ values for the samples as a whole ranged from −0.95 to 1.88, which falls within the range expected for marine carbonates. No significant isotopic variance among different carbonate features was identifiable from these limited data.

Hydrology

The chemical evolution of ground water is dependent on the path the ground water follows as it flows through an aquifer. Ground-water flow in an aquifer responds to areal differences in potential, moving from areas of high potential to areas of low potential. Because the Upper Floridan aquifer is generally bounded at both the top and bottom by significantly less permeable units, ground water within the aquifer can be assumed to flow approximately parallel to the upper and lower surfaces of the aquifer. The directions of flow can be determined from the areal distribution of potential, which can be mapped using the altitude of water levels in wells that are isolated in the aquifer.

Bush and Johnston (1988) estimated and mapped the ground-water potentiometric surface for the Upper Floridan aquifer prior to any ground-water withdrawals. This potentiometric surface has been reproduced for the study area in figure 13. Flow lines drawn perpendicular to the potentiometric contours indicate the directions of ground-water flow, and the map shows that ground water flowed generally from updip parts of the aquifer toward the coast, converging near Port Royal Sound. The ground water was discharged by upward leakage through the confining bed to Port Royal Sound, the Atlantic Ocean, and to streams along the flow field. Aquifer recharge from the surface and overlying sediments occurred in updip areas where the aquifer crops out or is shallow, and in some areas near the coast. Smith (1988) used a steady-state simulation of ground-water flow in the Upper Floridan aquifer to show that the most significant recharge to the aquifer near the coast occurred from overlying sediments on the islands surrounding Port Royal Sound and in an area near Beaufort, S.C. (fig. 14). Recharge prior to pumping ranged from as much as 4 inches per year (in./yr) on the north end of Hilton Head Island to 6 in./yr on the islands to the north of Port Royal Sound. The recharge area near Beaufort supplied about 6 in./yr to the aquifer. These recharge areas existed where the upper confining unit is thinner and probably provides less confinement. Smith's simulation indicates that only minor recharge (less than 2 in./yr) occurred in the area between the islands and the upgradient outcrop areas.

Since 1880, the flow system in the Upper Floridan aquifer has been altered by the effects of ground-water pumping. The most significant withdrawals of ground water occur in the Savannah, Ga. area, where approximately 70 million gallons per day (Mgal/d) were pumped in 1984 (Clark and others, 1985). The potentiometric surface of the Upper Floridan aquifer in 1984, as modified from Smith (1988), is shown in figure 15. A cone of depression centered on Savannah has had a negligible effect on the direction of flow in the aquifer to the west and north of Savannah; however, east of the depression the flow directions have changed markedly from prepumping conditions. The flow paths that originally extended to the northeast beneath Hilton Head Island had reversed direction in 1984, heading southwestward beneath Hilton Head Island toward the center of the cone of depression near Savannah. In addition, Smith's simulation of ground-water flow indicates that in 1984 the rates of recharge had increased on Hilton Head Island from 0–4 to 3–8 in./yr in response to lowered ground-water potentials in the aquifer.

The presence of a wedge of high-salinity water underlying fresher water in the aquifer beneath Port Royal Sound adds another constraint on flow within the system. The location of the high-salinity wedge in 1984 (Smith, 1988) coincided with its theoretical prepumping position as based on Hubbert's (1940) interface equation. The similarity of the locations is consistent with the probability that the flow system was approximately at steady state prior to pumping. At steady state the freshwater would be expected to flow over the high-salinity wedge and discharge to the surface, as described by Cooper and others (1964) for similar conditions in off-shore Florida. Because the boundary between freshwater and high-salinity water in such a system is not a sharp interface (due to diffusion and dispersion), the discharging freshwater transports some of the high-salinity water out of the aquifer, causing a flow in the high-salinity water toward the interface (Cooper and others, 1964). The lowering of ground-water potential in the Hilton Head Island area caused a reversal of freshwater flow, and the freshwater would no longer discharge over the

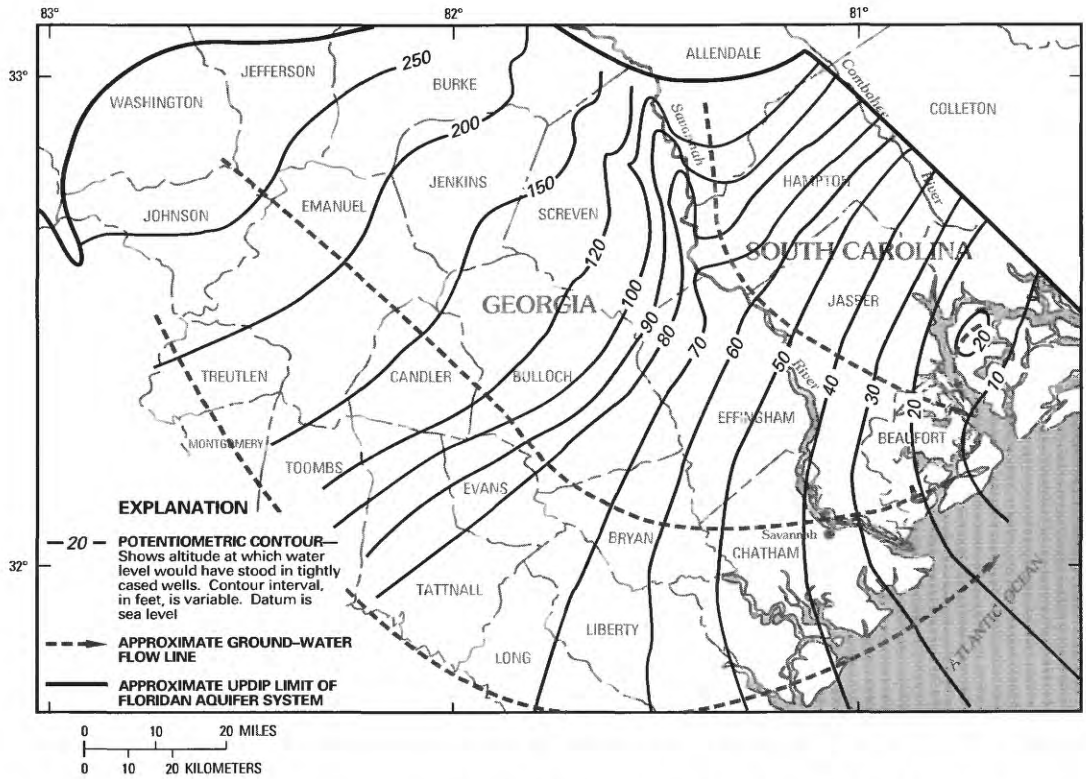

Figure 13. Estimated potentiometric surface and approximate flow lines in the Upper Floridan aquifer prior to pumping (modified from Bush and Johnston, 1988).

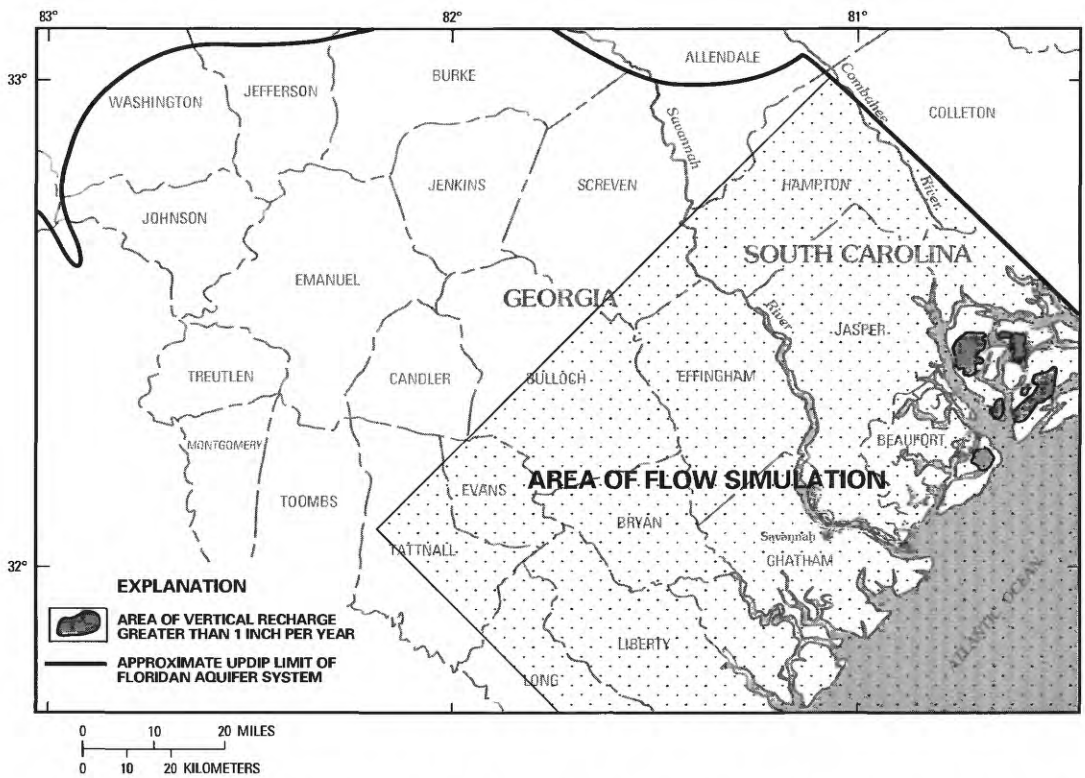

Figure 14. Areas of vertical recharge to the Upper Floridan aquifer prior to pumping based on a steady state numerical flow model (modified from Smith, 1988).

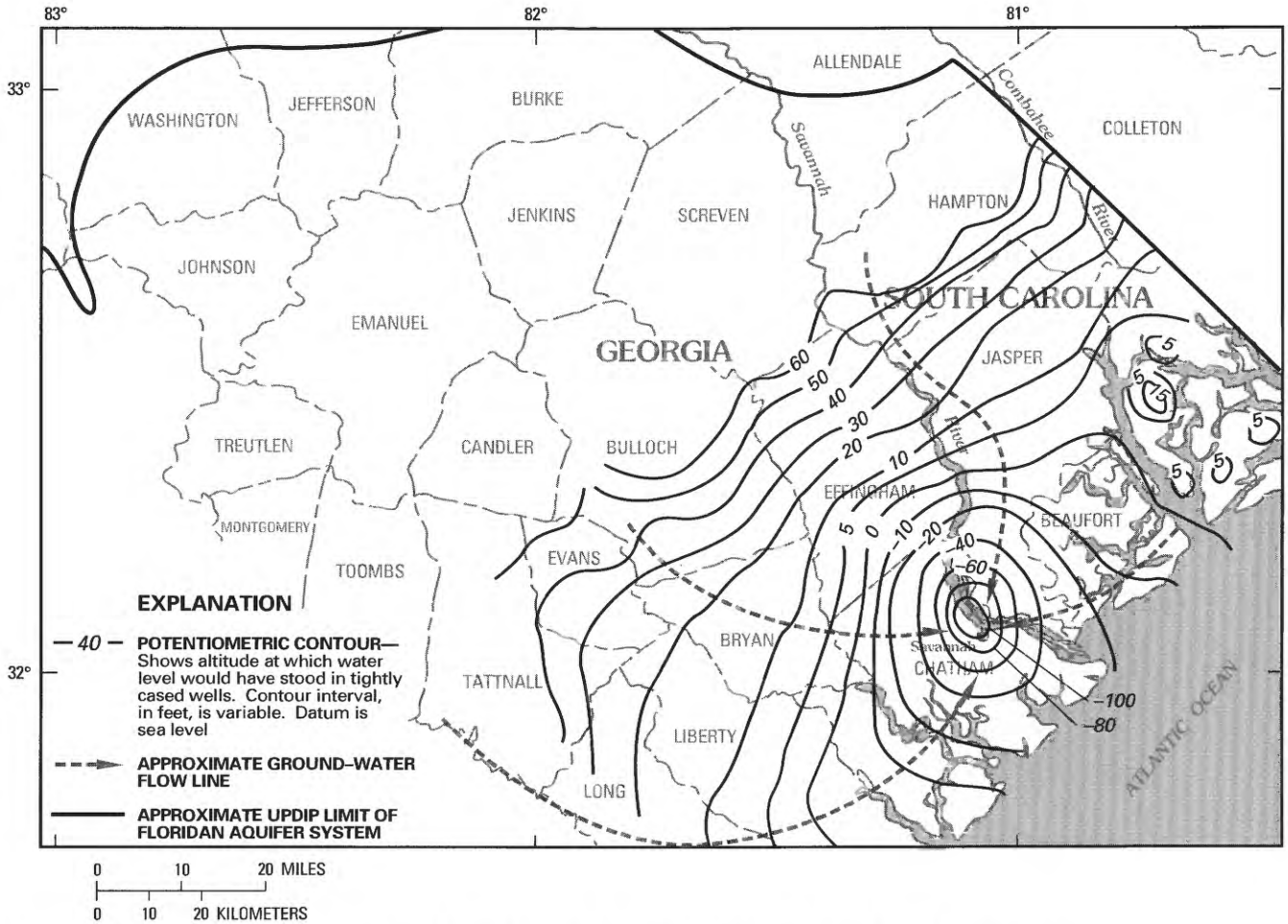

Figure 15. Potentiometric surface of the Upper Floridan aquifer in 1984 (modified from Smith, 1988).

high-salinity wedge. Rather, the location of the interface would be expected to move in the new direction of ground-water flow. The extent to which this intrusion of saltwater has occurred, and the rate at which it is expected to proceed in the future, is addressed in a report by Smith (1993).

CHEMICAL EVOLUTION AND DIAGENETIC PROCESSES

The composition of ground water in the study area varies from very low salinity to compositions that are similar to seawater. Chloride is most often used to demonstrate this variability, but differences also exist in a host of other constituents. In this study, the primary parameters used to interpret the geochemical system are calcium, magnesium, sodium, potassium, chloride, sulfate, sulfide, fluoride, bromide, silica, aluminum, phosphate, dissolved inorganic carbon (DIC), ammonia, nitrate, pH, oxygen-18, deuterium, and the isotopes of carbon, carbon-13 and carbon-14. These components constitute greater than 99 percent of the dissolved substances in the water. Variations in the concentrations of these constituents in ground water within the study area may be the result of mixing processes and chemical interactions of the ground water with its geologic environment and are used in this study to develop conceptual models of these processes.

The distribution of chloride concentrations in the Upper Floridan aquifer in the Port Royal Sound area is shown in figure 16. The chloride distribution actually varies in three dimensions, as shown by Smith (1993), but for the purposes of this presentation is represented in two dimensions. The values in figure 16 are the maximum values measured in each of the wells.

The distribution of chloride in the aquifer near Port Royal Sound is probably controlled by both distant and local sources of seawater and freshwater. The location of the high-salinity wedge, which as described earlier, closely coincides with its expected steady state position as determined with the Hubbert equation, suggests that much of the high-salinity water may be the landward extension of old seawater that recharged the aquifer at some distance

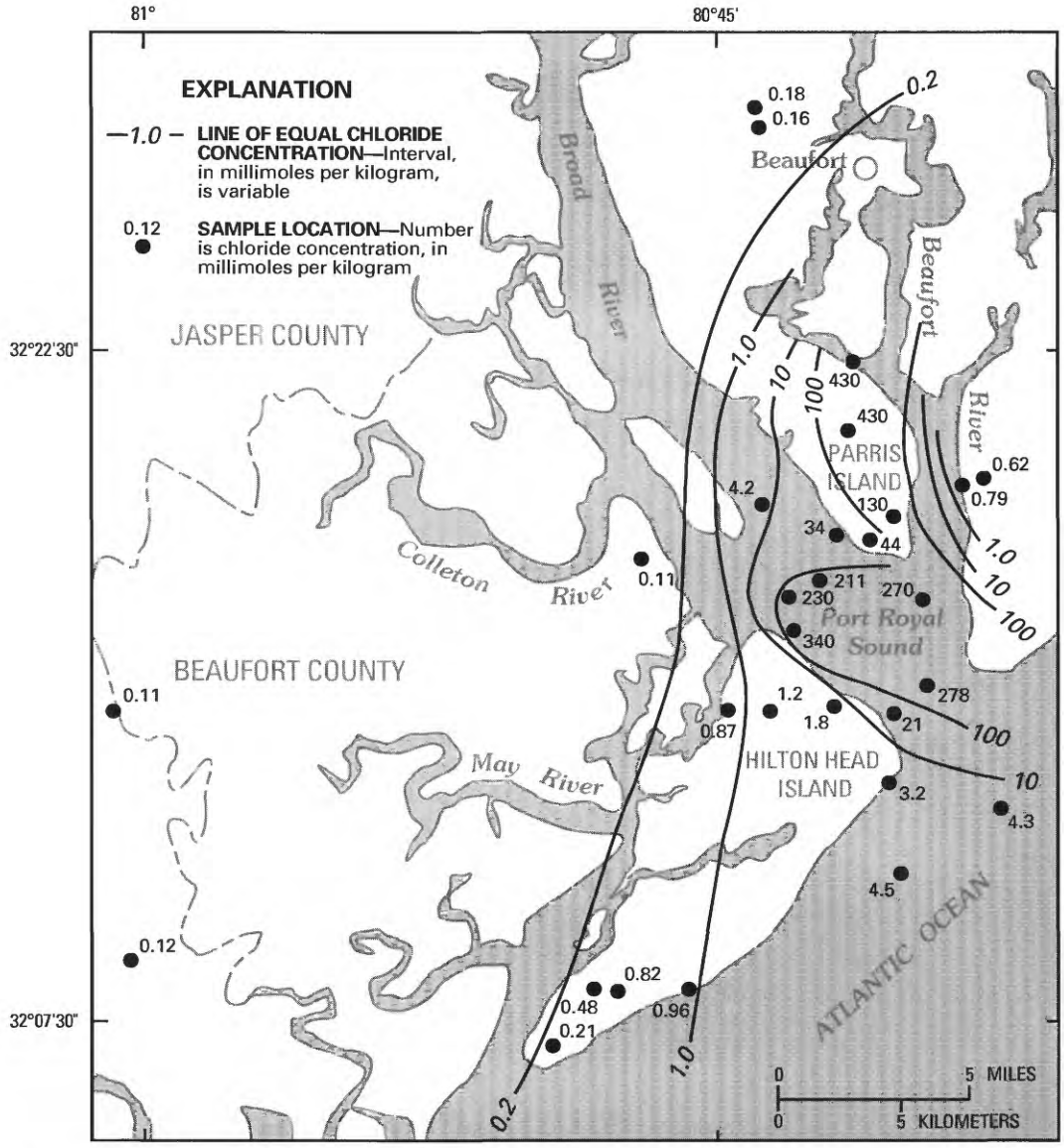

Figure 16. Concentration of chloride in ground water in the Upper Floridan aquifer.

offshore. Old freshwater in the aquifer flowed to the Port Royal Sound area after recharging the aquifer near its distant outcrops inland. Local recharge to the aquifer through overlying sediments by younger ocean water and younger freshwater is indicated by high carbon-14 activities measured on dissolved inorganic carbon in ground-water samples from this and other studies (Back and others, 1970).

Most of the carbon-14 in ground water is derived from atmospheric carbon dioxide dissolved in rain, or from soil carbon dioxide that dissolves in infiltrating water in shallow sediments. Carbon-14 is a radioactive isotope that decays with a half-life of 5,730 years. As ground water flows deeper in the subsurface and away from the surface source of modern carbon dioxide, the carbon-14 activity of carbon in the water is depleted by radioactive decay. The carbon-14 activity of a ground-water sample is, therefore, an indication of the amount of time elapsed since the water was at the surface, and the apparent age of the ground water can be calculated. However, other geochemical processes may also dilute the amount of carbon-14 in solution, so unless these other geochemical processes can be identified and quantified, exact ages are indeterminable. In this study, the uncertainties inherent in the geochemical reaction models and the very low activities (near detection limit) of some samples precluded the calculation of ground-water ages. Large differences in carbon-14 activity of ground water in the study area are probably still roughly indicative of relative age differences, however.

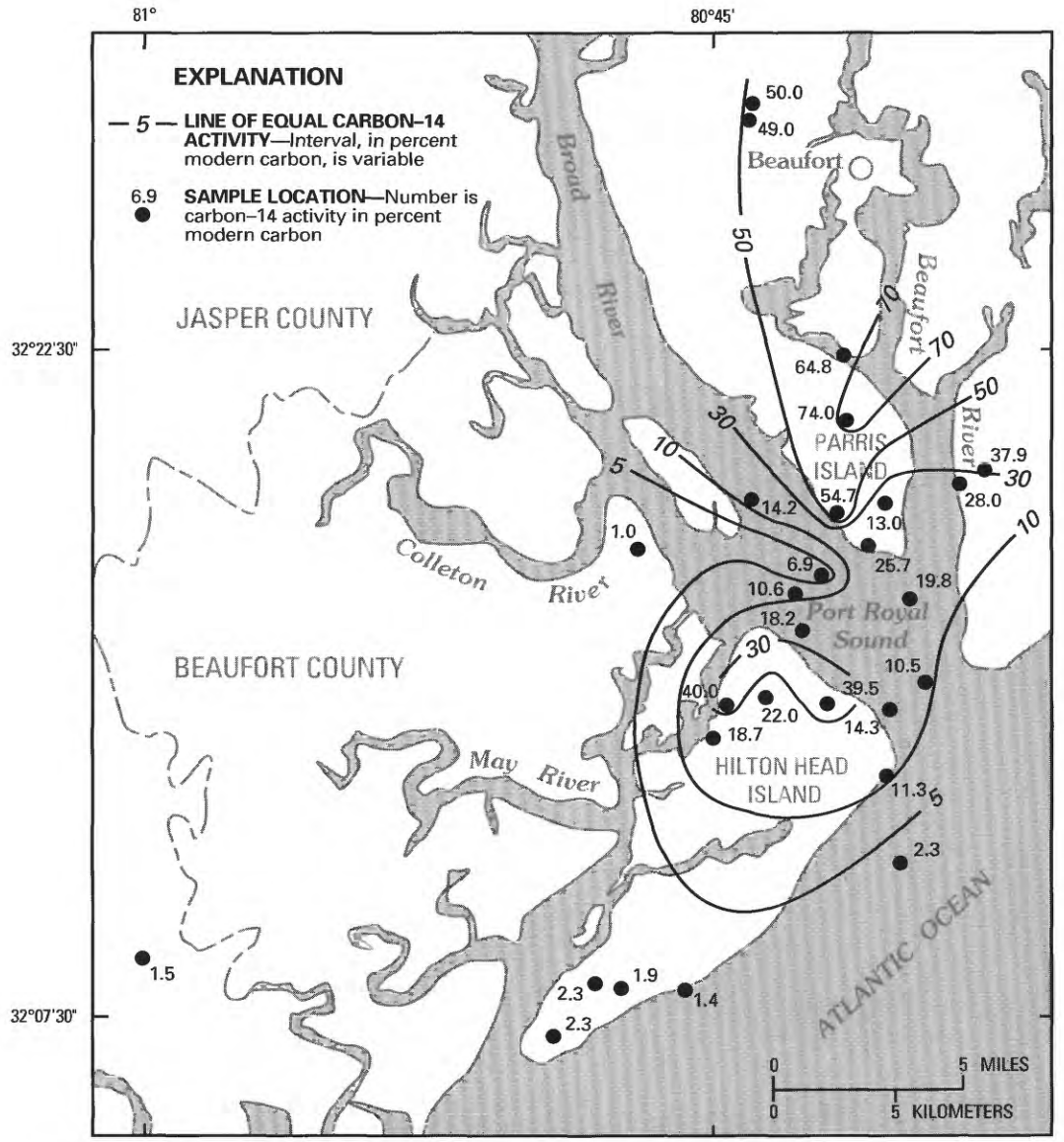

Figure 17. Distribution of carbon-14 activity in ground water in the Upper Floridan aquifer.

The distribution of carbon-14 activity in the aquifer is shown in figure 17. The activity values are in units of percent modern carbon (PMC), a ratio between the measured specific activity of the sample to that of a modern standard [0.95 oxalic acid, National Institute of Standards and Technology (NIST)]. Carbon samples were prepared from ground water by precipitating dissolved inorganic carbon as strontium carbonate from the water sample after raising the pH to approximately 11 with sodium hydroxide that was free of carbon dioxide. The procedure is described in detail in Busby and others (1983). Carbon-14 activity as well as $\delta^{13}C$ measurements were performed on carbon dioxide gas prepared from the strontium carbonate precipitate and oxalic acid standard. The specific activity of the carbon dioxide generated from the oxalic acid standard was corrected to a $\delta^{13}C$ value of -19 per mil (‰) and age corrected to 1950 prior to calculation of PMC activity values according to accepted procedures.

Near-modern carbon-14 activities exist in the area near Port Royal Sound and north toward Beaufort, decreasing to the south and west (fig. 17). The high activities reflect a local, young source of water recharging the area. The two highest carbon-14 activities were measured in wells BFT–795 (64.8 PMC) and BFT–566 (74.0 PMC). Both of these samples were 79 percent seawater, based on chloride concentration. The high carbon-14 activities show that the primary origin of water in the area of these wells is probably modern seawater. Farther north, samples BFT–124 and BFT–121 exhibit high carbon-14 activities for very low-salinity samples, indicating a modern source of

freshwater. The low carbon-14 activities (less than 3.0 PMC) bordering the area to the south and west reflect domination by the characteristically older, low-salinity ground water in the Upper Floridan aquifer upgradient and west of Port Royal Sound.

For the purposes of this investigation, the study area has been divided into two parts, a low-salinity zone and a mixing zone. The boundary between the two zones is delineated as the 0.2 millimoles per kilogram (mmol/kg) chloride concentration contour. This value was chosen because it represents a concentration of seawater in the system below which the concentrations of the other major seawater constituents are insignificant. To delineate the geochemical processes that have occurred in the mixing zone, it was first necessary to describe the nature of the fresh ground water that flowed into this area from upgradient. The results of this investigation are, therefore, presented in two parts: one covering the low-salinity zone and the other covering the mixing zone.

Data Sources

The chemical and isotopic analyses used for this investigation, arranged according to the sources of data, are given in table 7. As part of this project, 31 ground-water samples from 31 wells were collected and analyzed during 1984–1987. Analyses presented by Back and others (1970) of eight samples from the study area taken during 1965 and 1966 have been combined with the more recent samples and used in the geochemical reaction models applied to this study. All of these samples were collected from wells in South Carolina. To qualitatively extend the study area into Georgia and expand the coverage in South Carolina, analyses of samples collected between 1941 and 1981 were compiled from available data bases. Two analyses were taken from Hayes (1979), and five from Counts and Donsky (1963). The remainder of the analyses presented here were identified from points on the chloride distribution map of Sprinkle (1982), and the standard complete analyses were retrieved from the historical files of the U.S. Geological Survey. The latter analyses were not used in the formulation of geochemical reaction models due to insufficient precision of the reported pH values and incompleteness of the data. However, the analyses were suitable for qualitative interpretations based on ion concentrations.

Samples used as part of this study were collected and analyzed according to accepted standard procedures (Skougstad and others, 1979; Barnes, 1964; Busby and others, 1983). The sample interval in each well was chosen based on identification of the Upper Floridan aquifer from geophysical logs. Correspondence of the sample intervals reported by other authors to the Upper Floridan aquifer were checked by comparison of the reported intervals with the top and bottom of the Upper Floridan aquifer as mapped by Miller (1986). Only analyses with ionic balances [|(total cation equivalents−total anion equivalents)|/ total equivalents] of less than 7 percent were accepted for use in this study.

Low-Salinity Zone

Ground-Water Chemistry

The chemical composition of ground water in the Upper Floridan aquifer varies areally across South Carolina and northeastern Georgia. The chemistry changes in a systematic manner in the direction of ground-water flow, suggesting that the chemical variation reflects the evolutionary changes resulting from chemical reactions occurring as the ground water migrates through the aquifer.

Near the coast, elevated concentrations of chloride indicate that the ground water is mixed with seawater. This section of the report deals only with the chemical evolution of the low-salinity ground water in areas unaffected by seawater mixing.

A trilinear plot (fig. 18) of the major anions and cations measured in samples from 26 wells illustrates the chemical character of the low-salinity ground water in the Upper Floridan aquifer in the study area. Without exception, the major anions are dominated by bicarbonate. In contrast, the major cations show variation along the aquifer flow paths. An arrow on figure 18 shows the general direction of ground-water flow with respect to the plotted cation concentrations. Upgradient, the cations are dominated by calcium. This calcium bicarbonate type of water is the result of calcite dissolution in the aquifer and overlying sediments by recharging ground water. Downgradient of the recharge areas the sodium and magnesium cations become significant components of the ground water, indicating that other chemical reactions have affected the ground-water composition.

This evolutionary pattern is further illustrated in figures 19–28, where the areal distributions of concentrations are mapped for chloride, calcium, magnesium, sodium, potassium, silica, bicarbonate, fluoride, sulfate, and pH of the ground water in the Upper Floridan aquifer. Superimposed on the maps are flow lines that approximate ground-water flow paths in the aquifer based on the potentiometric surface of the aquifer (Bush and Johnston, 1988) prior to extensive ground-water development. These maps show that most of the ground water constituents either progressively increase or decrease along the flow paths. This is particularly evident for calcium, magnesium, sodium, bicarbonate, and pH, which, as will be shown, are the most significant reactants affecting the chemical evolution of the ground water in the Upper Floridan aquifer. Magnesium and sodium concentrations increase with distance downgradient, ranging from 0.02 mmol/kg to 0.49 mmol/kg and 0.08 mmol/kg to 0.74 mmol/kg, respectively.

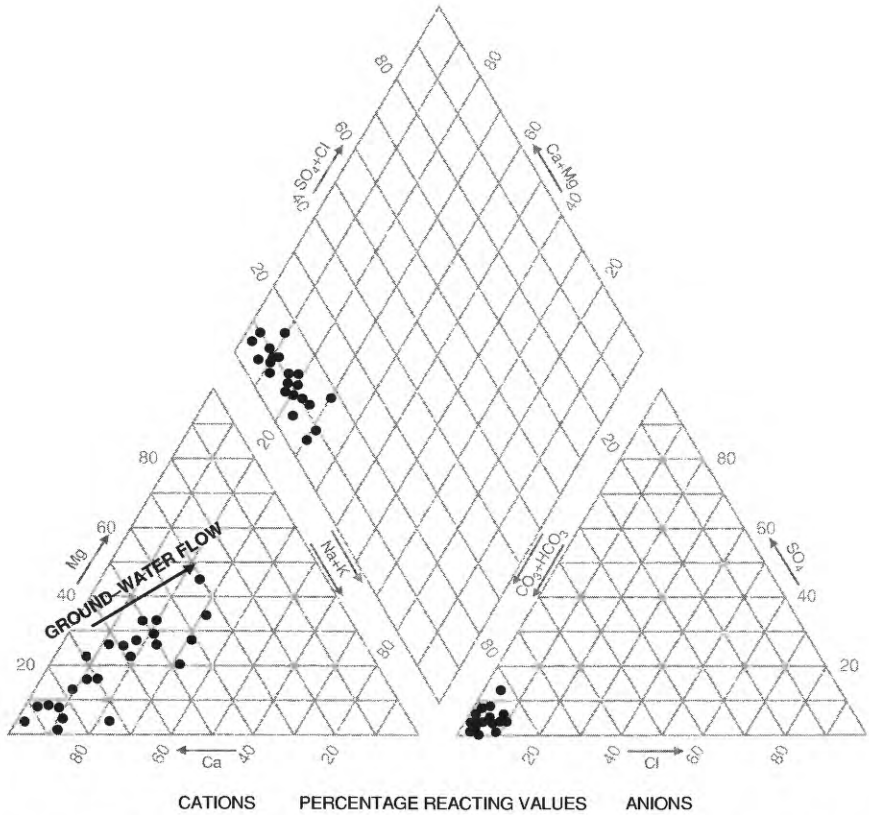

Figure 18. Trilinear plot of chemical analyses of ground water from the low-salinity zone of the Upper Floridan aquifer.

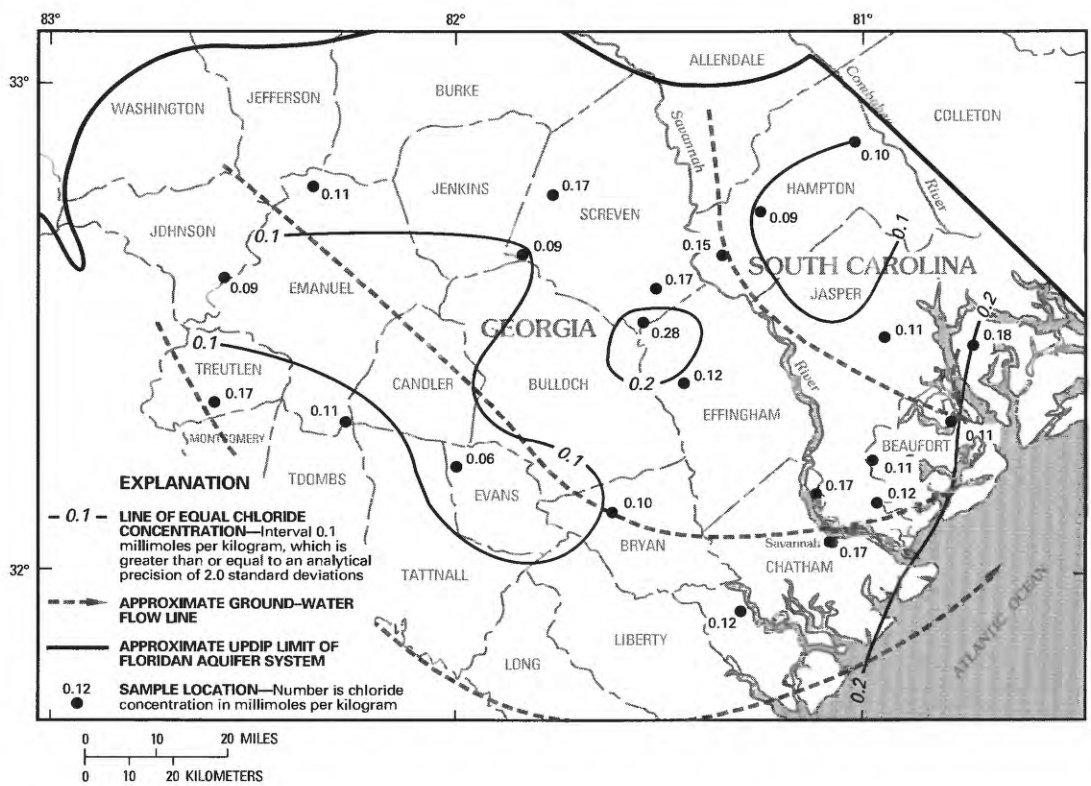

Figure 19. Chloride in ground water in the low-salinity zone of the Upper Floridan aquifer.

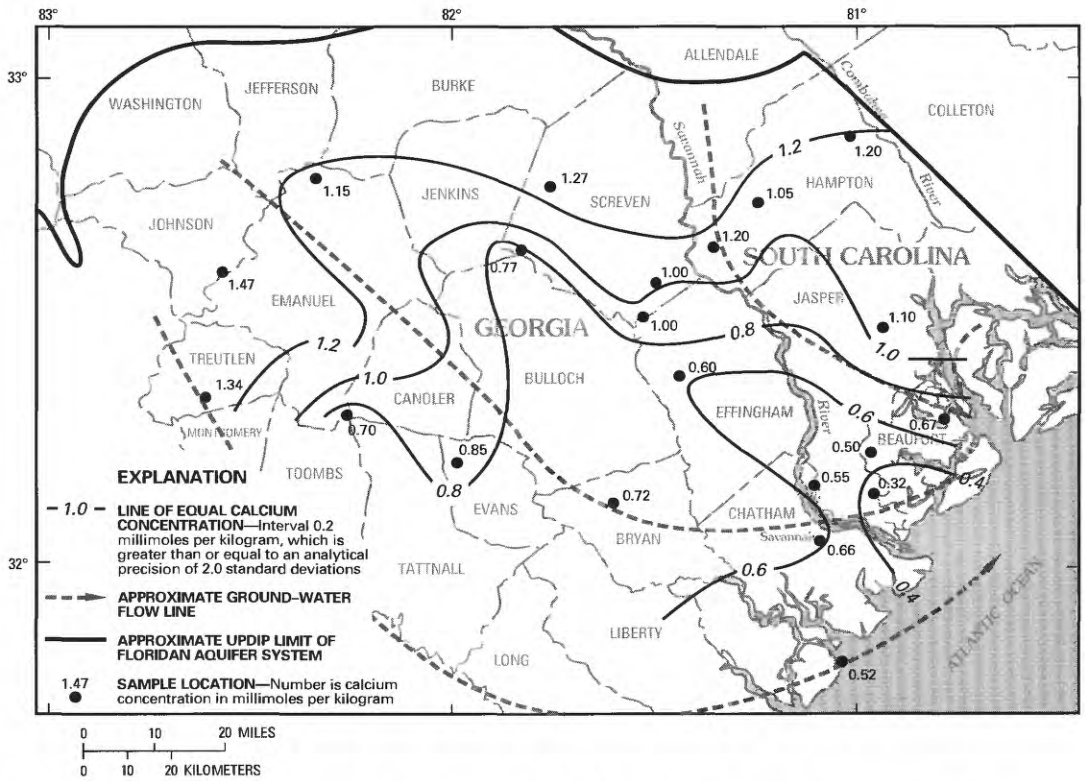

Figure 20. Calcium in ground water in the low-salinity zone of the Upper Floridan aquifer.

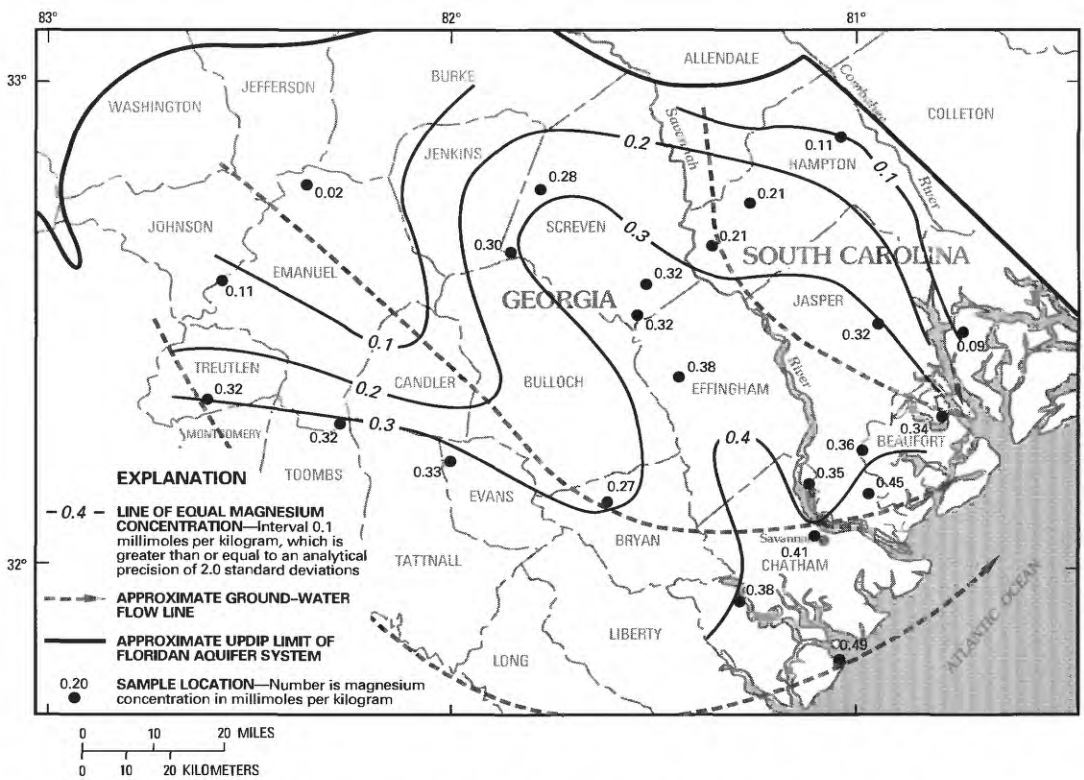

Figure 21. Magnesium in ground water in the low-salinity zone of the Upper Floridan aquifer.

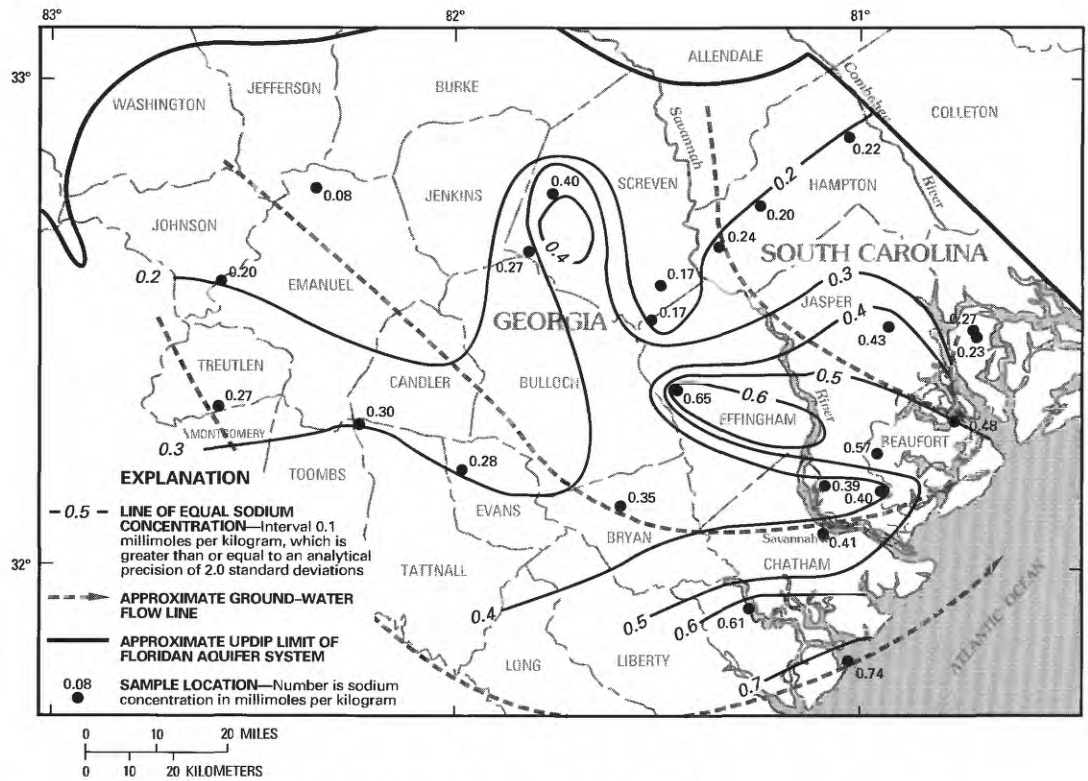

Figure 22. Sodium in ground water in the low-salinity zone of the Upper Floridan aquifer.

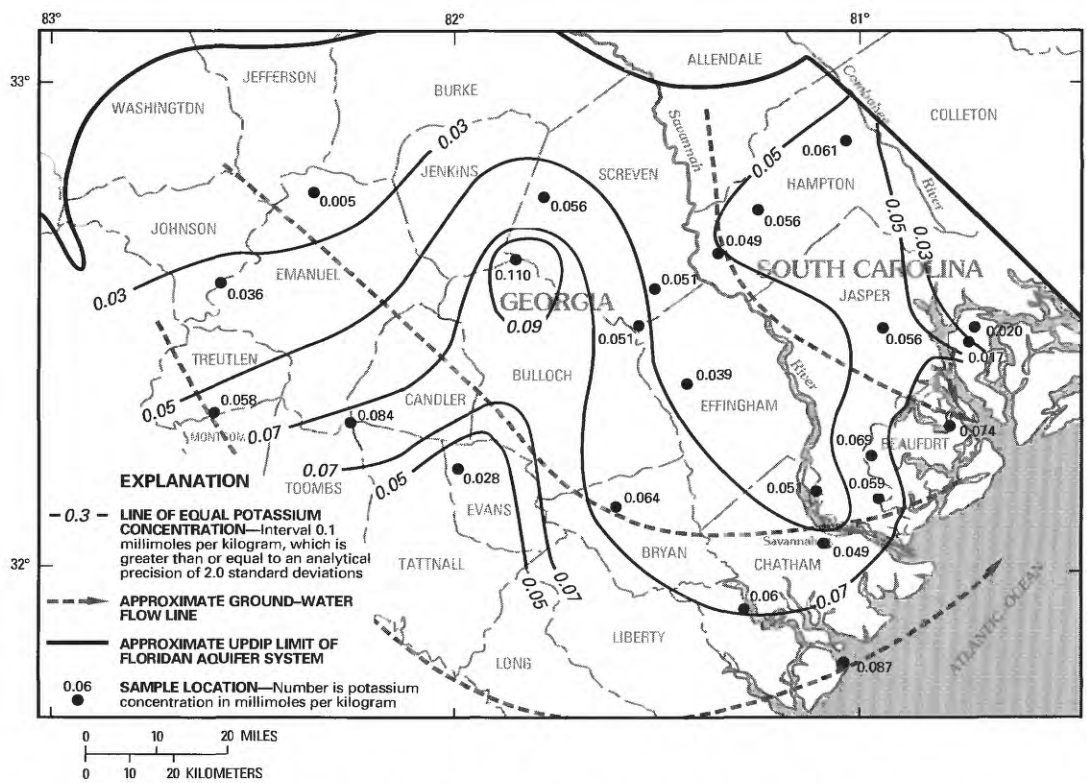

Figure 23. Potassium in ground water in the low-salinity zone of the Upper Floridan aquifer.

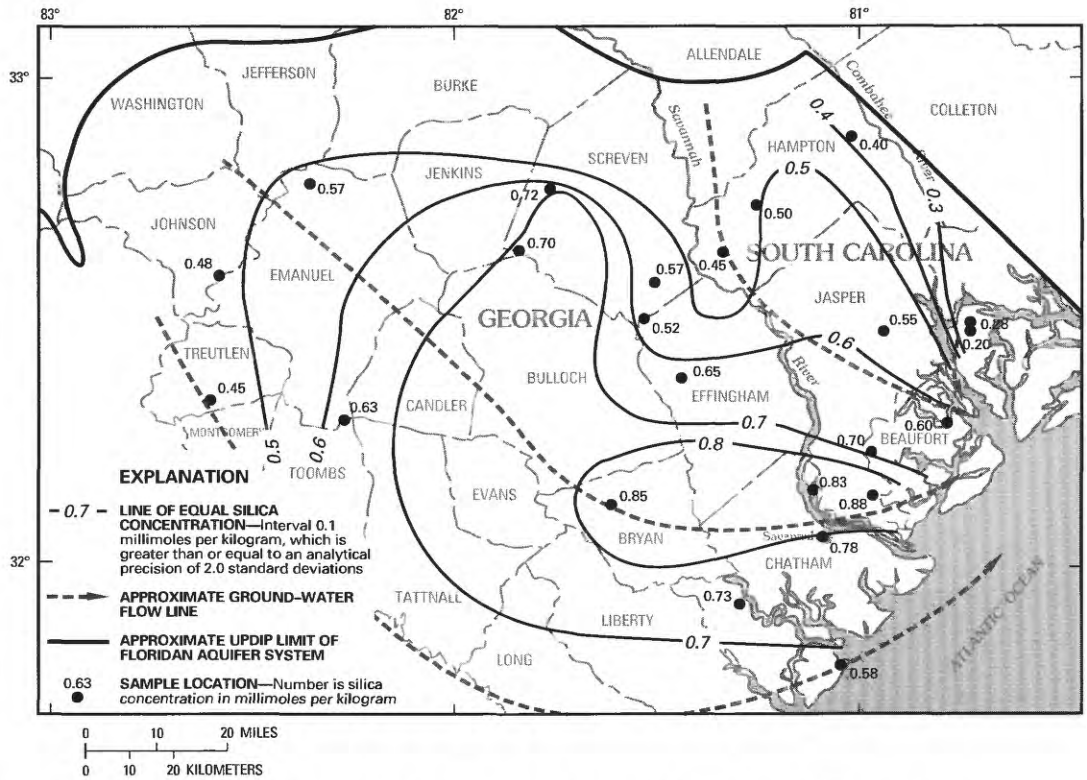

Figure 24. Silica in ground water in the low-salinity zone of the Upper Floridan aquifer.

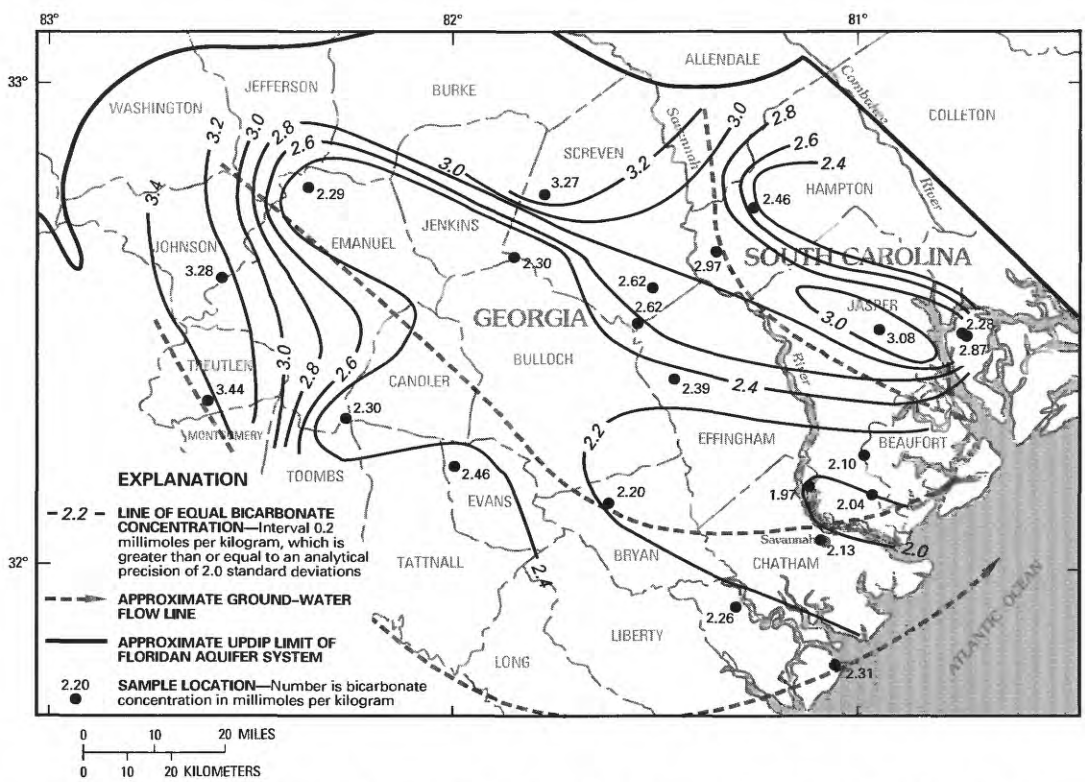

Figure 25. Bicarbonate in ground water in the low-salinity zone of the Upper Floridan aquifer.

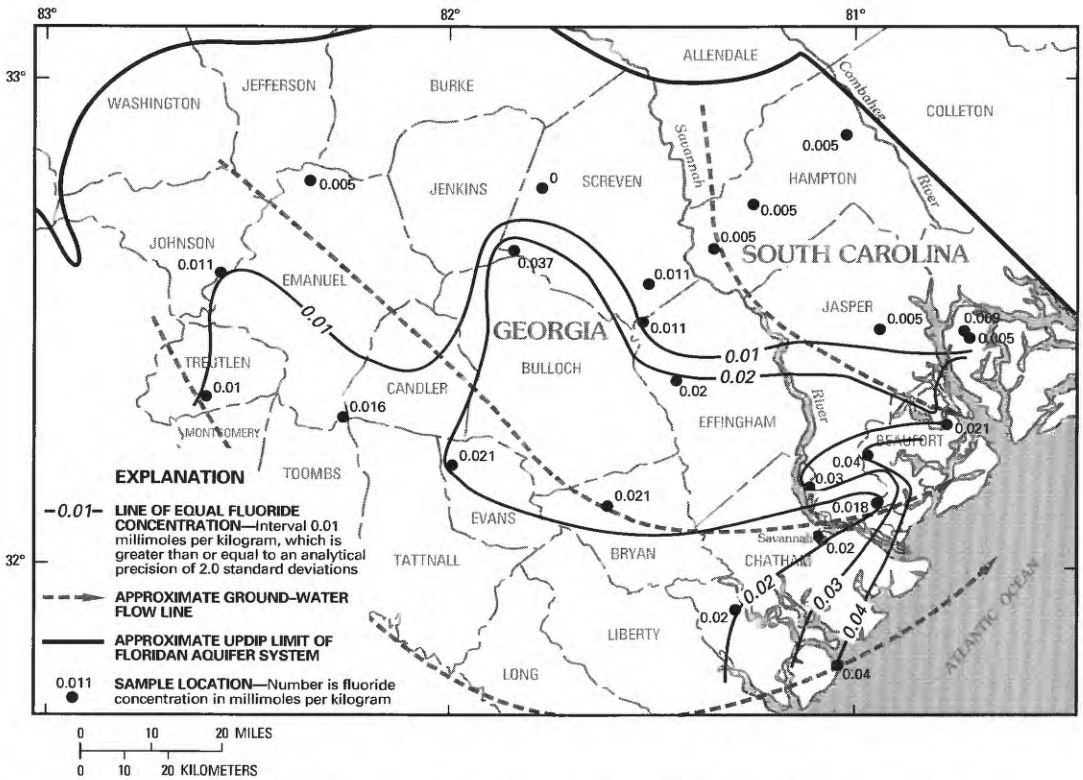

Figure 26. Fluoride in ground water in the low-salinity zone of the Upper Floridan aquifer.

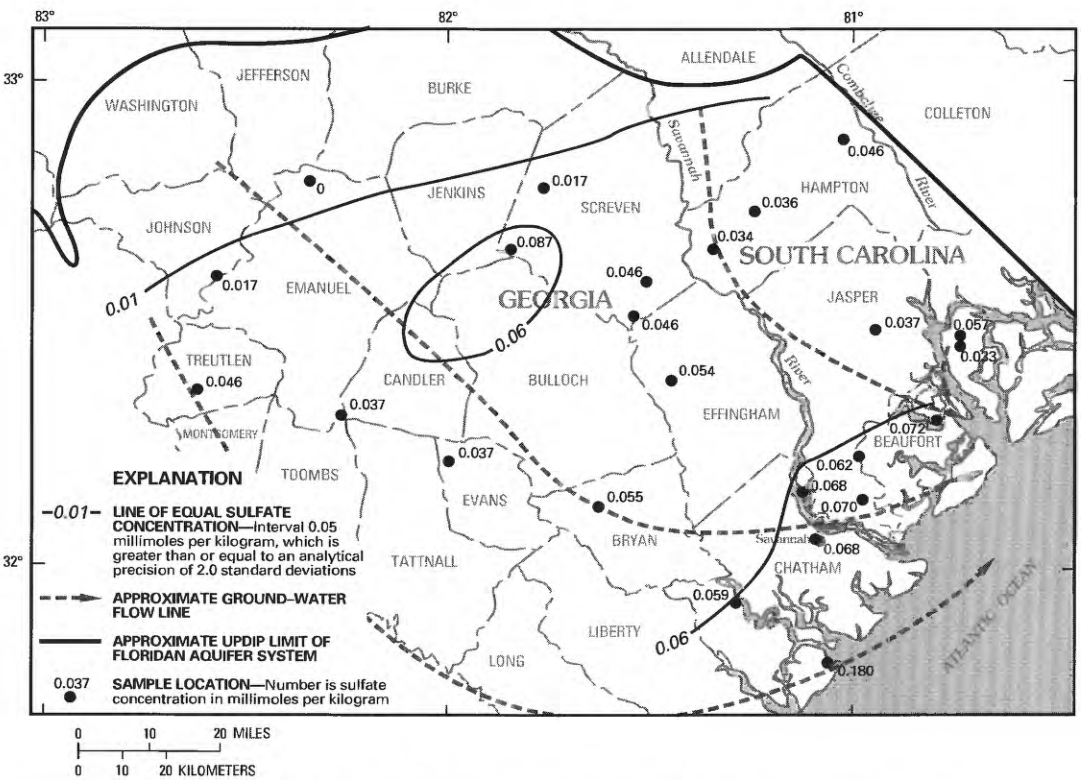

Figure 27. Sulfate in ground water in the low-salinity zone of the Upper Floridan aquifer.

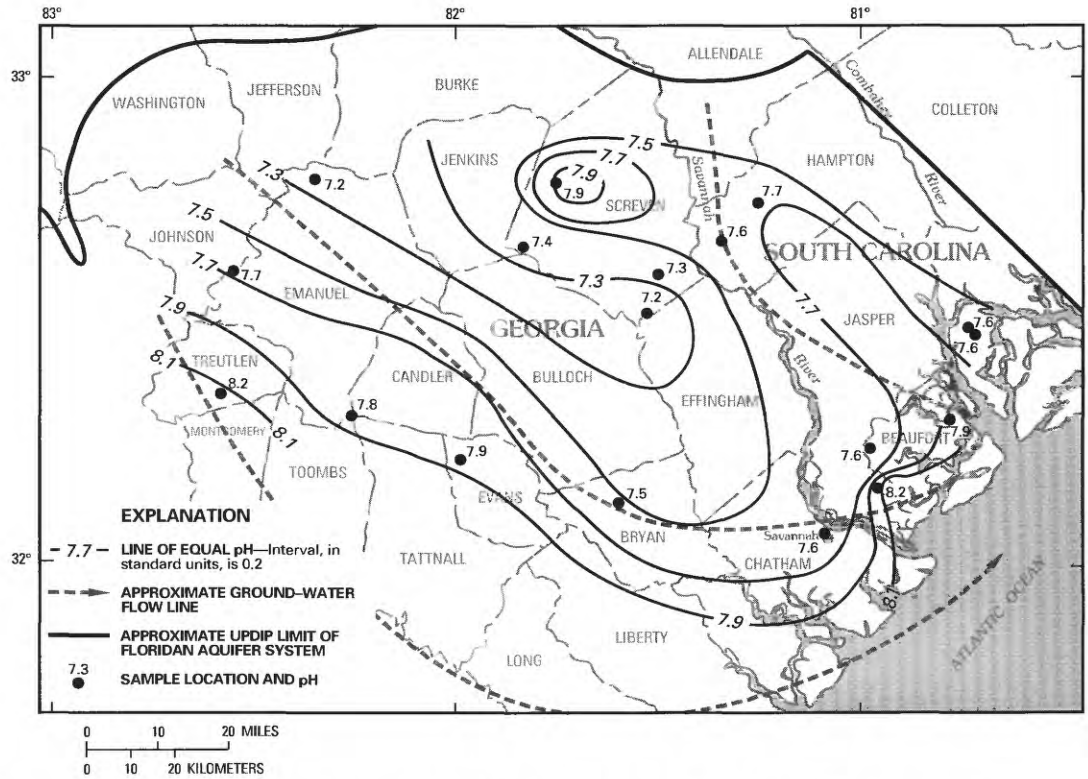

Figure 28. The pH in ground water in the low-salinity zone of the Upper Floridan aquifer.

The pH of the ground water also increases downgradient within a range of 7.2–8.2 pH units. Calcium and bicarbonate concentrations decrease downgradient, ranging from 1.47 to 0.37 mmol/kg and 3.44 to 1.97 mmol/kg, respectively. The changes in fluoride, potassium, and sulfate are not as consistent; however, each shows a net increase over the full length of any given flow path. Fluoride ranges from 0.000 to 0.04 mmol/kg; potassium ranges from 0.005 to 0.087 mmol/kg; and sulfate ranges from 0.00 to 0.72 mmol/kg. Fluoride, potassium, and sulfate, it turns out, appear to be only minor reactants in the geochemical evolution of the ground water in the Upper Floridan aquifer. Chloride ranges from 0.06 to 0.19 mmol/kg but does not exhibit a significant trend outside of the area of seawater mixing.

Because mixing of ground water of differing compositions does not play a role in this part of the study area, the exhibited chemical variation must be the result of some combination of dissolution, precipitation, and exchange reactions between the ground water, dissolved constituents, and such minerals in the aquifer as carbonates, silicates, sulfates, phosphates, and possibly organic matter. A model is presented in the following section that demonstrates the plausible influence of eight chemical processes on the evolution of the ground-water chemistry as well as diagenesis of the sediments that compose the aquifer. The processes include

1. Calcite dissolution,
2. Calcite precipitation,
3. Alkali feldspar incongruent dissolution,
4. Plagioclase feldspar (oligoclase) incongruent dissolution,
5. Cation exchange,
6. Anion exchange,
7. Gypsum dissolution, and
8. Carbon dioxide input.

Most notably, calcite precipitation in the aquifer occurs primarily in response to processes 1 and 4: calcite dissolution and oligoclase incongruent dissolution. The significance of oligoclase incongruent dissolution demonstrates the important effect that small amounts of unstable silicate minerals may impose on the diagenesis and chemical evolution of a predominantly carbonate aquifer.

Chemical Evolution Model

The consistency of patterns of chemical variation in the ground water across the study area suggests that a common set of chemical processes controls the chemical evolution of the ground water along each flow line. The problem is to identify the specific chemical processes and the relative effect of each process on the change in ground-water composition. Quantitative conceptual models

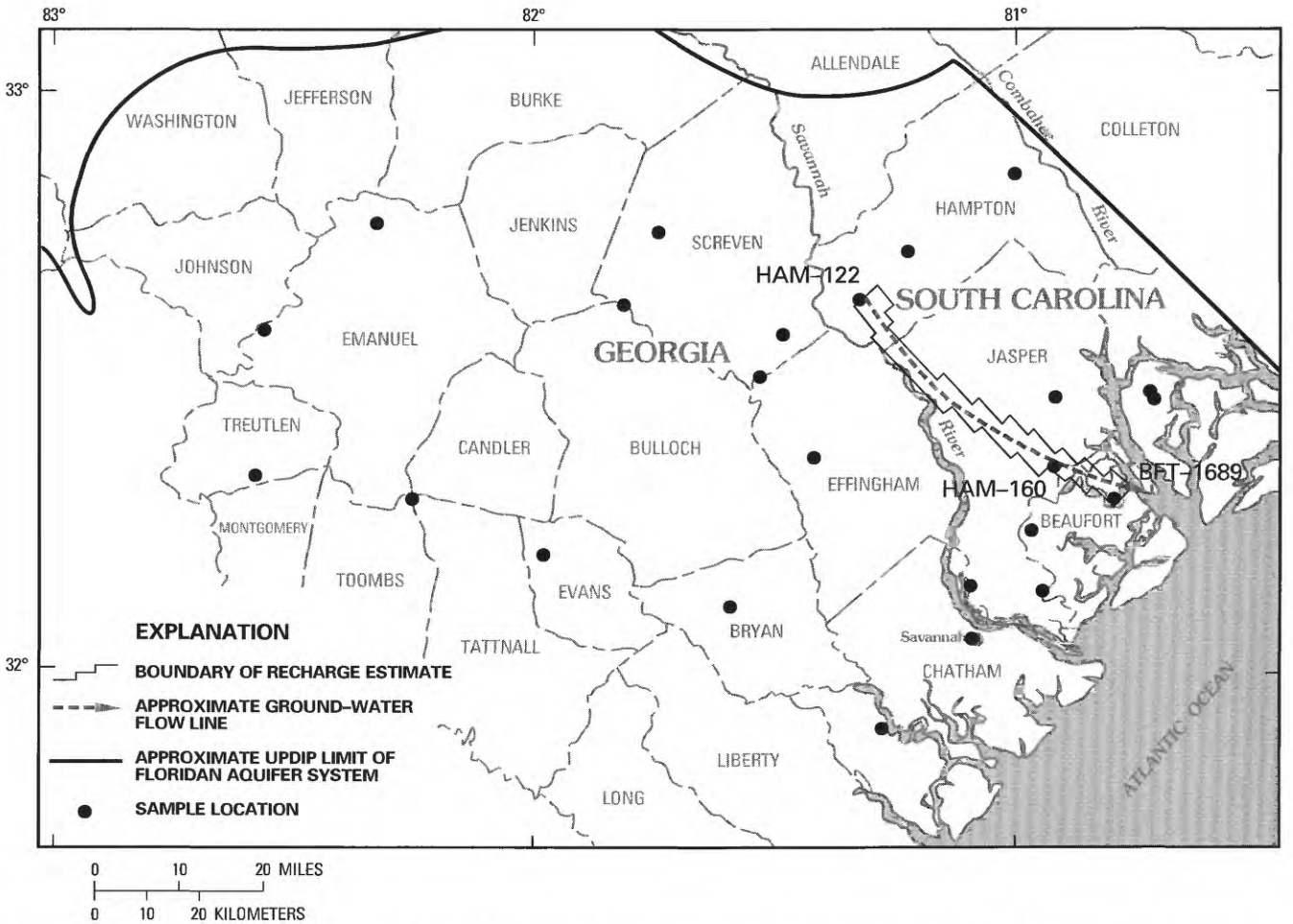

Figure 29. Approximate flow line used to model chemical evolution in the low-salinity zone of the Upper Floridan aquifer, and the boundary of the area used for the vertical recharge estimate.

explaining the evolutionary pattern can be formulated by first designating a ground-water flow-line segment for which the chemical composition of the ground water at each end-point of the flow line is accurately known. The modeling process then begins by hypothesizing possible chemical reactions based on plausible sources or sinks for the changing chemical constituents in the ground water along the flow-line segment. Minerals that may react with the ground water, acting as sources or sinks for the various ground-water constituents, are considered along with compounds such as carbon dioxide, which may be derived from organic processes in the subsurface. The limitations imposed by mineral saturation, mass balance, and isotope mass transfer are then applied to constrain the set of reactions into a conceptual model that quantitatively explains the chemical evolution of the ground water along the designated flow line, and qualitatively describes the similar patterns of changing ground-water composition observed along other flow lines in the study area.

Application of this approach to modeling the chemical evolution of the ground water requires that two assumptions be met regarding the hydrologic system:

1. Any change in the composition of the ground water along the designated flow-line segment can only be attributable to chemical reactions within the aquifer; and
2. The composition of the ground water at any given point on the flow line must approach constancy with time (steady state).

Violation of the first assumption would occur if the aquifer was not well confined, allowing a flux of dissolved ground-water constituents in or out of the aquifer, or if the effects of dispersion were significant. The second assumption might be violated if the ground-water flow has not maintained a state of equilibrium. The flow-line model for this study was formulated for the flow-line segment bounded upgradient by well HAM–122 and downgradient by well BFT–1689 (fig. 29). This segment was selected because of availability of good-quality chemical analyses of water samples from the two end-point wells and a reasonable compliance with the stated assumptions as follows.

Table 5. Chemical and isotope analyses of ground water at the model flow-line end-points

[mmol/kg, millimoles per kilogram; dashes indicate no data]

	Calcium (mmol/kg)	Magnesium (mmol/kg)	Sodium (mmol/kg)	Potassium (mmol/kg)	Chloride (mmol/kg)	Sulfate (mmol/kg)	Fluoride (mmol/kg)	Silica (mmol/kg)	Aluminum (mmol/kg)	Phosphate (mmol/kg)	Dissolved inorganic carbon (mmol/kg)	Carbon-13 (per mil)
HAM–122	1.2	0.21	0.24	0.049	0.15	0.034	0.0053	0.45	0.0004	0.0016	2.98	−10.5
	[1]±.1	±.01	±.02	±.004	±.03	±.028	±.004	±.02	±0.002	—	±.07	±.7
BFT–1689	.67	.34	.48	.074	.11	.072	.021	.60	.0008	.0019	2.35	−3.3
	±.05	±.02	±.03	±.007	±.03	±.032	±.004	±.02	±.002	—	±.07	±.7
Δ[2]	−0.53	+.13	+.24	+.025	−.04	+.038	+.016	+.15	+.0004	+.0003	−.63	—
	[3]±.15	±.03	±.05	±.011	±.060	±.060	±.008	±.04	±.004	—	±.14	—

[1] Symbol ± represents the precision of the analytical method (±1.0 standard deviation).

[2] The Δ value is judged to be significantly different from zero if the absolute value of Δ is greater than the computation standard error.

[3] For Δ, symbol ± represents the combined error of the computation.

The confining units above and below the Upper Floridan aquifer restrict vertical leakage to and from the aquifer to minimal amounts in the area of the designated flow-line segment. A steady state flow model (B.S. Smith, U.S. Geological Survey, written commun., 1987) was used to estimate recharge from overlying sediments within a 111-square-mile (mi^2) corridor along the flow line (fig. 29). The model indicated that the flow line lies in a net discharge area whose average areal upward discharge is 0.21 in./yr and average areal recharge is 0.025 in./yr. If water discharging from the aquifer has the same average composition as the water in the aquifer at the discharge point, discharge will not affect the composition of the aquifer water. However, water entering the aquifer as recharge will mix with the aquifer water and change its composition. The flow-model recharge estimate shows that recharge from overlying sediments to the aquifer is very low along the flow line; however, the cumulative effect on ground-water chemistry could still be significant. To simplify this discussion, the flow-line chemical reaction model will be formulated under the assumption that recharge along the flow-line segment is not significant, and the implications of this assumption will be discussed later.

Wigley and others (1978) demonstrate that dispersion effects are not significant when the change in concentration of a dissolved constituent is small over the dispersion length characteristic of the aquifer. The dispersion length is unknown for the Upper Floridan aquifer but for most aquifers is on the order of 10–500 ft. Ground-water compositional changes are minimal over these distances in the study area. Therefore, it can be assumed that the compositional change of the ground water is attributable only to chemical reactions within the aquifer.

The steady state assumption is harder to document because data are not available over the period required for flow from the upgradient end to the downgradient end on the flow-line segment (approximately 2,500 years based on estimates of hydraulic gradient, transmissivity, and porosity). Ground-water withdrawals during the past 80 years have modified the potentiometric surface in the study area, resulting in changes in the directions of ground-water flow; however, the orientation of the flow lines in the area of the designated flow-line segment has not been appreciably changed (fig. 15) for a significantly long time. For this study the system is assumed to closely approach steady state.

The chemical and isotope analytical values pertinent to formulation of the flow-line model are listed in table 5. Values from wells HAM–122 and BFT–1689 as well as the relative difference Δ between the two wells for each of the constituents are presented. Magnesium, sodium, silica, fluoride, and potassium each significantly increase in concentration along the flow-line segment, resulting in positive Δ values. The pH also increases. Calcium and DIC both significantly decrease, resulting in negative Δ values. The $\delta^{13}C$ values change from −10.5 to −3.3 ‰. As indicated by the confidence limits (±1.0 standard deviation) presented in table 5, the changes in concentration of chloride, sulfur, and aluminum are not significantly different from zero. The confidence limits were calculated based on the precision of the analytical methods.

The first step in formulating the flow-line model is to identify plausible sources and sinks for each of the chemical constituents that change concentration along the flow-line segment. The minerals used as plausible sources and sinks in this model are restricted to those identified in the aquifer by the standard techniques of petrography, X-ray diffraction, scanning electron microscopy, and microprobe analysis. Drill cuttings of the Upper Floridan aquifer sampled from well HAM–160, located on the flow-line segment (fig. 29), were used for the analyses.

The aquifer in the study area consists predominantly of low-magnesium calcite in the form of skeletal fragments, micrite, and sparry cements; however, silicate minerals

made up of quartz, clays, and feldspars also compose a significant fraction (24 percent) of the total matrix at the sample location. The clay minerals identified in aquifer samples were kaolinite, smectites, and illites. Other undifferentiated clays were also present. Plagioclase and alkali feldspars were detected in trace amounts along with gypsum, pyrite, and apatite minerals. Organic material was visually observed as a very dark component of the clay fraction. The minerals, their approximate concentration in the sediment, and their compositional ranges (if known) are presented in table 3.

Chemical Reactions

The potential for dissolution or precipitation of a specific mineral in an aqueous solution depends on the mineral's solubility and the composition of the aqueous solution. This potential is measured by the saturation index (SI) defined by Langmuir (1971) as

$$SI = \log(IAP/K)$$

where IAP is the ion activity product in aqueous solution of a given mineral and K is the equilibrium constant. A value of zero for SI indicates that an aqueous solution is at equilibrium with respect to the mineral. A negative value of SI indicates subsaturation of the solution with respect to the mineral, so that dissolution of the mineral is thermodynamically favored. A positive value of SI indicates supersaturation of the solution with respect to the mineral, so that precipitation of the mineral is thermodynamically favored.

The saturation indices for minerals similar to those identified in the aquifer are graphed in figure 30. An SI value is presented for each mineral in the solution at both the upgradient (HAM–122, open bars) and downgradient (BFT–1689, shaded bars) ends of the flow-line segment. Thermodynamic data used for the SI calculations were taken from Truesdell and Jones (1974), Parkhurst and others (1980), and Karaka and Barnes (1973). The SI value for oligoclase was calculated for the average oligoclase composition ($Ca_{0.28}Na_{0.72}Al_{1.28}Si_{2.72}O_8$) in the aquifer using thermodynamic data for the end-member feldspars, albite and anorthite, and assuming ideal mixing in the solid solution. The SI value for alkali feldspar was similarly calculated for the average composition ($K_{0.74}Na_{0.26}AlSi_3O_8$) using thermodynamic data for the end-member feldspars, albite and sanadine (high) and albite and microcline (low). (See Appendix for explanation of calculations.)

Based on the saturation indices of the minerals in contact with the ground water, feasible chemical reactions can now be formulated into a model that explains the change in chemical concentration of the ground water and does not violate the constraints of mineral solubility.

Calcite Dissolution and Precipitation

The saturation indices for ideal calcite (fig. 30) show that the ground water is very near equilibrium with respect to calcite at both the initial and final points on the flow-line segment. However, the negative Δ values for calcium and DIC indicate that calcite has probably precipitated. Simultaneously, a net increase in magnesium concentration of the ground water along the flow path shows that low-magnesium calcite, the only detected magnesium mineral, has dissolved. This apparent paradox is explained by examining the variation in the equilibrium constant, K_{cal}, of calcites containing differing amounts of magnesium.

Plummer and MacKensie (1974) demonstrate the variation of K_{cal} in relation to the amount of magnesium contained in calcite. The solubility of the mineral reaches a minimum near 2 or 3 percent magnesium carbonate (fig. 31). The solubility increases slightly for calcite with less magnesium carbonate and significantly as the amount of magnesium carbonate increases up to about 25 percent. Calcite from the Upper Floridan aquifer, along the flow-line segment, varies compositionally from $Ca_{0.94}Mg_{0.06}CO_3$ to $Ca_{0.98}Mg_{0.02}CO_3$ (fig. 12). The solubility variation within this range is small but sufficient enough that unstable calcite is favored to dissolve simultaneously with precipitation of stable calcite, as in the following reactions:

$$Ca_XMg_{(1-X)}CO_3 + H^+ \rightarrow XCa^{++} + (1-X)Mg^{++} + HCO_3 \quad (1)$$
(dissolution)

$$YCa^{++} + (1-Y)Mg^{++} + HCO_3^- \rightarrow Ca_YMg_{(1-Y)}CO_3 + H^+ \quad (2)$$
(precipitation)

For these reactions to account for the negative Δ value for DIC, the precipitation reaction must occur to a greater extent than the dissolution reaction. This would require some mechanism to drive the ground water toward supersaturation with respect to calcite. Also, to account for the positive Δ value for magnesium, the dissolving calcite phase must contain a higher concentration of magnesium than the precipitating phase.

Feldspar Incongruent Dissolution

Supersaturation of the ground water with respect to calcite could be achieved by contributing calcium or by raising the pH, both of which may be accomplished with a mechanism involving dissolution of feldspars. Oligoclase is thermodynamically favored to dissolve at both ends of the flow-line segment, as shown in figure 30. Dissolution of oligoclase is consistent with positive Δ values for silica, sodium, and pH. The observation that the concentration of aluminum does not change along the flow-line segment indicates that the oligoclase dissolution is typically

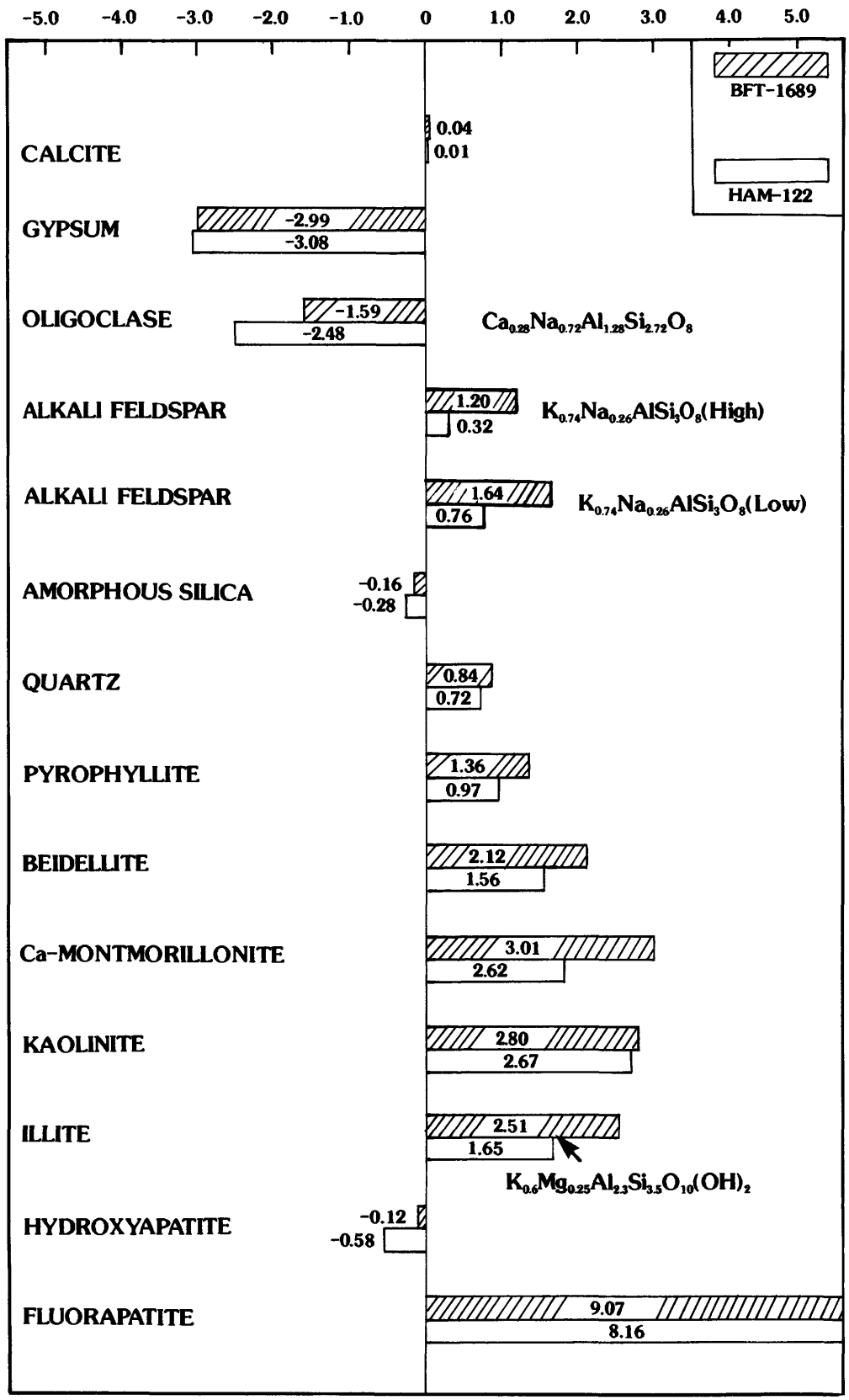

Figure 30. Saturation indices with respect to minerals for ground-water samples from wells BFT–1689 and HAM–122 based on thermodynamic data from compilations of Parkhurst and others (1980), Karaka and Barnes (1973), and Truesdell and Jones (1974).

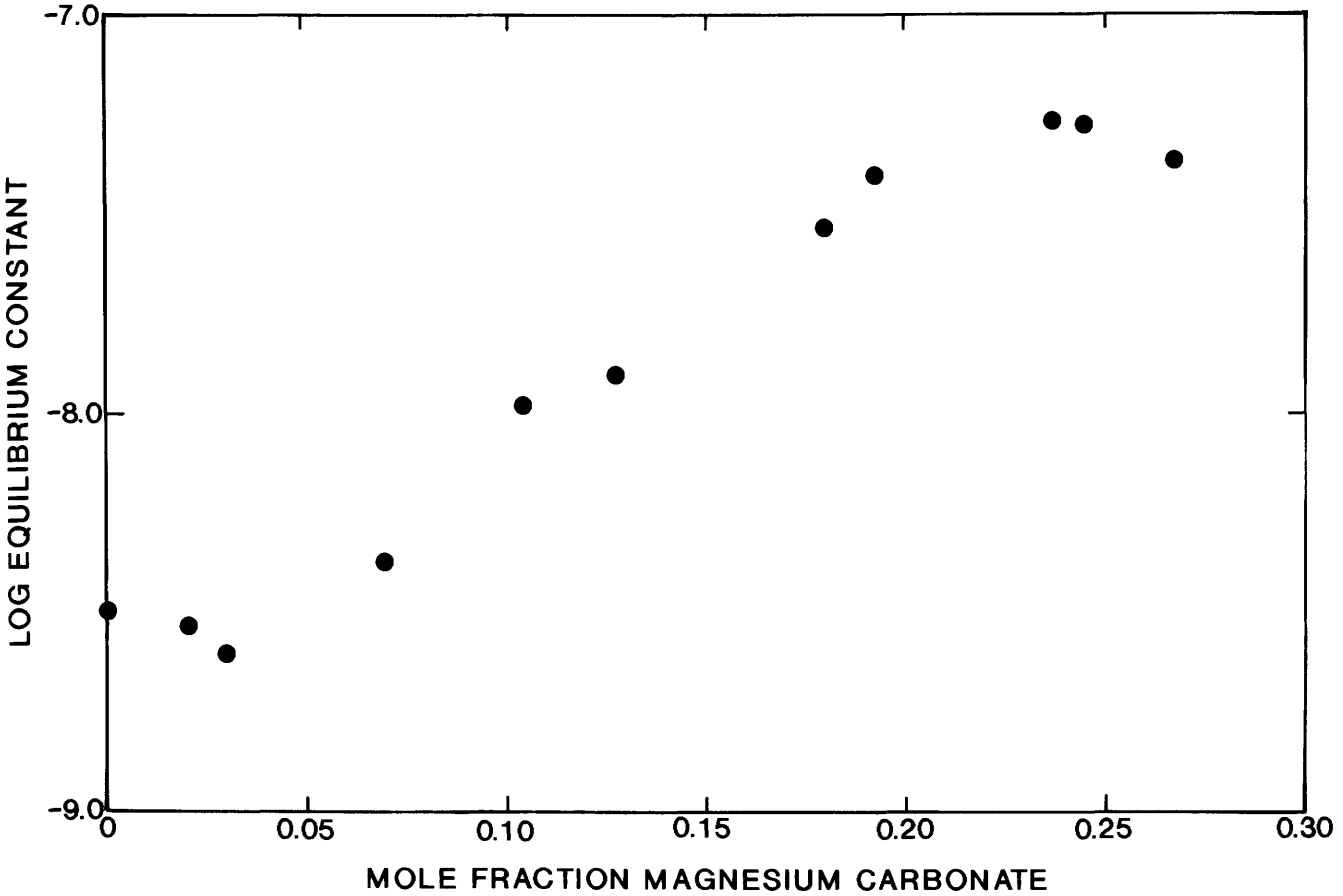

Figure 31. Estimated magnesium-calcite stabilities at 25°C and 1.0-atm total pressure (modified from Plummer and MacKensie, 1974).

incongruent, involving the precipitation of clays, as in the following representative reaction:

$$Na_{0.72}Ca_{0.28}Al_{1.28}Si_{2.72}O_8 + 1.0382H_2O + 0.6904H^+ \rightarrow$$
(oligoclase)

$$0.6271Ca_{0.0205}Al_2(Al_{0.041}Si_{3.959})O_{10}(OH)_2 + 1.1481Ca^{++}$$
(pyrophyllite-beidellite)

$$+0.4260Na^+ + 0.3781Si(OH)_4 \qquad (3)$$

The dissolution of the average oligoclase identified in the aquifer is described in equation 3. The reaction includes simultaneous formation of a simple clay mineral, intermediate in composition between pyrophyllite and beidellite. The reaction results in a hydrogen ion deficit and a surplus of sodium, calcium, and silicic acid in the products. The concentration of aluminum does not change. Consistent with this reaction, figure 30 shows that in addition to oligoclase being favored to dissolve, a number of clay minerals, including pyrophyllite and beidellite, are significantly favored to precipitate.

The saturation indices for alkali feldspar show that the ground waters at both ends of the flow-line segment appear to be supersaturated. However, the SI value for the high-temperature and -pressure form of alkali feldspar at HAM-122 is very close to zero, causing uncertainty as to whether the mineral is favored to precipitate or dissolve. Incongruent dissolution of alkali feldspar would be consistent with positive Δ values for silica, potassium, sodium, and pH, as shown in the following representative reaction:

$$K_{0.74}Na_{0.26}AlSi_3O_8 + 2H_2O + H^+ \rightarrow$$
(alkali feldspar)

$$0.5Al_2Si_4O_{10}(OH)_2 + 0.74405K + 0.2589Na + 1.001Si(OH)_4 \qquad (4)$$
(pyrophyllite)

The dissolution of alkali feldspar, of the average composition identified in the aquifer, with simultaneous formation of pyrophyllite, a simple dioctahedral clay mineral, is described in equation 4. Again, aluminum is conserved. The feasibility of this reaction is uncertain based on the saturation indices for alkali feldspars presented in figure 30; however, the reaction will be included in the proposed model to account for the positive Δ value observed for potassium. Subsequently, it will be shown that the influence of this reaction is of minor significance.

Although both of these incongruent dissolution reactions are plausible, they are probably not unique examples of feldspar to clay reactions that could satisfactorily model the system. The large number of possible clay mineral products and the likelihood of feldspar compositions differing from those presented above suggest that other incongruent dissolution reactions are feasible. In the model, proposed reactions 3 and 4 will be used to demonstrate that feldspar to clay reactions in general are a plausible explanation for the observations.

Cation Exchange

The presence of smectite in the aquifer, along with other clays, indicates the system's potential for cation exchange reactions. A reversible calcium-for-sodium exchange has been included in the model in the following form:

$$\text{Ca-clay} + 2\text{Na}^{+} \leftrightarrow \text{Na}_2\text{-clay} + \text{Ca}^{++} \quad (5)$$

Anion Exchange

The ground water may be supersaturated or subsaturated with respect to apatite, depending on the apatite composition (fig. 30). Hydroxyapatite would be thermodynamically favored to dissolve, while fluorapatite would be favored to precipitate. The composition of the apatite in the aquifer with respect to fluorine and hydroxyl was not determined. If apatite does dissolve in the ground water, it apparently does so only slightly. The Δ value for phosphate is 0.0003 mmol/kg, which corresponds to 0.0001 mmol of apatite dissolving per kilogram of water. This is a very minor contribution to the chemical evolution of the ground water.

The lack of apatite dissolution suggests that the apatite in the aquifer primarily consists of the more stable form of the mineral, fluorapatite. An increase in fluorine concentration of 0.016 mmol/kg in ground water along the flow-line segment can be explained by an exchange of hydroxide ions for fluoride in the apatite crystal lattice in the following reaction:

$$\text{Ca}_5(\text{F}_x,\text{OH}_{1-x})(\text{PO}_4)_3 + \text{OH}^{-} \rightarrow \text{Ca}_5(\text{F}_{x+1},\text{OH})(\text{PO}_4)_3 + \text{F} \quad (6)$$

This process is documented in the Cretaceous sand aquifers in South Carolina (Zack, 1980), where apatitic shark teeth have contributed high levels of fluoride to the ground water.

Gypsum Dissolution

The saturation indices for gypsum show that the ground water is subsaturated with respect to the mineral at both the initial and final points on the flow-line segment and gypsum is, therefore, thermodynamically favored to dissolve. Dissolution of gypsum would contribute both sulfur, in the form of sulfate, and calcium to the ground water, consistent with the reaction

$$\text{CaSO}_4 \leftrightarrow \text{Ca}^{++} + \text{SO}_4^{=} \quad (7)$$

An alternative explanation for the source of sulfate to the ground water is pyrite oxidation. The reaction requires an electron acceptor such as oxygen. The oxidation-reduction potential of the ground water is unknown, so the feasibility of this reaction cannot be evaluated; however, the Δ value for sulfur is not significantly different from zero, indicating that gypsum dissolution and pyrite oxidation are of minor importance to the chemical evolution of the ground water. For the purpose of the model computations, gypsum dissolution will be used to balance the small change in sulfur concentration.

Carbon Dioxide Generation

The final reaction included in the model involves the flux of carbon dioxide into the ground water:

$$\text{CO}_2(\text{aqueous}) + \text{H}_2\text{O} \rightarrow \text{H}_2\text{CO}_3 \quad (8)$$

Carbon dioxide may enter the ground-water system from the atmosphere, or it may be generated by processes in the subsurface. These processes will be discussed later in the report. At this point, the possibility of carbon dioxide input to the aquifer will be dealt with by, first, formulating a model under the assumption that no source of carbon dioxide exists. This assumption restricts the possible sources of carbon in the model to calcite dissolution. Subsequently, the possible influence of carbon dioxide input to the system will be explored.

Mass Balance

The set of eight chemical reactions hypothesized thus far is consistent with the constraints of mineral solubility. The next step is to quantify the set of reaction equations by applying mass balance calculations. Some combination of the equations, in the direction they are written, must be able to account for all changes in the chemistry of the ground water along the flow-line segment for the model to be consistent with the observations. A solution to the mass balance will result in a set of reaction coefficients that quantify the relative contribution of each reaction to the total chemical change along the flow-line segment.

A unique algebraic solution to such a mass balance problem requires that the number of proposed reaction equations be equal to the number of constituents considered in the reacting minerals and other compounds. For this model, eight reactions describing eight plausible sources and sinks have been proposed, corresponding to eight constituents. The mass balance is solved, and reaction coefficients are obtained by solving the eight equations simultaneously.

Because reactions 1 and 2 contain calcites of unknown composition, the mass balance can only be solved by substituting artificial values for these unknown compositions. The resulting reaction coefficients for equations 1

and 2 will be strictly dependent on the choice of values for the calcite compositions. These unknowns do not affect the resulting reaction coefficients of the other reactions though, so the mass balance can be solved for now using arbitrary calcite compositions for the purpose of testing the plausibility of the model. It will be shown later that the actual reaction coefficients for the calcite reactions can be estimated on the basis of mass transfer of isotopes.

The solution to the mass balance for the reactions formulated above is as follows:

Reaction coefficient (mmol/kg)	Reaction	
	Calcite dissolution	
4.9634	$Ca_{0.94}Mg_{0.06}CO_3+H^+ \rightarrow 0.94Ca^{++}+0.06Mg^{++}+HCO_3^-$	(9)
	Calcite precipitation	
5.5934	$0.97Ca^{++}+0.03Mg^{++}+HCO_3^- \rightarrow Ca_{0.97}Mg_{0.03}CO_3+H^+$	(10)
	Plagioclase feldspar incongruent dissolution	
0.4908	$Na_{0.72}Ca_{0.28}Al_{1.28}Si_{2.72}O_8+0.4744H_2O+1.2546H^+ \rightarrow 0.6271Ca_{0.0205}Al_2(Al_{0.041}Si_{3.959})O_{10}(OH)_2+0.2671 Ca^{++}+0.7200Na^++0.2373Si(OH)_4$	(11)
	Alkali feldspar incongruent dissolution	
0.0336	$K_{0.74}Na_{0.26}AlSi_3O_8+2H_2O+H^+ \rightarrow 0.500Al_2Si_4O_{10}(OH)_2 +0.7440K^++0.2589Na^++1.001Si(OH)_4$	(12)
	Cation exchange	
0.0610	$Ca\text{-clay}+2Na^+ \rightarrow Na_2\text{-clay}+Ca^{++}$	(13)
	Anion exchange on apatite	
0.0157	$Ca_5(F_z, OH_{1-z})(PO_4)_3+OH^- \rightarrow Ca_5(F_{z-1}OH_2)(PO_4)_3+F^-$	(14)
	Gypsum dissolution	
0.0380	$CaSO_4 \rightarrow Ca^{++}+SO_4^=$	(15)
	CO_2 input	
0.000	$CO_2(gas) \rightarrow CO_2(aqueous)$	(16)

The sum of these equations yields a reaction that quantitatively describes the change in chemical composition of ground water in the Upper Floridan aquifer along the flow-line segment.

The fact that a mass balance solution exists that is compatible with the hypothetical set of reactions demonstrates that the model as formulated can be considered a plausible explanation for the chemical evolution of the ground water. However, it does not necessarily imply that the model is a unique explanation of the system. The model shows that the chemical evolution of the ground water along the flow-line segment is fully explained by seven chemical reactions (assuming that carbon dioxide input is zero). The process is dominated by the dissolution and precipitation of calcite, although it must be remembered that the reaction coefficients for reactions 1 and 2 are based on arbitrary calcite compositions. The mass balance requires that relatively more calcite precipitate than dissolve, resulting in a net precipitation of calcite cements that is driven primarily by the incongruent dissolution of oligoclase. Oligoclase incongruent dissolution, in combination with the minor effects of alkali feldspar incongruent dissolution, cation exchange, and gypsum dissolution, has maintained a slight degree of supersaturation in the ground water with respect to the precipitating calcite by contributing calcium and raising the pH.

Among the initial assumptions used in the formulation of the model was that recharge to the aquifer primarily occurs near the beginning of the flow lines, and that recharge downgradient of these areas has been insignificant. Previous discussion showed that results of a ground-water flow simulation support this assumption, but it has not been conclusively shown that recharge along the flow-line segment from overlying sediments can be neglected. If recharge along the flow-line segment is significant, the composition of the ground water along the flow lines actually reflects a process of mixing between recharge water and aquifer water originating upgradient. Ground-water samples collected from recharge areas are compositionally similar to each other but differ compositionally from ground water downgradient (fig. 18). Thus, it is reasonable to assume that if significant recharge has occurred along the flow line, the recharge component of ground water, having mixed with water in the aquifer, is similar in composition to the recharge water observed upgradient. The effect of this sort of mixing on the ground-water composition would be to dilute the effect of the chemical processes occurring in the aquifer. A correction for this simple mixing process in the chemical mass balance along the flow line would require that the reaction coefficients of each of the chemical reactions be increased in the model to account for the dilution. While this adjustment would affect the specific magnitudes of the chemical reactions in the model, it causes no inconsistency in the proposed set of chemical reactions or their relative magnitudes.

Isotope Mass Transfer

The proposed model has thus far met the constraints imposed by mineral solubility and mass balance. For the model to be plausible, it must also be consistent with the mass transfer of isotopes. Carbon is a primary participant in the chemical evolution of the ground water along the flow-line segment. Therefore, the change in the $\delta^{13}C$ of the DIC in ground water between the end-points on the flow-line segment (see table 5) must be consistent with that predicted by the model. If it is assumed that isotopic changes are independent of reaction path, that is to say, they are primarily dependent on the net stoichiometry of the reactions, then the mass transfer of the isotopes can be described by mathematical relations that incorporate values

for equilibrium fractionation between the solid and aqueous phases. The derivation of these relations is presented in Wigley and others (1978).

Because at this point the model still assumes that there is no source of carbon from input of carbon dioxide, the only available source of carbon is dissolving calcite, while the only sink for carbon is calcite precipitation. Based on $\delta^{13}C$ values of -10.5 at the upgradient end and -3.3 at the downgradient end of the flow-line segment, the ratio of the carbon input rate to the carbon output rate can be calculated using the notation of Wigley and others (1978):

$$\beta R - R^* = (\beta R_0 - R^*)\frac{mC}{mC_0}^{(\beta\Gamma/1-\Gamma)} \qquad (17)$$

where β $1 + (\alpha_{ps} - 1)/\Gamma$

Γ ratio of carbon input rate to carbon output rate;

R^1 $m^{13}C/m^{12}C$ of the DIC at the downgradient end of flow-line segment;

$R_0{}^1$ $m^{13}C/m^{12}C$ of the DIC at the upgradient end of flow-line segment;

R^{*1} $m^{13}C/m^{12}C$ of the source carbon (calcite or carbon dioxide);

mC concentration of the DIC at the downgradient end of the flow-line segment, mmol/kg;

mC_0 concentration of DIC at the upgradient end of the flow-line segment, mmol/kg;

$m^{13}C$ concentration of carbon-13, mmol/kg;

$m^{12}C$ concentration of carbon-12, mmol/kg;

α_{ps} carbon-13 fractionation factor between the solution and the precipitating solid (calcite).

Values for mC_0 and mC are listed in table 5. Values for R and R_0 can be determined from $\delta^{13}C$ values in table 5. R^* can be determined from the $\delta^{13}C$ value of the dissolving calcite, which is assumed to fall within the range of $\delta^{13}C$ values measured for calcite in the aquifer ($+1.88$ to -0.95) listed in table 4. A value for α_{ps} is calculated from figure 2 and equation 22 in Wigley and others (1978) to be 1.0026. Substituting the maximum measured value of $\delta^{13}C$ of the source carbon ($+1.88$, $R^* = 1.00188$) sets a lower limit on Γ of 0.8600. The upper limit on Γ is 1.0000, since the carbon input rate must be less than the carbon output rate because a deficit of DIC (0.63 mmol/kg) occurs along the flow-line segment. These limiting values for Γ can be used to solve for a range of reaction coefficients for the calcite dissolution and precipitation reactions. This calculation will be demonstrated using a value for Γ of 0.9205, which corresponds to a value of 0.0 for the $\delta^{13}C$ of the dissolving calcite, a commonly used approximation for marine calcites and within the range of measured values in table 4.

Defining

$$Ca_XMg_{(1-X)}CO_3$$

as the amount (mmol/kg) of dissolving calcite, and

$$Ca_YMg_{(1-Y)}CO_3$$

as the amount (mmol/kg) of precipitating calcite, the mass balance on DIC can be written

$$Ca_XMg_{(1-X)}CO_3 - YCa_YMg_{(1-Y)}CO_3 = \Delta DIC \qquad (18)$$

where ΔDIC is the change in concentration of DIC in the ground water (-0.63 mmol/kg). Substituting

$$\Gamma = \frac{Ca_XMg_{(1-X)}CO_3}{Ca_YMg_{(1-Y)}CO_3} = 0.9205$$

into equation 18, the amounts of dissolving and precipitating calcite can be determined, resulting in

$$Ca_XMg_{(1-X)}CO_3 = 7.2945 \text{ mmol/kg} \qquad (19)$$

$$Ca_YMg_{(1-Y)}CO_3 = 7.9245 \text{ mmol/kg} \qquad (20)$$

These values are equivalent to reaction coefficients and replace the arbitrary coefficients determined for the calcite reactions in the mass balance.

The variables X and Y in equation 18 define the average composition of the dissolving and precipitating calcites with respect to calcium and magnesium. Values for X and Y are dependent on the reaction coefficients for dissolving and precipitating calcite, and can be calculated if the reaction coefficients are known. This is demonstrated as follows by using the reaction coefficients determined above for the case $\Gamma = 0.9205$. Consider

$$XCa_XMg_{(1-X)}CO_3 - YCa_YMg_{(1-Y)}CO_3 = \Delta Ca_c \qquad (21)$$

$$\Delta Ca_c = \Delta Ca_T - \Delta Ca_{CE} - \Delta Ca_G - \Delta Ca_{ID} \qquad (22)$$

where ΔCa_c change in concentration of calcium in the ground water due to the combined effect of calcite precipitation and calcite dissolution;

ΔCa_T total observed change in concentration of calcium in the ground water;

ΔCa_{CE} change in concentration of calcium in the ground water due to cation exchange;

ΔCa_G change in the concentration of calcium in the ground water due to gypsum dissolution;

ΔCa_{ID} change in the concentration of calcium in the ground water due to incongruent dissolution of plagioclase to clay.

By substituting reaction coefficient values from the mass balance into equations 21 and 22, a function of Y results,

$$X(7.2945) - Y(7.9245) = -0.7600 \qquad (23)$$

[1]For all forms of R,

$$R = \left(\frac{\delta^{13}C}{1000} + 1\right)Rstd$$

where $Rstd = m^{13}C/m^{12}C$ of the respective isotopic standard (PDB).

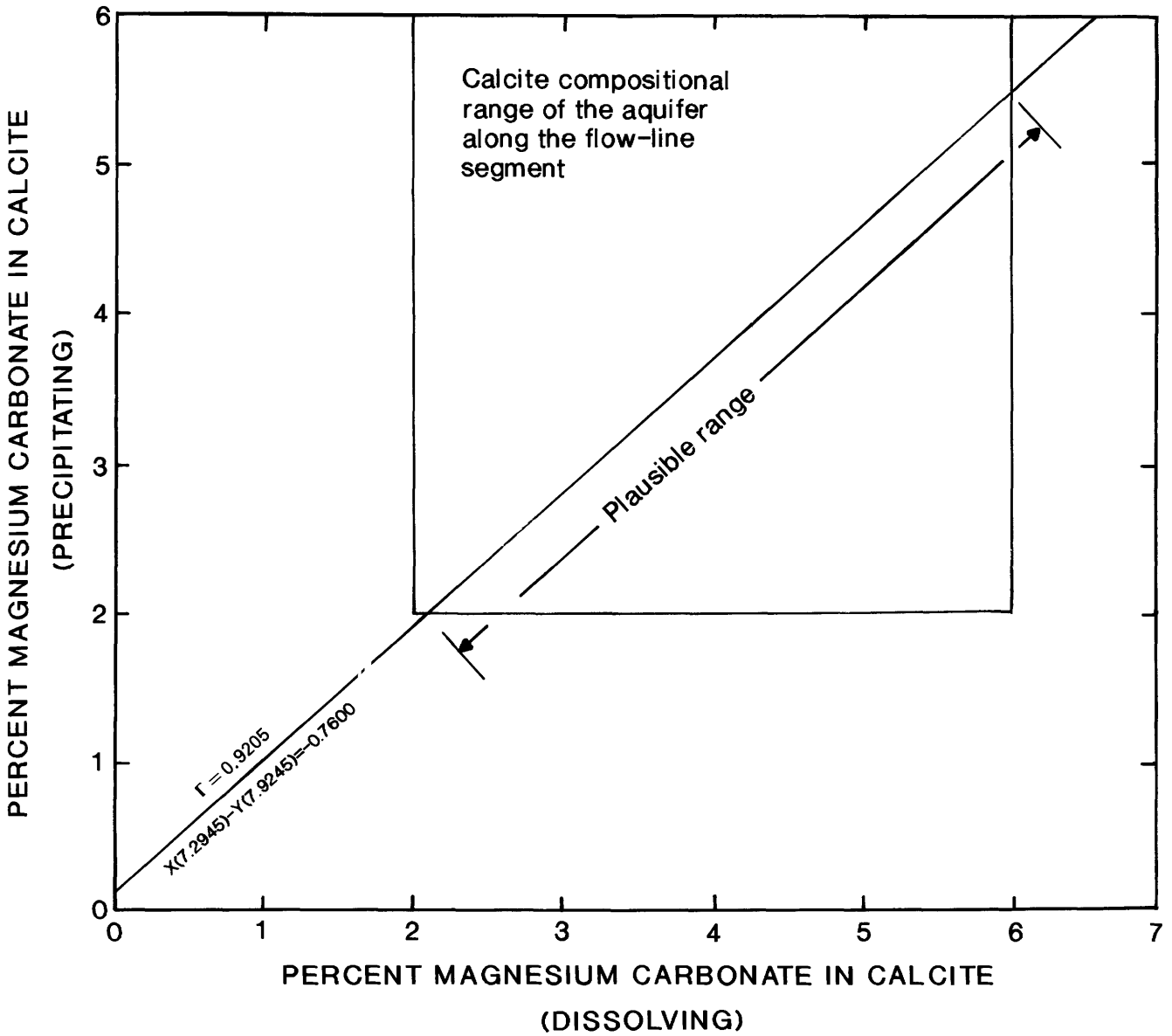

Figure 32. Plausible compositional ranges of dissolving and precipitating calcite in the low-salinity zone of the Upper Floridan aquifer based on mass balance and carbon-13 mass transfer.

such that pairs of values for X and Y can be computed, describing the possible average compositions of the dissolving and precipitating calcite. Figure 32 is a plot of the function. The possible compositions described by the function are further restricted in this aquifer to the compositions identified in mineral samples, which ranged between $Ca_{0.94}Mg_{0.06}CO_3$ and $Ca_{0.98}Mg_{0.02}CO_3$. This additional restriction is illustrated by the box outline in figure 32.

Substitution of the reaction coefficients calculated in equations 19 and 20 into the mass balance solution yields the following plausible model of the chemical evolution of the ground water along the flow-line segment:

Reaction coefficient (mmol/kg)	Reaction	
	Calcite dissolution	
7.2945	$Ca_XMg_{(1-X)}CO_3+H^+ \rightarrow XCa^{++}+_{(1-X)}Mg^{++}+HCO_3^-$	(24)
	Calcite precipitation	
7.9245	$YCa^{++}+(1-Y)Mg^{++}+HCO_3^- \rightarrow Ca_YMg_{(1-Y)}CO_3+H^+ \rightarrow$	(25)
	Plagioclase feldspar incongruent dissolution	
0.4908	$Na_{0.72}Ca_{0.28}Al_{1.28}Si_{2.72}O_8+0.4744\ H_2O+1.2546H^+ \rightarrow$ $0.6271\ Ca_{0.0205}Al_2(Al_{0.041}Si_{3.959})O_{10}(OH)_2+0.2671$ $Ca^{++}+0.7200Na^++0.2373Si(OH)_4$	(26)

Reaction coefficient (mmol/kg)	Reaction	
	Alkali feldspar incongruent dissolution	
0.0336	$K_{0.74}Na_{0.26}AlSi_3O_8+2H_2O+H^+ \rightarrow 0.500Al_2Si_4O_{10}(OH)_2$ $+0.7440K^+ +0.2589Na^+ +1.001Si(OH)_4$	(27)
	Cation exchange	
0.0610	$Ca\text{-clay} +2Na^{++} \rightarrow Na_2\text{-clay}+Ca^{++}$	(28)
	Anion exchange on apatite	
0.0157	$Ca_5(F_z, OH_{1-z})(PO_4)_3+OH^- \rightarrow Ca_5(F_{z-1}OH_2)(PO_4)_3+F^-$	(29)
	Gypsum dissolution	
0.0380	$CaSO_4 \rightarrow Ca^{++}+SO_4^=$	(30)
	CO_2 input	
0.000	$CO_2(gas) \rightarrow CO_2(aqueous)$	(31)

The reaction coefficients have not changed from those calculated in the mass balance solution except for calcite dissolution and calcite precipitation. This model is consistent with mineral solubility, mass balance, and isotope mass transfer of carbon-13. However, this model is based on an assumed average $\delta^{13}C$ value of 0.0 for the dissolving calcite, which resulted in a value of 0.9205 for Γ. As indicated earlier, the actual value of Γ may range between 0.8600 and 1.0000 based on the range of $\delta^{13}C$ measured from calcite in the aquifer and mass balance on DIC. Reaction coefficients for dissolving and precipitating calcite are calculated to be 3.8700 and 4.2042, respectively, corresponding to a value for Γ of 0.8600. They approach infinity as Γ approaches 1.0000. Extremely high reaction coefficients for dissolving and precipitating calcites are unlikely, but even at the lower limit for these values, it is still evident that the model is dominated by the dissolution and precipitation of calcite.

A model, which incorporates seven chemical reactions between ground water and minerals, has now been formulated, providing a plausible explanation of the chemical evolution of the ground water along the flow-line segment. The model is shown to be consistent with mineral solubility, mass balance, and carbon isotope mass transfer.

Carbon Dioxide Input

Thus far the assumption was made that calcite constituted the only source of carbon even though dissolved carbon dioxide to the aquifer may also contribute significantly to the DIC in the ground water. At this point the possible effects of carbon dioxide input to the aquifer will be considered.

The carbon dioxide in ground water may originate from different sources. Atmospheric carbon dioxide gas may dissolve in surface water or rain before infiltration. Carbon dioxide may also be derived from plant respiration in the root zone or by oxidation of reduced carbon during decomposition of organic compounds in the sediments that constitute the aquifer and overlying beds. Atmospheric carbon dioxide ($P_{CO_2}=10^{-3.5}$) generally contributes only a small amount of the dissolved carbon dioxide in ground water. Respiration and organic decomposition in the soil or root zone can contribute large amounts ($P_{CO_2}=10^{-1.0}$) of dissolved carbon dioxide to shallow ground water (Fontes, 1980). The degree of carbon dioxide contribution that occurs deeper in the subsurface is not well known.

Oxidative decomposition of organic matter, resulting in carbon dioxide as a product, requires oxidation of the organic carbon by some electron acceptor. A number of dissolved constituents, among them oxygen, sulfate, nitrate, and nitrite, can act as electron acceptors in the process of oxidation of organic carbon. It can be shown, as follows, that the plausible influence of these types of reactions along the flow line is limited by the mass transfer of carbon-13 to less than about 22 percent of the total carbon input.

The carbon dioxide in soils and associated with the oxidation of organic matter generally has $\delta^{13}C$ values similar to that of the bulk organic matter in the sediments ($\sim -23.0‰$) (Fontes, 1980). Recent evidence shows, however, that the $\delta^{13}C$ of various components of the bulk organic matter varies significantly (Spiker and Hatcher, 1984) and that the carbon dioxide products of organic matter decomposition may have $\delta^{13}C$ values as high as $-10‰$ (F.H. Chapelle and P.B. McMahon, U.S. Geological Survey, written commun., 1987). To investigate the plausible influence of carbon dioxide input on the proposed chemical reaction model, it was necessary to consider this full range of possible carbon-13 input. Using equation 17, along with the measured values for mC, mC_0, R, and R_0, possible values for the $\delta^{13}C$ of the total source carbon (carbon dioxide plus dissolved calcite) can be calculated for a range of values of Γ. Based on these calculated values of source carbon $\delta^{13}C$, the input of carbon dioxide relative to the total carbon input along the flow line can be calculated for any assumed $\delta^{13}C$ values for carbon dioxide and calcite according to

$$a\delta^{13}C_{CO_2}+b\delta^{13}C_{calcite}=\delta^{13}C_{total\ input} \quad (32)$$

where $\delta^{13}C_{CO_2}$ average $\delta^{13}C$ value assumed for carbon input from carbon dioxide contribution;

$\delta^{13}C_{calcite}$ average $\delta^{13}C$ value for carbon input from calcite dissolution;

$\delta^{13}C_{total\ input}$ average $\delta^{13}C$ value calculated for the total source carbon;

a percentage input of carbon dioxide relative to the total carbon input;

b percentage input of carbon from calcite dissolution relative to the total carbon input.

A plot of the percent input of carbon dioxide with respect to Γ for assumed $\delta^{13}C_{CO_2}$ values of $-23.0‰$ and $-10.0‰$ is shown in figure 33. The $\delta^{13}C$ of dissolving

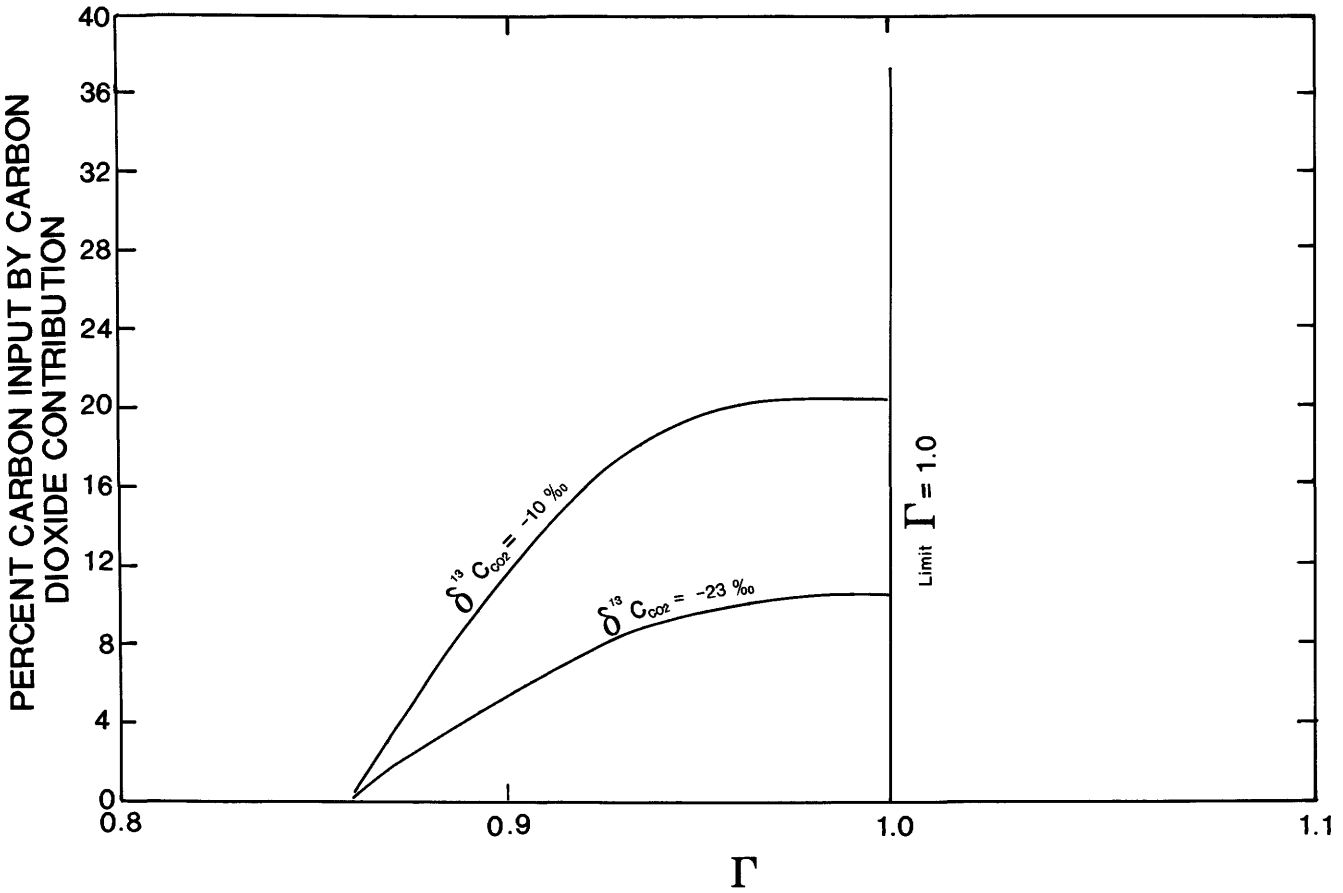

Figure 33. Plausible input of carbon dioxide ($\delta^{13}C_{CO_2}$ = −23.0‰ and −10.0‰) as a function of Γ, expressed as a percentage of total inorganic carbon input, and calculated using the maximum $\delta^{13}C$ value measured for calcite in the aquifer (+1.88).

calcite used for the calculations was +1.88, the maximum value measured for calcite in the aquifer, resulting in a conservative estimate of carbon input from dissolving calcite, and therefore a maximum estimate of carbon dioxide input. A limit on the plotted functions is approached where Γ=1.000 because the mass balance on carbon requires that the total output of carbon exceed the total input of carbon by 0.63 mmol/kg. The plots in figure 33 illustrate that for the expected range of $\delta^{13}C$ values for carbon dioxide, the contribution of carbon dioxide relative to the total input of carbon is limited to less than about 22 percent.

Another process of organic carbon decomposition, methanogenesis, may be of some importance in this geochemical system. Consistent with the observed carbon isotopic evolution along the flow-line segment, this mechanism produces carbon dioxide and methane, and the methanogenic carbon dioxide is typically characterized by very high $\delta^{13}C$ values.

Methanogenesis is known to occur under anaerobic conditions in sediments. The likelihood of methanogenic activity in freshwater aquifers has been argued by Chapelle and Knobel (1985), citing carbon isotope evidence.

The current literature cites two types of biogenic processes as primarily responsible for methanogenesis: (1) fermentation of acetate or other compounds capable of transferring methyl groups, and (2) reduction of carbon dioxide. Of the two processes, acetate fermentation is probably the source of about 70 percent of methane formation in freshwater environments (Whiticar and others, 1986). In this process, methane is derived from the methyl group of acetate or a similar compound according to the following reaction:

$$C^*H_3COOH \rightarrow C^*H_4 + CO_2 \qquad (33)$$

This contrasts with the second process, in which carbon dioxide is reduced using hydrogen as an electron acceptor, and both the carbon dioxide and hydrogen are derived from organic molecules, as in the following reactions (Claypool and Kaplan, 1974):

$$2CH_2O+2H_2O\rightarrow 2CO_2+4H_2$$
$$CO_2+H_2O\rightarrow HCO_3^-+H^+$$
$$4H_2+HCO_3^-+H^+\rightarrow CH_4+3H_2O \quad (34)$$

Net reaction $2CH_2O\rightarrow CH_4+CO_2$

The isotope fractionation effects that occur during these processes are not completely understood. A review by Whiticar and others (1986) of studies comparing measured carbon isotope data for carbon dioxide–methane pairs in sediments with calculated thermodynamic equilibrium values indicates that freshwater systems tend to deviate from thermodynamic equilibrium. They suggest that measured carbon isotope values reflect the kinetic fractionation effects of the metabolic processes, which occur significantly faster than thermodynamic exchange equilibria can be reached. They also show that the degree of carbon isotope fractionation differs for the two processes of acetate fermentation and carbon dioxide reduction.

Contribution of methanogenic carbon dioxide to the ground water is a possible mechanism for the increase in the $\delta^{13}C$ of dissolved carbonate species along the flow-line segment. Unfortunately, uncertainties concerning the carbon-13 content of methanogenic carbon dioxide preclude the application of carbon-13 mass transfer calculations with the available data. However, consideration of the mass balance of magnesium and carbon constrains the contribution of methanogenic carbon dioxide to a maximum of about 67 percent of the total carbon input to the system, as shown in the following. In the absence of any magnesium source other than dissolving calcite, the amount of dissolving calcite relative to total carbon input is a function of δMg_T, the compositions of the dissolving and precipitating calcites, Γ, and the total input of carbonate species to the ground water according to

$$(Ca_XMg_{(1-X)}CO_3)(1-X)-(Ca_YMg_{(1-Y)}CO_3)(1-Y) = \Delta Mg_T \quad (35)$$

Substitution of

$$\Gamma=\frac{I}{(Ca_YMg_{(1-Y)}CO_3)} \quad (36)$$

yields

$$(Ca_XMg_{(1-X)}CO_3)(1-X)- I/\Gamma(1-Y)=\Delta Mg_T$$

where

$(Ca_XMg_{(1-X)}CO_3)$ amount of dissolving calcite;
$(Ca_YMg_{(1-Y)}CO_3)$ amount of precipitating calcite;
I total input of carbon;
ΔMg_T total observed change in concentration of magnesium in the ground water.

The plot in figure 34 was calculated from equation 36 using a value of 1.0 for Γ (maximum limit on Γ, since the mass balance on carbon requires that the amount of output carbon exceed the amount of input carbon), and dissolving and precipitating calcite compositions of $Ca_{0.94}Mg_{0.06}CO_3$ and $Ca_{0.98}Mg_{0.02}CO_3$, respectively. These calcite compositions represent the largest compositional deviation observed along the flow-line segment and, therefore, result in the maximum possible input of magnesium with respect to the amount of calcite dissolved. The calculation is, therefore, conservative with respect to carbon input by calcite dissolution and indicates the maximum expected methanogenic carbon dioxide input. The plot shows the possible values for percentages of carbon input due to methanogenic carbon dioxide with respect to total carbon input, and indicates that high percentage input of methanogenic carbon dioxide requires high values of total carbon input. The maximum methanogenic carbon dioxide input is limited to about 67 percent due to the asymptotic nature of the function.

It has been shown that the plausible sources of carbon input into the ground water along the flow line cannot necessarily be restricted to calcite dissolution, as was assumed in the initial flow-line model. Dissolved carbon dioxide may also have contributed to the total carbon input. However, although the possibility of carbon dioxide contribution cannot be eliminated, the maximum limit of these contributions was established from the mass balance of magnesium and mass transfer of carbon-13. Nonmethanogenic carbon dioxide could not contribute more than about 22 percent of the total carbon input, while methanogenic carbon dioxide is limited to less than 67 percent. While carbon dioxide contributions of this magnitude would result in substantial changes in the reaction coefficients determined from the mass balance calculations presented earlier, the proposed list of chemical reactions used in the model would not change. Due to the carbon dioxide input, proportionately less dissolution of calcite would be required as a source of carbon. However, as indicated in figure 34, the total carbon input must increase as the carbon dioxide input increases, resulting in an increase in actual calcite dissolution. In response to the increase in calcite dissolution, calcite precipitation must also increase to maintain the magnesium and carbon mass balances. The precipitation of calcite must be driven by increasing pH and calcium contribution from incongruent dissolution of oligoclase and alkali feldspar, cation exchange, and gypsum dissolution.

Mixing Zone

Ground-Water Chemistry

The ground water in the Upper Floridan aquifer near the coast, being characterized by variable, elevated concentrations of chloride (fig. 16), has a different chemical composition than that in the inland parts of the aquifer. Chloride concentrations generally increase in a northeast-

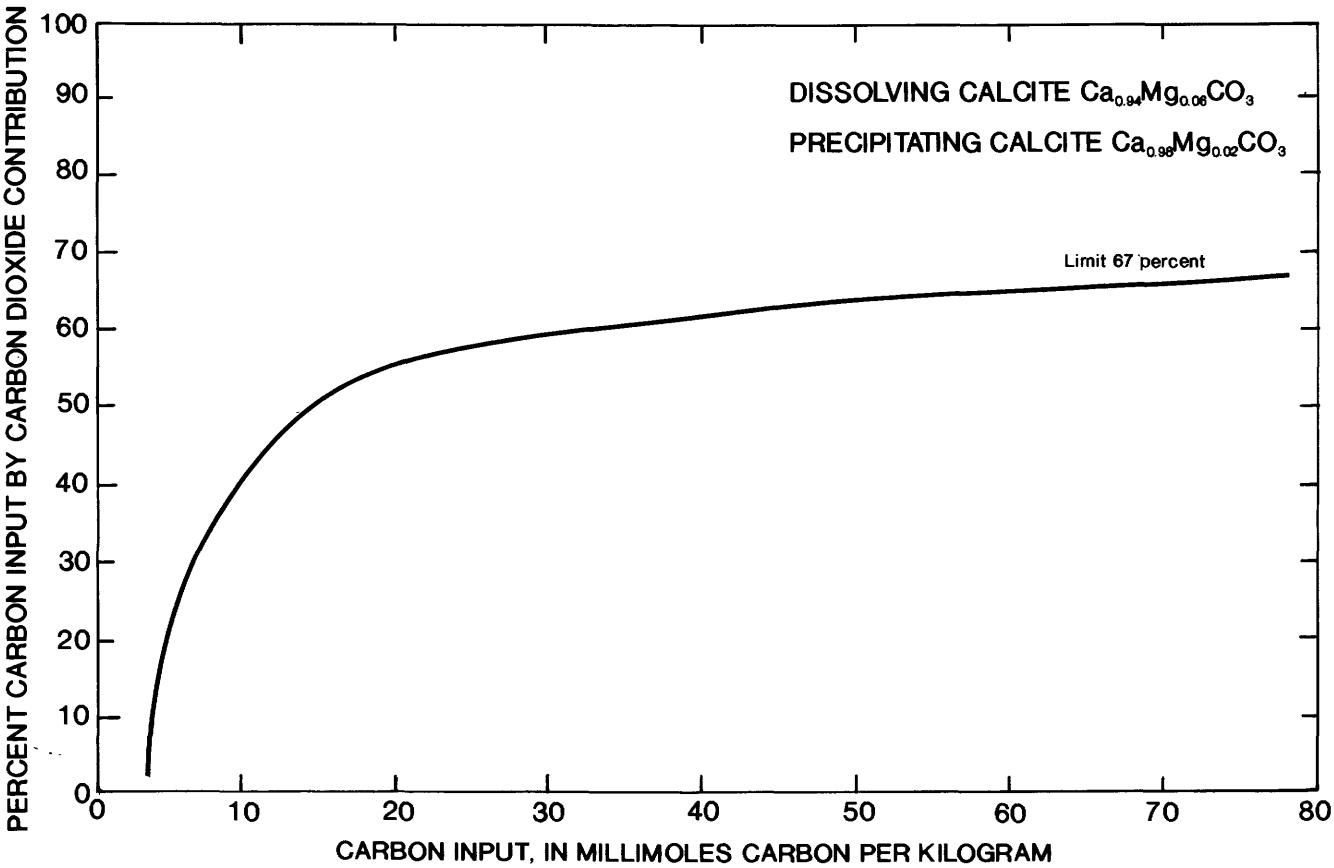

Figure 34. Plausible input of methanogenic carbon dioxide expressed as a percentage of total inorganic carbon input.

erly direction across the area, ranging as high as 430 mmol/kg in the areas of Parris Island and north of Port Royal Sound. The variation in chloride concentration is indicative of seawater, containing 566 mmol/kg of chloride, mixing with low-salinity ground water. For the purposes of this study, the part of the aquifer where this process occurs will be designated the mixing zone and will be delineated by chloride concentrations greater than 0.20 mmol/kg.

Models

This section discusses the formulation of a conceptual model that describes the chemical processes that have affected the ground-water evolution and diagenesis of sediments in the mixing zone of the Upper Floridan aquifer. The data for this study show that the ground-water composition is not the result of a conservative mixing process but rather a combination of mixing and chemical processes in the aquifer or in the sediments through which the aquifer is recharged. The chemical processes include reactions between the ground water, its dissolved constituents, minerals in the aquifer, and other compounds, such as carbon dioxide, derived from organic processes. Conservative mixing models were first used to identify conservative and nonconservative chemical behavior. Subsequently, plausible chemical reactions were hypothesized to formulate a conceptual geochemical reaction model, which was evaluated and modified to meet the constraints of mineral saturation and mass balance calculations while explaining the deviation of sample compositions from compositions expected from conservative mixing. The conceptual model indicates that ground-water composition in the mixing zone can be plausibly explained by a combination of processes, including equilibration with carbonate minerals, input of dissolved carbon dioxide to the ground water, and several other mineral/ground-water reactions. In general, these processes might be expected to influence diagenesis of the carbonate aquifer by causing either a net dissolution or net precipitation of the carbonate minerals, depending on the relative magnitudes of the processes. Mass balance calculations for each of 10 samples show that in the mixing zone investigated here, diagenesis has been dominated by net dissolution of carbonate minerals.

Conservative Mixing

Within the mixing zone, should simple mixing of seawater with low-salinity ground water be the dominant process, independent of any chemical reactions or additional input, the concentrations of all the dissolved

Table 6. Chemical analysis of Nordstrom's

	Degrees Celsius	pH	Concentration (millimoles/kilogram)					
			Calcium	Magnesium	Sodium	Potassium	Aluminum	Barium
Nordstrom's seawater[1]	25.0	8.22	10.7	55.1	485	10.6	0.000077	0.00015
Port Royal Sound average.[2]	—	7.95	9.2	42.5	387	9.6	—	—

[1] Analysis is from Nordstrom and others (1979).

[2] Values represent the means of measurements made in 1970 (South Carolina Water Resources Commission, 1972) at water quality station 1, located off the north end of Hilton Head Island.

constituents would be proportional to the degree of mixing. Stated another way, the constituents would exhibit conservative behavior. Chloride can generally be considered a conservative constituent in environments such as the Upper Floridan aquifer, where chloride minerals are absent. Therefore, conservative mixing models can be formulated using chloride to indicate the degree of mixing between seawater and low-salinity ground water. The hypothesis of conservative mixing for the other constituents can be tested by comparing the measured concentrations with those predicted by the models.

Seawater

The models formulated in this study assume that the high-salinity component of water in the mixing zone can be approximated by the chemical composition of surface seawater as reported by Nordstrom and others (1979). The analyses are presented in table 6. Several constituents of seawater, such as calcium, magnesium, sodium, potassium, chloride, sulfate, fluoride, and bromide, are essentially conservative elements in the open ocean. Nordstrom's seawater analysis, therefore, can be assumed to represent the concentrations of these constituents, relative to chloride, for the seawater that has entered the aquifer. Other constituents may vary considerably throughout the oceans, due primarily to biological activity, and for these, Nordstrom's data may not reflect the composition of seawater that has entered the Floridan aquifer. The similarity of Nordstrom's analysis to local seawater was checked for most of the constituents by comparison with the average composition of surface samples collected from Port Royal Sound (South Carolina Water Resources Commission, 1972) (table 6). All concentrations of constituents in the average Port Royal Sound water are somewhat lower than those in Nordstrom's analysis, indicative of some dilution of the seawater in the sound. A comparison of the constituent to chloride ratios indicates that, with the exception of silica, the relative concentrations of the constituents are very comparable between the two sets of analyses. It will be shown that the variations that do exist do not affect the conclusions drawn in this study.

Low-Salinity Ground Water

The compositional variability within the study area of low-salinity ground water in the Upper Floridan aquifer was described previously. The chemical analyses of ground-water samples from the low-salinity region of the aquifer show that the compositions generally vary with distance along flow paths. Prior to significant pumping from the aquifer, the ground-water flow configuration for the study area (fig. 13) was such that low-salinity ground water of varying composition converged on the mixing zone. This effect was combined with the probability of local recharge. It is evident that the low-salinity component of the conservative mixing model cannot be represented by a single analysis, but rather must consist of a sequence of compositions that satisfactorily encompasses the ranges of individual constituent concentrations in the low-salinity ground water.

Testing for Conservative Behavior

Concentrations of several ground-water constituents measured in samples from within and immediately surrounding the mixing zone, namely, bromide, calcium, DIC, pH, magnesium, sodium, potassium, sulfate, silica, fluoride, sulfide, ammonia, and phosphate, are plotted with respect to the concentration of chloride in each sample (figs. 35–47). Where available, the confidence intervals (± 1.0 standard deviation) for the constituent analyses are indicated by error bars. The plotting fields have been divided into two parts to distinguish samples representing low-salinity ground water from those collected in the mixing zone.

Superimposed on the plots of figures 35–47 are curves representing the boundaries of the conservative mixing models. Seawater constituent concentrations (Nordstrom and others, 1979) representing the high-salinity component of the model are plotted in the upper right.

seawater sample and Port Royal Sound water

Concentrations (millimoles/kilogram)									
Strontium	Silica	Choride	Total inorganic carbon	Sulfate	Nitrate	Ammonium	Phosphate	Fluoride	Bromide
0.096	0.074	566	2.13	29.3	0.0048	0.0017	0.00065	0.076	0.87
—	0.006	509	2.01	23.5	—	0.0027	0.00043	—	—

When available, average concentrations of constituents in seawater from Port Royal Sound have been plotted as a comparison with Nordstrom's data. The low-salinity end of the model was constructed for each constituent on the basis of the concentration range of that constituent in the low-salinity samples. The low-salinity samples used to establish these ranges were from wells BFT–124, BFT–121, BFT–136, BFT–1689, and BFT–206. Samples from wells BFT–124 and BFT–121 were collected from an area of known aquifer recharge indicated by the potentiometric high near Beaufort in figure 13, and represent the younger, locally recharged component of low-salinity water. Low-salinity samples from wells BFT–136, BFT–1689, and BFT–206 were collected from points in the aquifer near the ends of long flow paths extending from inland recharge areas, and represent the older, distantly recharged, low-salinity ground water. The boundaries of the conservative mixing model constitute a mixing envelope. Analyses that plot outside of the envelope exhibit nonconservative behavior. Sample analyses that plot within the envelope may or may not exhibit conservative behavior, but nonconservative behavior cannot be proven.

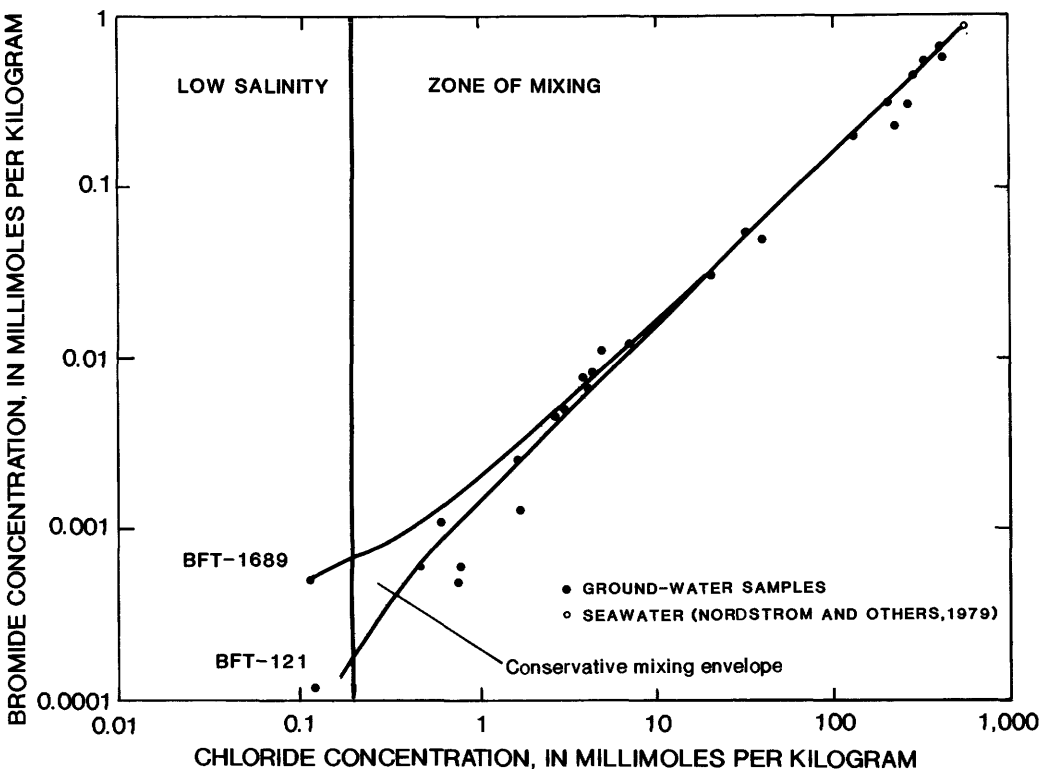

Figure 35. Bromide to chloride relation in the mixing zone compared to the conservative mixing model.

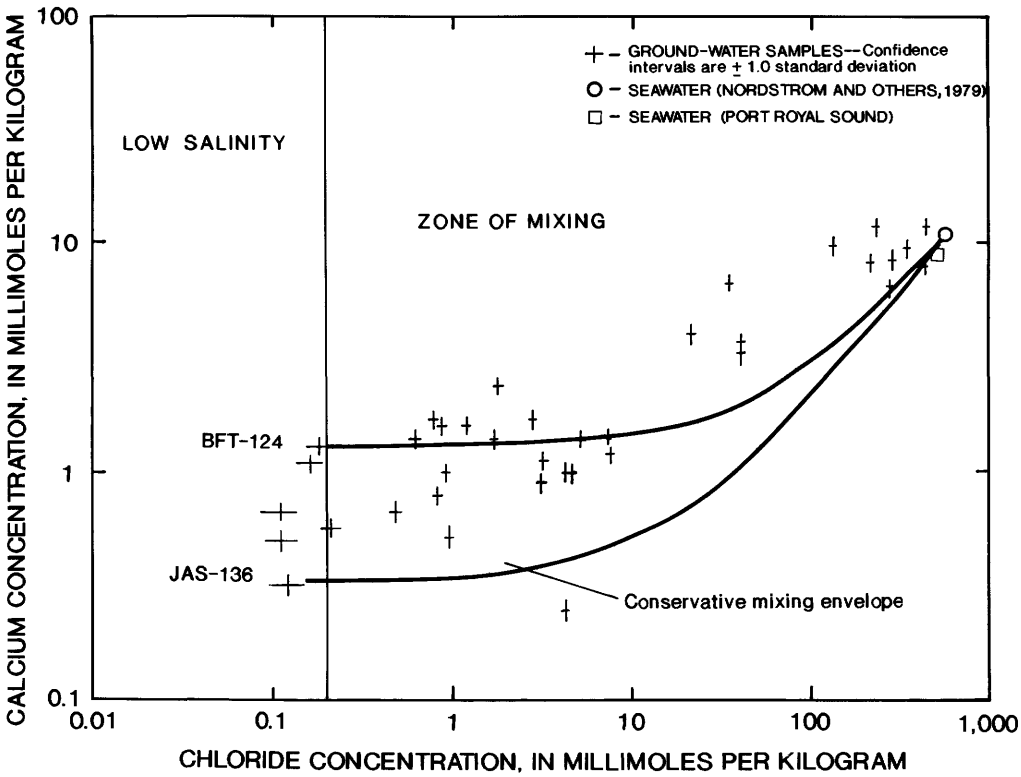

Figure 36. Calcium to chloride relation in the mixing zone compared to the conservative mixing model. (The analytical precision is indicated as ±1.0 standard deviation.)

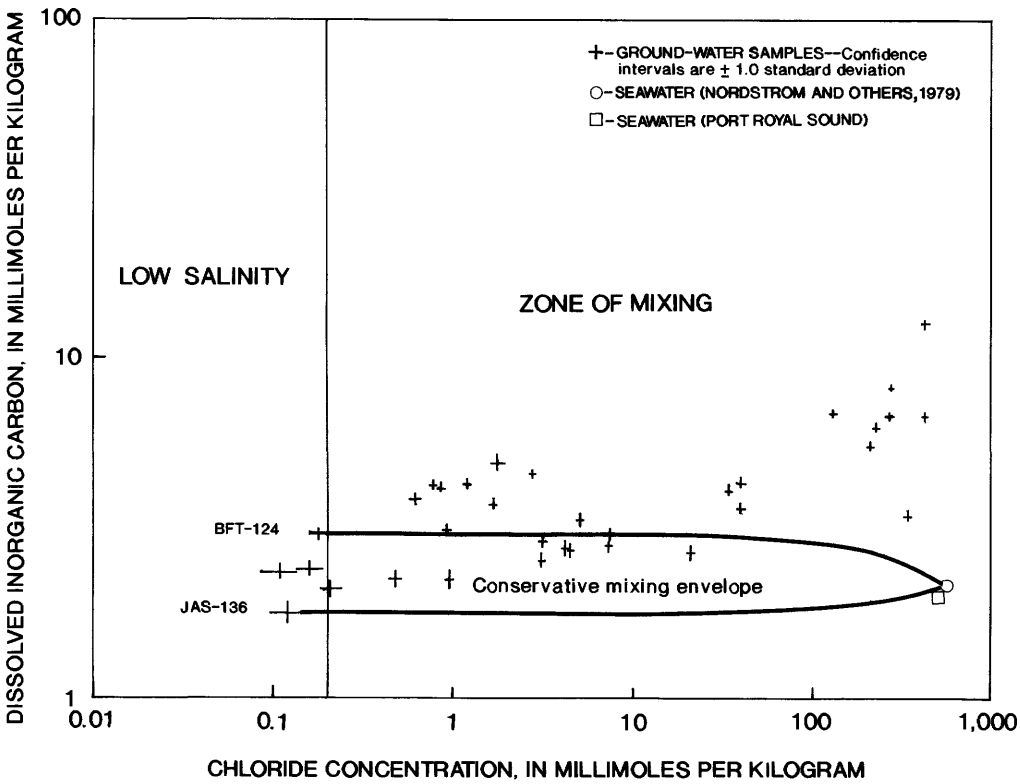

Figure 37. Dissolved inorganic carbon to chloride relation in the mixing zone compared to the conservative mixing model. (The analytical precision is indicated as ±1.0 standard deviation.)

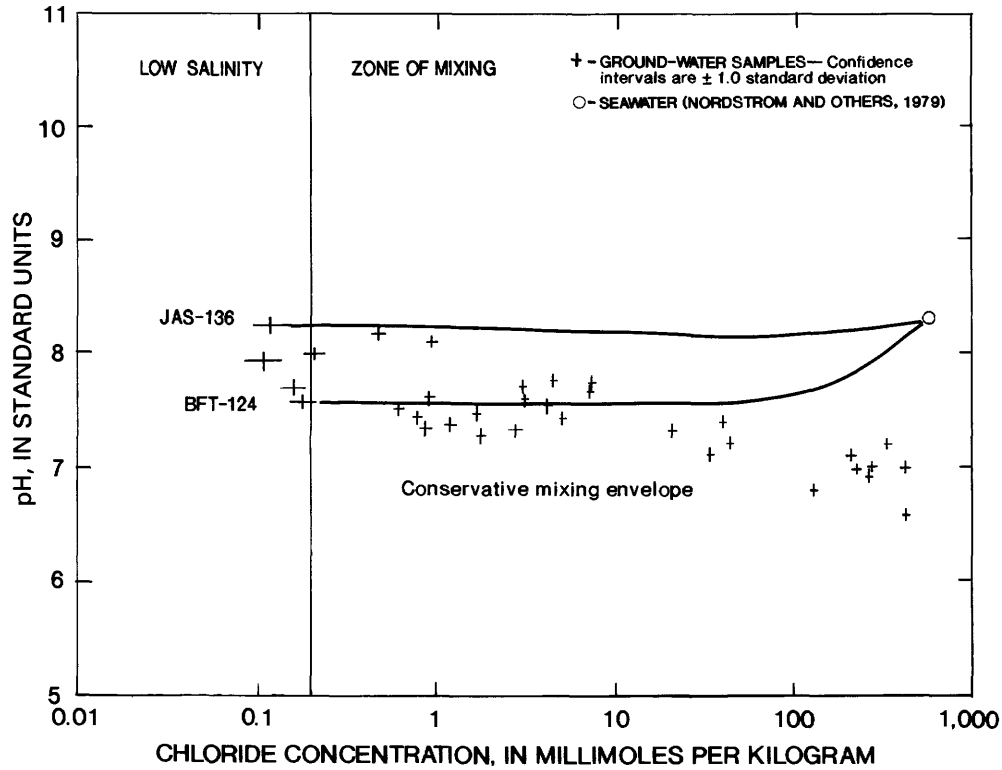

Figure 38. The pH to chloride relation in the mixing zone compared to the conservative mixing model. (The analytical precision is indicated as ±1.0 standard deviation.)

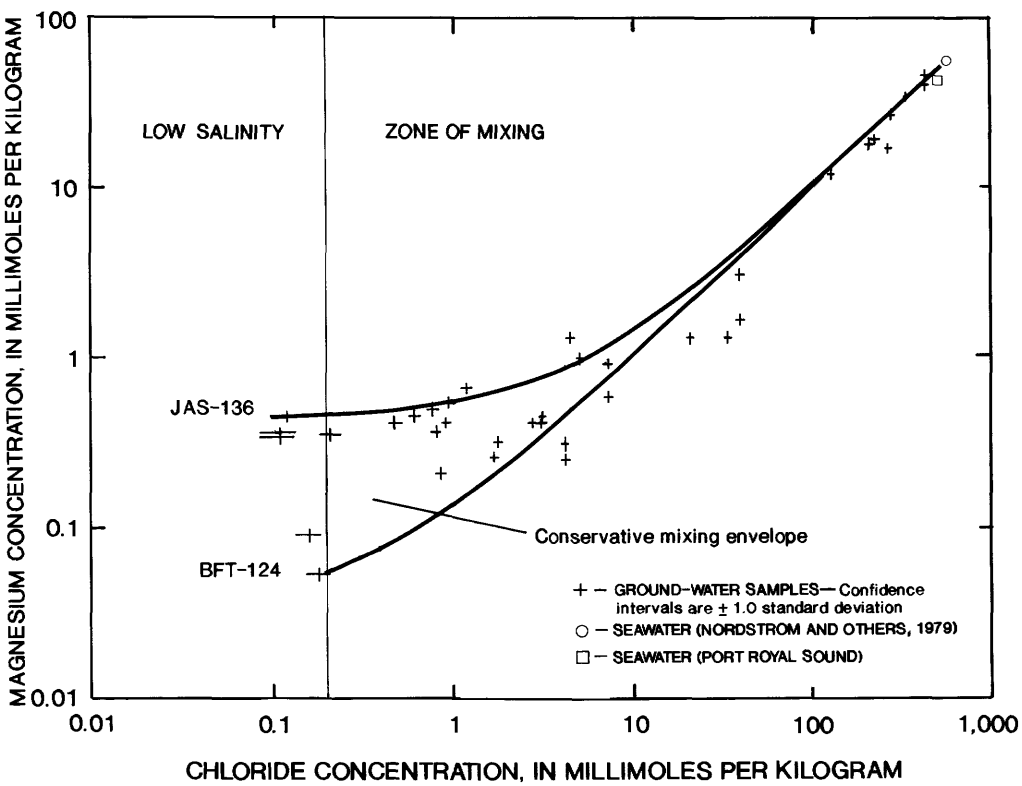

Figure 39. Magnesium to chloride relation in the mixing zone compared to the conservative mixing model. (The analytical precision is indicated as ±1.0 standard deviation.)

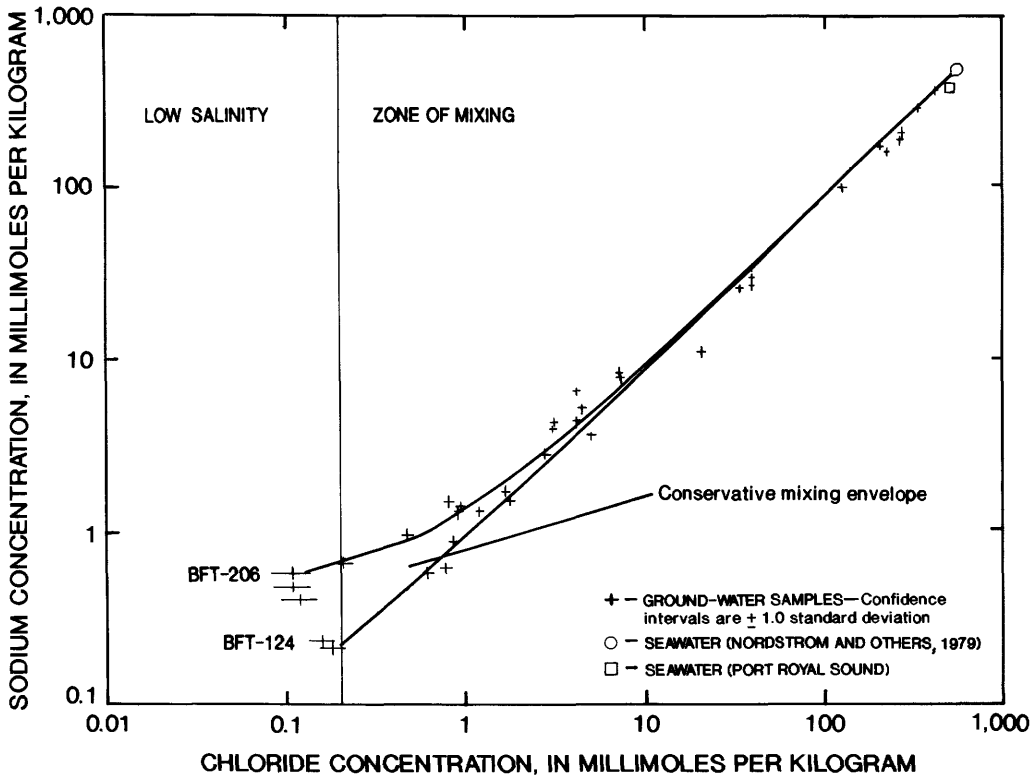

Figure 40. Sodium to chloride relation in the mixing zone compared to the conservative mixing model. (The analytical precision is indicated as ±1.0 standard deviation.)

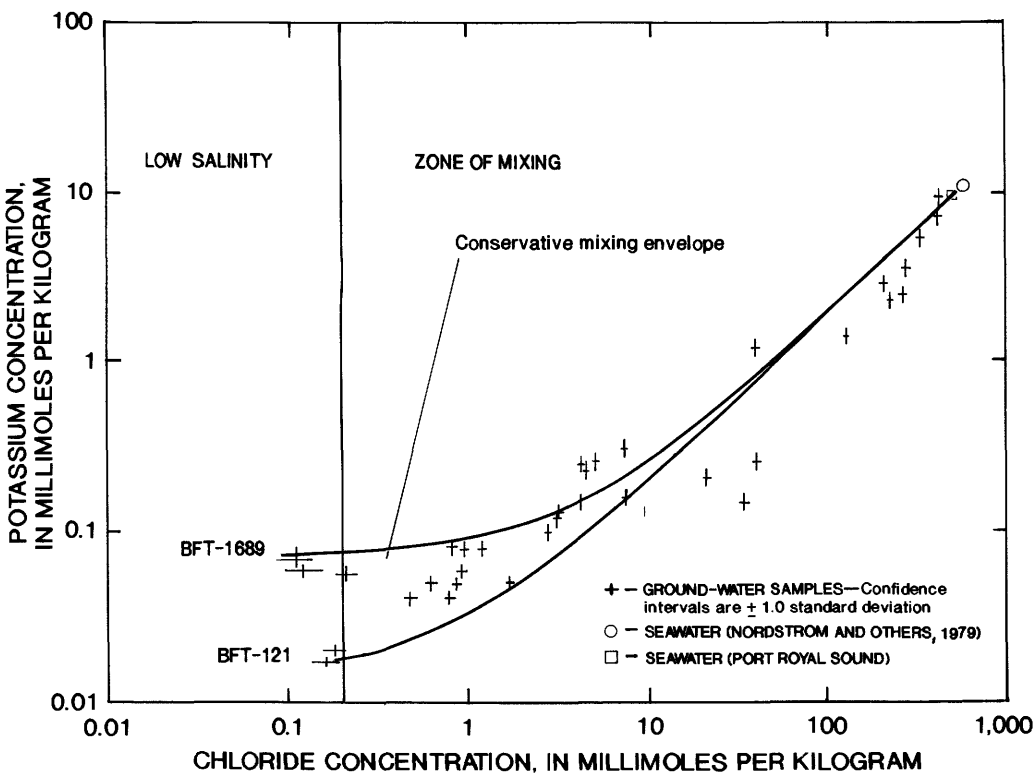

Figure 41. Potassium to chloride relation in the mixing zone compared to the conservative mixing model. (The analytical precision is indicated as ±1.0 standard deviation.)

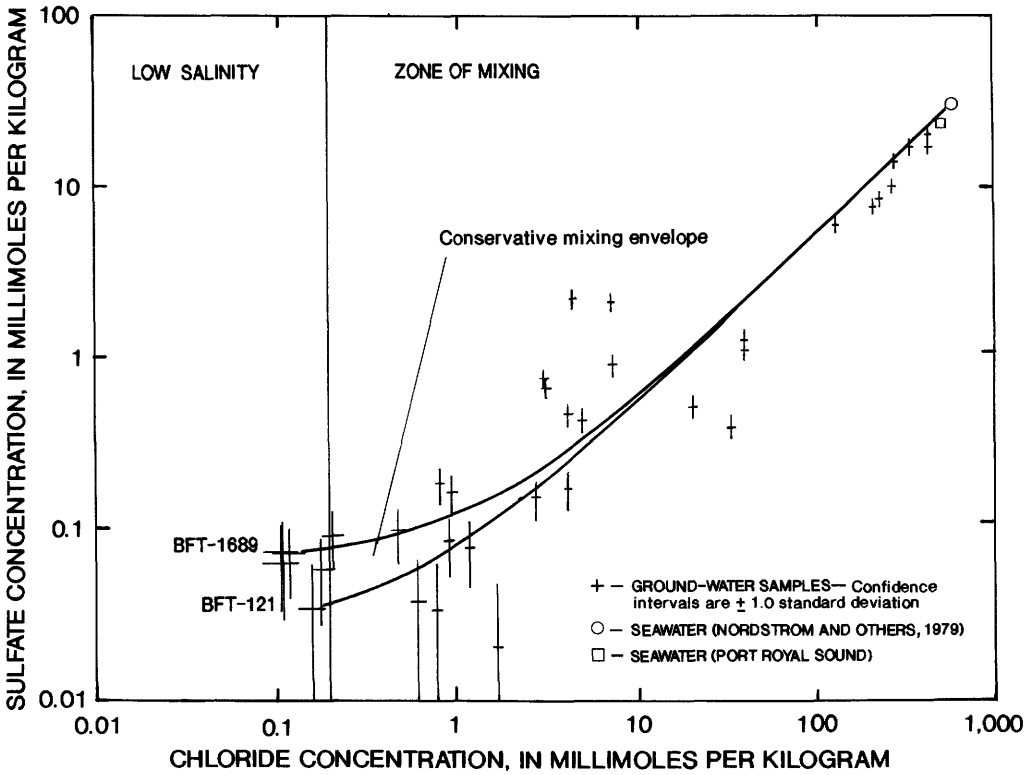

Figure 42. Sulfate to chloride relation in the mixing zone compared to the conservative mixing model. (The analytical precision is indicated as ±1.0 standard deviation.)

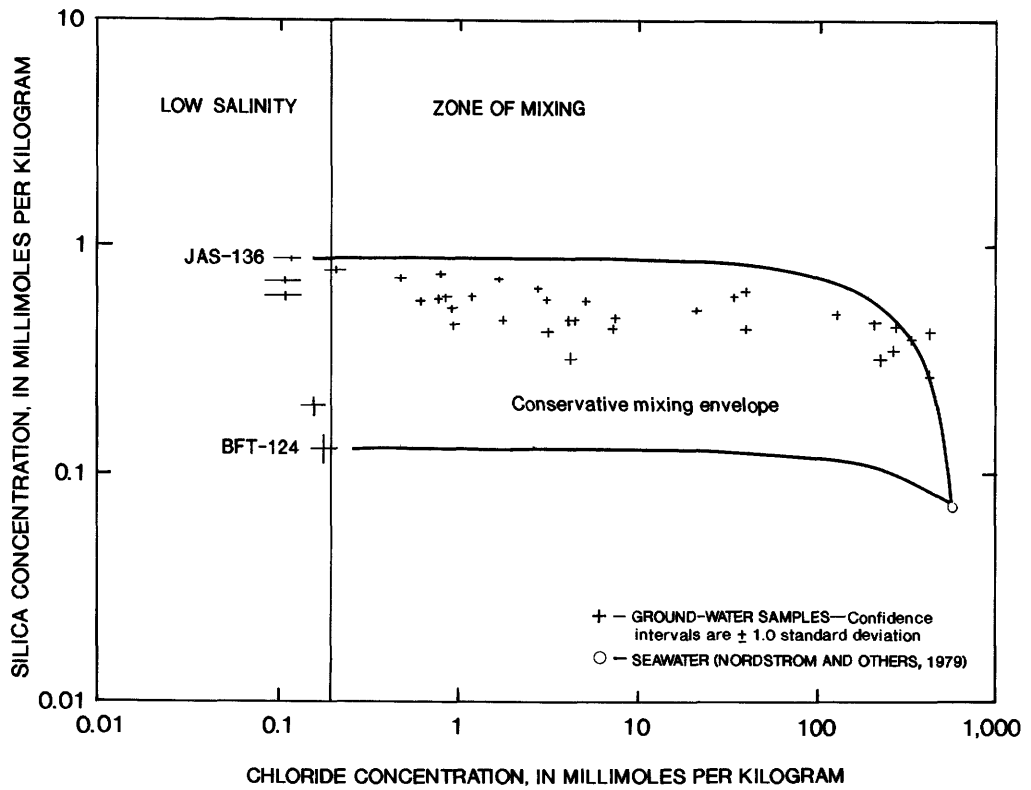

Figure 43. Silica to chloride relation in the mixing zone compared to the conservative mixing model. (The analytical precision is indicated as ±1.0 standard deviation.)

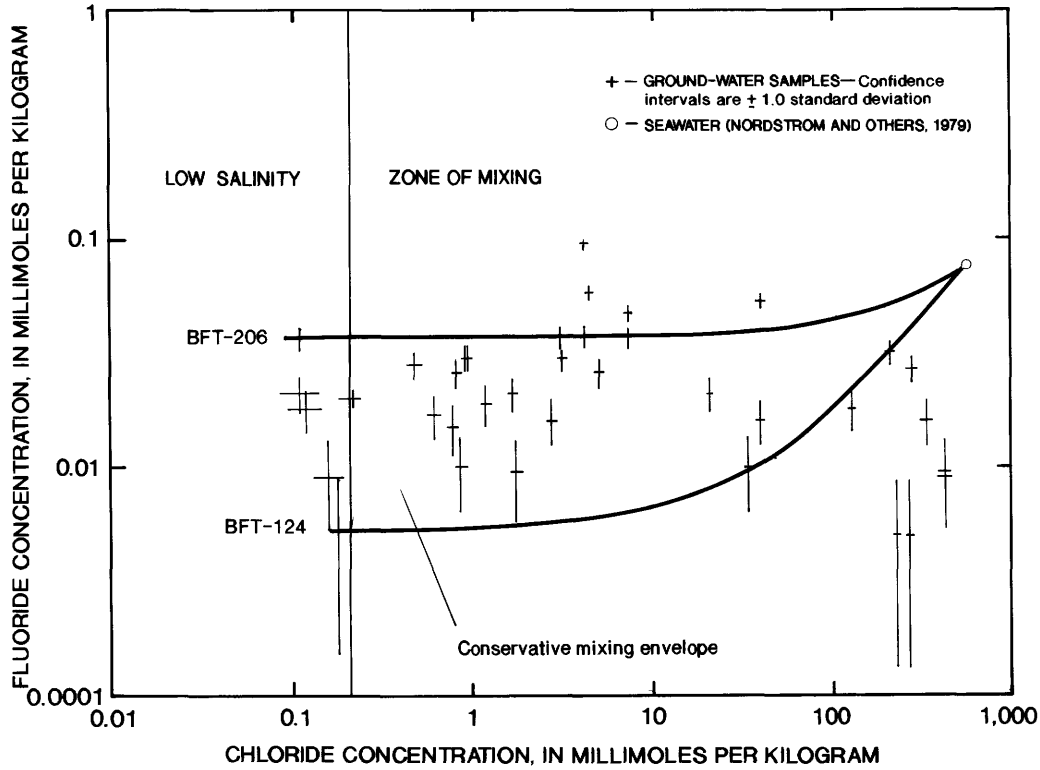

Figure 44. Fluoride to chloride relation in the mixing zone compared to the conservative mixing model. (The analytical precision is indicated as ±1.0 standard deviation.)

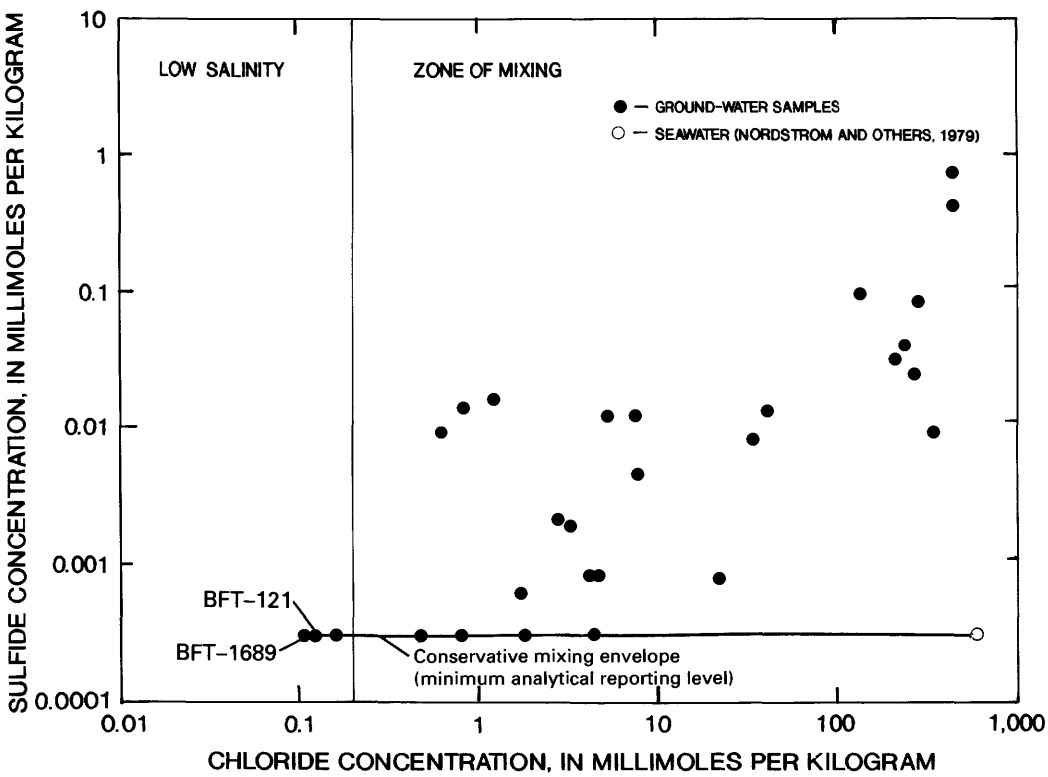

Figure 45. Sulfide to chloride relation in the mixing zone compared to the conservative mixing model.

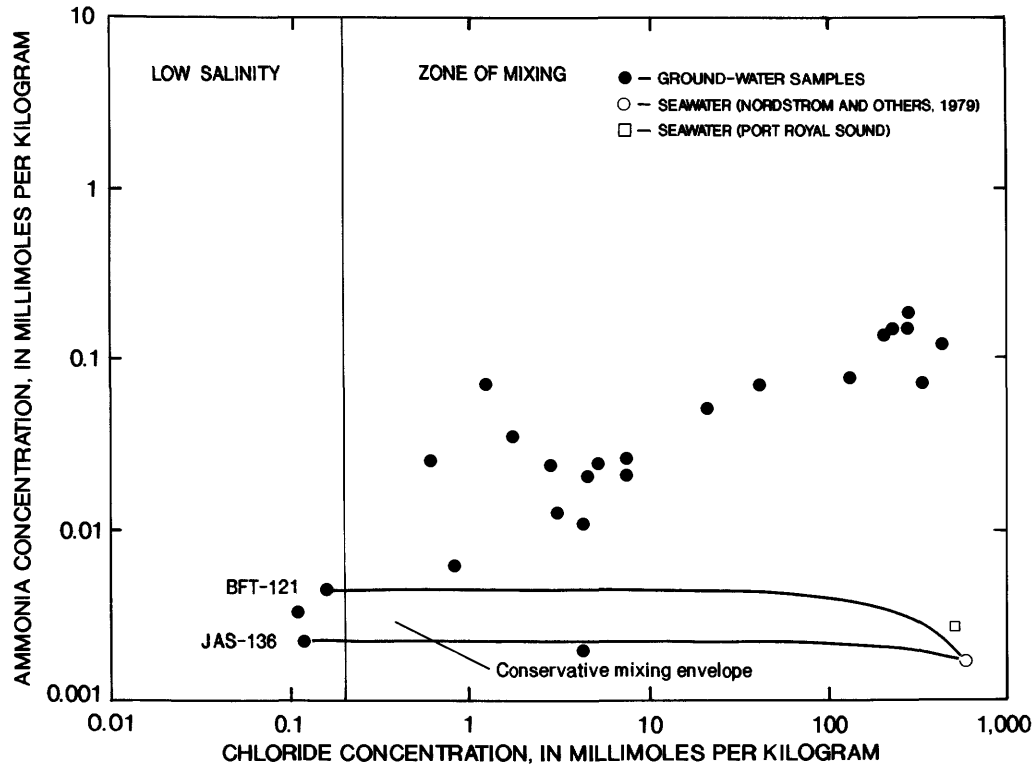

Figure 46. Ammonia to chloride relation in the mixing zone compared to the conservative mixing model.

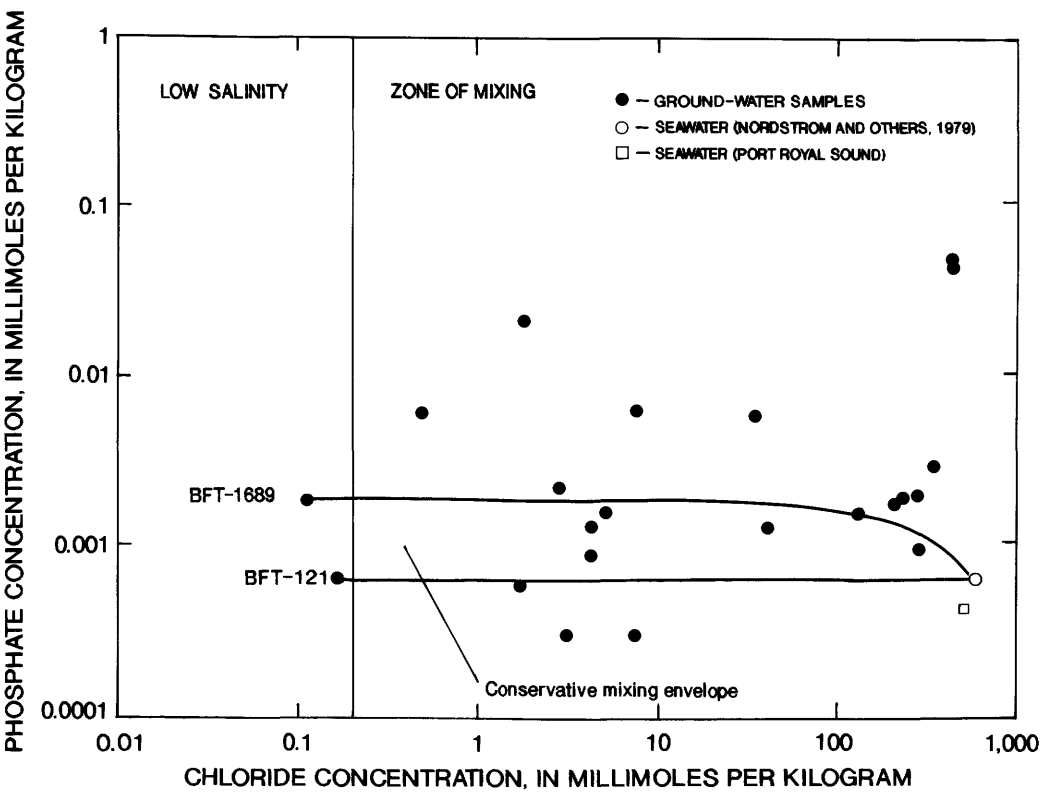

Figure 47. Phosphate to chloride relation in the mixing zone compared to the conservative mixing model.

Most of the bromide values exhibit conservative behavior throughout the mixing zone (fig. 35). Bromide, like chloride, is expected to act conservatively because bromine minerals are absent from the reactive sediments. The excellent correlation between chloride and bromide shown here identifies seawater as the source of high-salinity water as opposed to brine water, which typically exhibits higher bromide to chloride ratios than does seawater. Six of the values fall slightly below the conservative mixing envelope. These deviations are probably the result of combined errors in the analyses of bromide and chloride.

The other plots in figures 36–47 show that several calcium and DIC values are significantly higher than predicted by the conservative mixing model, while pH values are significantly lower than what the model predicts. The concentrations of magnesium, sodium, potassium, fluoride, and sulfate all deviate from the conservative mixing model, both positively and negatively. Silica values, with the exception of one sample, are not significantly different from expected for conservative mixing. Ammonia, sulfide, and phosphate values trend higher than predicted by the conservative mixing model.

The data in figures 36–47 show that the composition of the ground water in the zone of mixing cannot be attributed only to simple mixing of seawater with low-salinity ground water. The data indicate that sources exist for calcium and DIC, while magnesium, sodium, potassium, fluoride, and sulfate appear to have been both added and removed from the solutions. Similarly, the data in figures 45–47 show that a source of ammonia, sulfide, and phosphate also has existed. Some interaction between the ground water and its environment has effected these changes in composition and has caused a decrease in pH.

Limitations of the Conservative Mixing Models

The conservative mixing models presented above are strictly simulations of mixing between three samples assumed to represent the true end-member compositions of water types in the study area. The model limitations are directly related to how well the chosen sample compositions match the true end-members. The uncertainties inherent in the model and the implications of these on interpretations are discussed here.

The end-member compositions of the low-salinity end of the conservative mixing model are representative of the low-salinity ground water existing in the Upper Floridan aquifer in areas immediately surrounding the mixing zone. The evolution of the low-salinity water can be explained in terms of three stages. Rainwater represents the first stage. The second stage includes infiltration of the rainwater and subsequent vertical flow through the sediments overlying the Upper Floridan aquifer. The third stage begins when the water contacts the Upper Floridan, and includes all the changes that occur as the ground water flows horizontally through the aquifer. All of the low-salinity samples collected represent some point in the third stage. Samples from wells BFT–124 and BFT–121, which were used as end-members in the conservative mixing models, represent the earliest time sampled in stage three because they were collected from an area where the aquifer receives significant recharge from overlying sediments. This recharge area is identified by a potentiometric mound in figure 13. Relative to low-salinity samples collected from areas some distance downgradient of recharge areas, samples from BFT–124 and BFT–121 are characterized by high concentrations of calcium and DIC, and low concentrations of magnesium, sodium, potassium, sulfate, fluoride, and silica. These samples reflect the interaction of rainwater with minerals and organically derived compounds in the overlying sediments during recharge, plus some degree of interaction in the Upper Floridan as well.

Because the constituent concentrations of BFT–124 and BFT–121 are considerably higher than the concentrations in local coastal rainfall (Back and others, 1970), it is evident that significant chemical interaction has occurred between some combination of minerals, organically derived compounds, and water during stage two and the earliest part of stage three. The effects of the interactions that occurred at that time cannot be discerned from deviations of sample compositions from the conservative mixing model because BFT–124 and BFT–121 define the earliest evolutionary composition in the model. Any nonconservative behavior may be underestimated if the sample of interest is derived from a significant amount of locally recharged water.

Another limitation of the conservative mixing model concerns the seawater composition. The high-salinity end-member of the conservative mixing model is represented by Nordstrom's seawater analysis. The sample composition is typical of surface seawater conditions. The measured deviations of ground-water constituents from the conservative mixing model, therefore, not only reflect changes in the seawater composition that may have occurred in the Upper Floridan aquifer, but also that occurred prior to or during contact with sediments through which the seawater has passed en route to recharge the aquifer.

Reactions With Minerals and Organically Derived Compounds

The nonconservative behavior exhibited by the mixing zone ground water must be explained by chemical interaction of the water and its dissolved constituents with minerals and organically derived compounds in the aquifer. The Upper Floridan aquifer, in the mixing zone, consists predominantly of calcite in the form of skeletal fragments, micrite, and sparry cements. Other minerals identified in minor to trace amounts were quartz, gypsum, pyrite, plagioclase, alkali feldspar, kaolinite, smectite, and illite (table 2). Dolomite and apatite were not identified in the Upper Floridan aquifer zone of mixing, but both are known to exist in sediments immediately overlying the aquifer

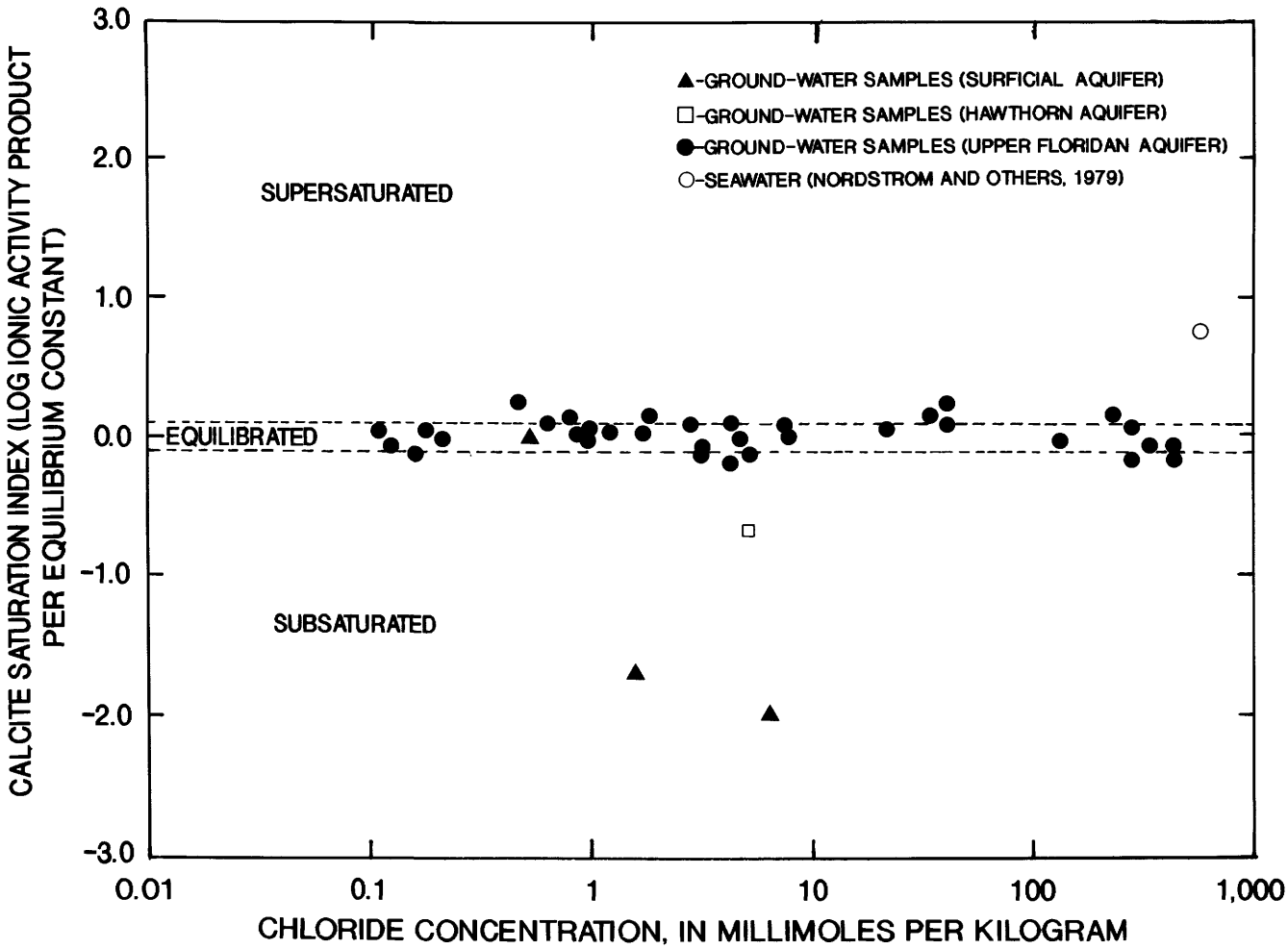

Figure 48. Saturation states, with respect to calcite, of ground water from the surficial, Hawthorn, and Upper Floridan aquifers; and saturation state of seawater with respect to calcite.

(L. McCarten, U.S. Geological Survey, written commun., 1985). Trace amounts of apatite were also identified in the Upper Floridan aquifer updip of the mixing zone. All of these minerals must initially be considered as potential participants in the chemical evolution of ground water in the mixing zone. Additionally, carbon dioxide, hydrogen sulfide, ammonia, phosphate, and organic acids, derived primarily from organic processes (decomposition of organic compounds, respiration), may be important reactants in the ground-water system.

The plausibility of reactions occurring between the detected minerals, dissolved constituents, and the ground water can be tested against mineral saturation constraints. This testing has been done as follows.

Calcite

Saturation indices with respect to calcite, of Upper Floridan aquifer ground-water samples from the mixing zone and the immediate surrounding area, are plotted relative to chloride concentration in figure 48. Values also are plotted for ground water from the surficial aquifer and the Hawthorn Formation, and from Nordstrom's seawater analysis. Saturation index values that fall within 0.1 units of zero are considered to be in equilibrium with calcite based on the precision of the analyses for calcium, carbonate species (alkalinity), and pH (Langmuir, 1971). Despite significant supersaturation of seawater, the ground-water samples from the Upper Floridan aquifer are all very near equilibrium with respect to calcite. In contrast, the calcite saturation indices for three of the four ground-water samples from the surficial and the Hawthorn aquifer indicate subsaturation. All of these shallower samples are from recharging areas on Hilton Head Island (BFT–1812, BFT–1816) and Parris Island (BFT–1842, BFT–1843). They show that calcite saturation generally increases with depth as the recharging water reacts with disseminated carbonate minerals in the shallow clastic sediments. These data probably reflect the combination of kinetic effects as well as variations in availability of carbonate minerals in the shallow sediments overlying the limestone aquifer.

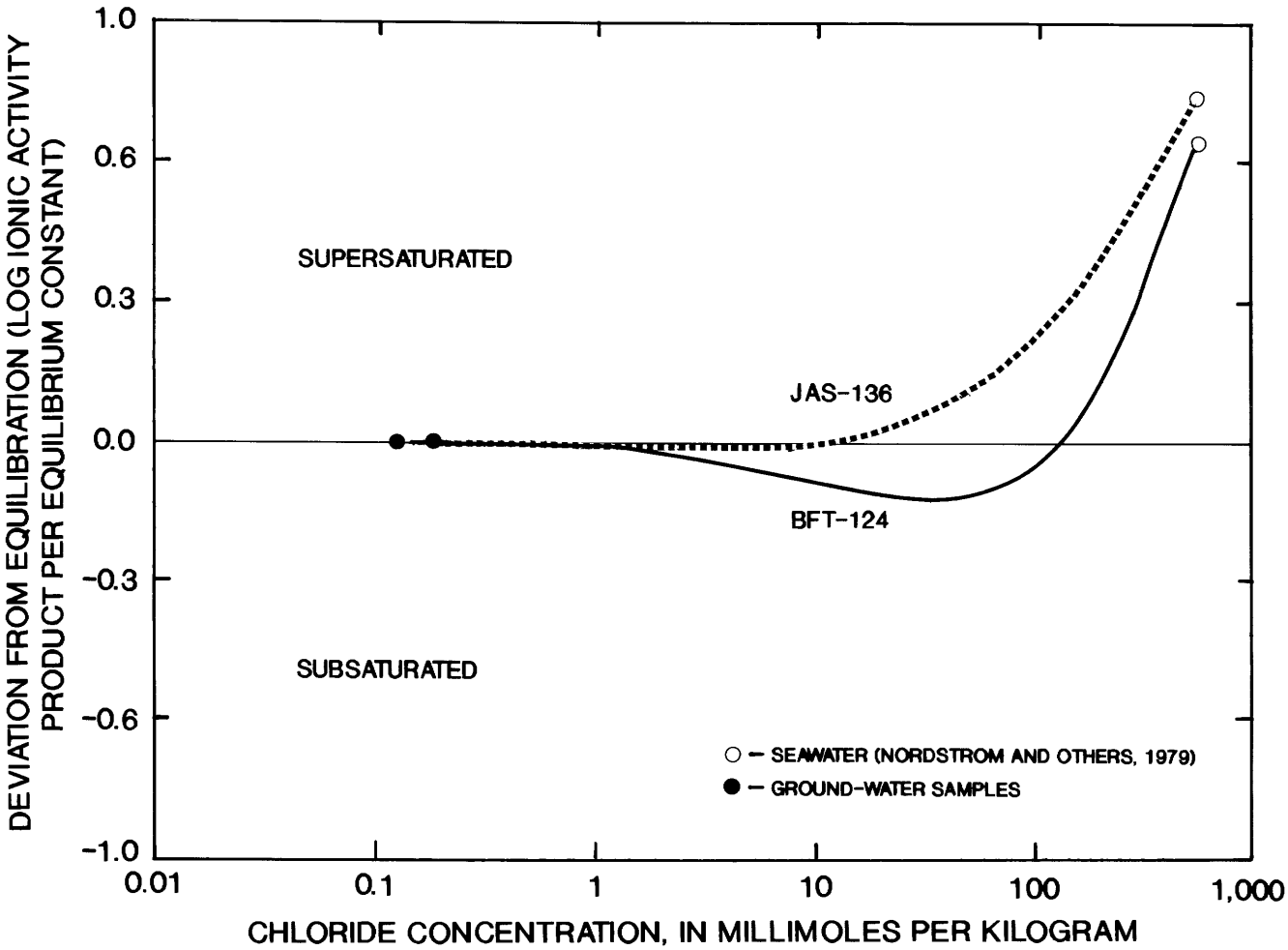

Figure 49. Deviation from equilibrium, with respect to calcite, of simulated mixtures of seawater with samples from wells JAS–136 and BFT–124.

Mixing of seawater with the low-salinity, calcite-equilibrated ground water in the aquifer would be expected to produce solutions that are either supersaturated or subsaturated with respect to calcite, depending on the proportion of mixing. This is illustrated in figure 49, where the saturation indices have been calculated using equilibrium speciation calculations for mixture compositions predicted by the conservative mixing model (using samples JAS–136 and BFT–124 as the low-salinity end-members). The state of saturation deviates from that of either BFT–124 or JAS–136 as seawater is mixed at various concentrations represented by chloride. The deviations from equilibrium indicate that high salinities are conducive for precipitation of calcite. At lower salinities the solutions can dissolve calcite. The tendency of the mixed solutions to be subsaturated at lower salinities is a function of several factors (Wigley and Plummer, 1976), the most significant of which are a redistribution of inorganic carbon species that occurs upon mixing, and the nonlinear dependence of ion activity on ionic strength. This tendency of conservatively mixed waters to deviate from calcite equilibrium, coupled with the tendency for the ground-water samples from the mixing zone to be in equilibrium with calcite, suggests that the mixed ground water has either dissolved or precipitated calcite to attain equilibrium. Ground water mixed with a high percentage of seawater has probably precipitated calcite, while ground water mixed with a low percentage of seawater has probably dissolved calcite.

The saturation indices used to construct figure 49 were calculated for pure calcite (calcium carbonate). Measurements of calcite composition in the zone of mixing show that the calcite actually contains between 0.008 and 0.039 mole fraction magnesium carbonate. Any effect of this deviation from pure calcite is shown to be undetectable, as follows.

The relative position of the ground-water samples and seawater with respect to equilibrium with calcite of varying magnesium carbonate composition is shown in figure 50. The logarithms of the ion activity products of the ground-water samples are plotted as a series of frequency diagrams for several calcite compositions. The logarithms of the ion activity products of seawater are plotted separately for the

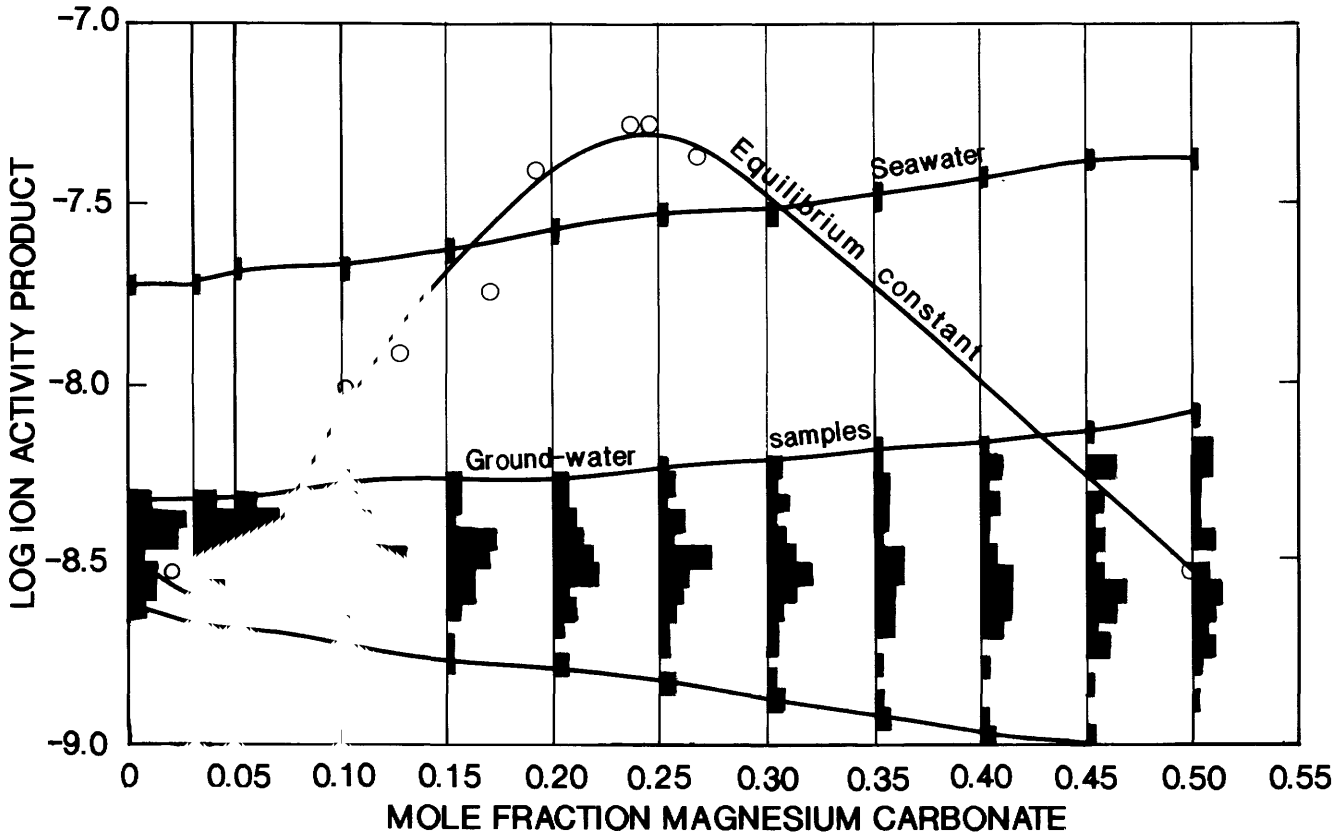

Figure 50. Relation between ion activity product and equilibrium constant with respect to calcite of varying magnesium carbonate content for ground water and seawater. Equilibrium constant values are from Plummer and MacKensie (1974).

same calcite compositions (ion activity products were calculated for samples and seawater using temperatures varying between 19.8 and 25°C). Equilibrium constants are plotted for different calcite compositions at 25°C, as estimated by Plummer and MacKensie (1974), and the approximate curve representing the continuum of these points has been extrapolated to the equilibrium constant for dolomite at 25°C) (Parkhurst and others, 1980). The temperature differences between ion activities and equilibrium constants results in negligible errors for comparison purposes. Ion activity products that fall below the equilibrium constant curve indicate subsaturation with respect to calcite of the indicated composition. Ion activity products that fall above the curve indicate supersaturation. The figure shows that within the compositional range of calcites in the aquifer (0.008–0.039 mole fraction magnesium carbonate) the variation of equilibrium constants is not significantly different from the equilibrium constant of pure calcite (0.0 mole fraction magnesium carbonate) relative to the distribution of products of ground-water ion activity.

The ground water appears to be equilibrated with calcites in this compositional range. Except for calcite within the compositional range of 0.16–0.31 mole fraction magnesium carbonate, seawater is supersaturated with respect to all calcite, and therefore the potential has existed for precipitation of a wide range of calcite compositions (fig. 50). Because the ion activity products of the ground-water samples fall well below the equilibrium constant curve between about 0.07 and 0.42 mole fraction magnesium carbonate, equilibrium with calcite in this composition range does not appear to exert much control on the ground-water compositions. However, the plausibility of precipitation of calcites of widely varying compositions must be considered.

Calcite reactions can be represented by the following equation:

$$x\mathrm{Ca}+(1-x)\mathrm{Mg}+\mathrm{CO_3^{=}}\leftrightarrow \mathrm{Ca}_x\mathrm{Mg}_{(1-x)}\mathrm{CO_3} \qquad (37)$$

Precipitation of calcite would be a sink for calcium, magnesium, and inorganic carbon. Dissolution of calcite would be a source of these constituents. Both of these alternatives appear to be plausible in the mixing zone.

Dolomite

The saturation indices with respect to dolomite for the ground-water samples are plotted in figure 51. Superimposed on the plots are simulated curves representing the saturation indices that would be expected in conservative mixtures of seawater with each of the low-salinity end-

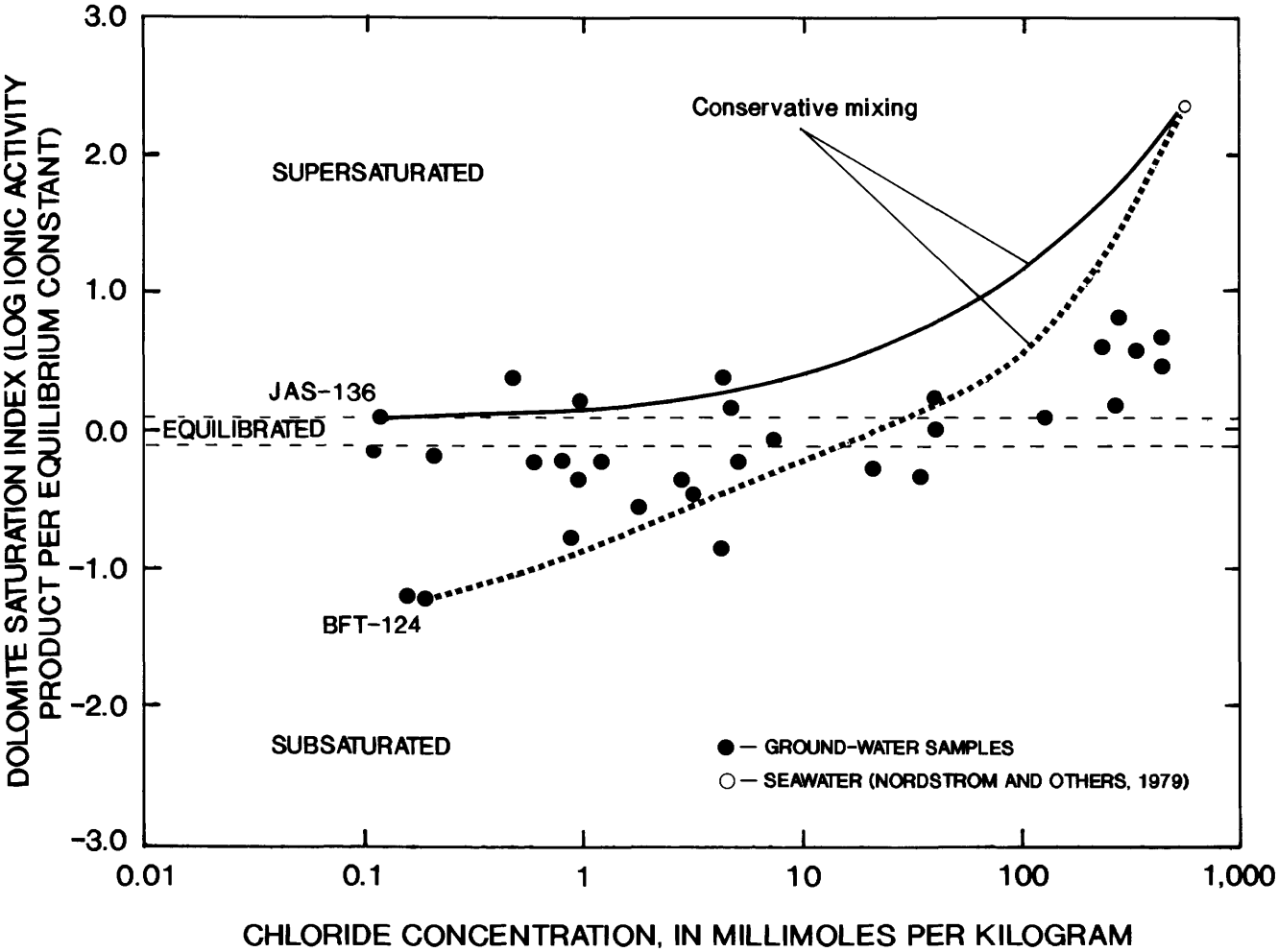

Figure 51. Saturation states with respect to dolomite of ground water compared to simulated values predicted by conservative mixing.

member samples (BFT–124 and JAS–136). For the ground-water samples, saturation indices that fall within ±0.1 of zero are considered to be in equilibrium with dolomite. This value is based on the precision of analysis for calcium, magnesium, carbonate species (alkalinity), and pH (Langmuir, 1971).

The conservative mixing curves in figure 51 show that, depending on the low-salinity end-member and the degree of mixing with seawater, both dissolution and precipitation of dolomite have been possible within the zone of mixing. As with calcite, at high salinities, precipitation is favored. Only a small percentage of the ground-water samples falls within the range of dolomite equilibrium, however, indicating that equilibration with the mineral does not control the ground-water composition. Dolomite was not detected by X-ray diffraction, microprobe, or alizarin red-S staining in the Upper Floridan aquifer, further suggesting minimal influence of dolomite in that part of the system. However, dolomite does occur in the Miocene siliciclastic sediments immediately overlying the Upper Floridan aquifer and may influence the composition of ground water that flows through these sediments and recharges the Upper Floridan aquifer. Dolomite dissolution would be a source of calcium, magnesium, and inorganic carbon for the ground water, whereas dolomite precipitation provides a sink for these constituents. The reaction is represented by

$$CaMg(CO_3) \leftrightarrow Ca^{++} + Mg^{++} + 2CO_3^{=} \qquad (38)$$

Dolomite dissolution also serves to increase the calcite saturation index by increasing the activity of calcium and carbonate in the ground water. The opposite effect would occur in response to dolomite precipitation. Both dolomite dissolution and precipitation must be considered plausible reactions in the system.

Silicates

The silicate minerals identified in the Upper Floridan aquifer were minor to trace amounts of quartz, feldspars, and clay minerals. Because silica concentrations do not deviate from the conservative mixing model (fig. 43), for modeling purposes, it can only be assumed that silicate dissolution and precipitation reactions are of minor significance in the chemical evolution of the mixing-zone ground water.

In contrast, some of these silicate minerals, particularly the smectite clays, may be significant participants in cation exchange reactions by providing the sites for exchange. Other minerals may serve the same purpose. Magnesium, sodium, and potassium deviate in groundwater samples, both above and below the conservative mixing model, as shown in figures 39, 40, and 41. Seawater is enriched with these constituents relative to the low-salinity water and would be expected to exchange these ions for calcium as the seawater encroaches on fresher parts of the aquifer, where exchange sites have been dominated by calcium. Exchange sites associated with the lower-salinity water tend to be saturated with calcium, which is the dominant cation in solution. The opposite effect would be expected under conditions of low-salinity water encroachment into parts of the aquifer containing higher-salinity water, as may occur during recharge from the surface. Here, calcium would be removed from solution to replace sodium, potassium, and magnesium ions on exchange sites. Cation exchange, the reaction direction dependent on hydrologic flow conditions, can explain the nonconservative behavior of sodium, potassium, and magnesium in the zone of mixing. Ion exchange may be an important factor in the regulation of carbonate mineral dissolution and precipitation through its controls on calcium activity in the ground water.

The plausible cation exchange reactions can be represented by the following equations:

$$CaX + 2Na^{+} \leftrightarrow Ca^{++} + Na_2X \quad (39)$$

$$CaX + 2K^{+} \leftrightarrow Ca^{++} + K_2X \quad (40)$$

$$CaX + Mg^{++} \leftrightarrow Ca^{++} + MgX \quad (41)$$

These may occur in either direction and must be considered as plausible reactions in the system.

Gypsum

The conservative mixing model predicts subsaturation with respect to gypsum across the entire mixing sequence (fig. 52). Therefore, gypsum is favored to dissolve. The reaction is written

$$CaSO_4 \leftrightarrow Ca^{++} + SO_4^{=} \quad (42)$$

Dissolution of gypsum results in an increase in the activity of calcium in the ground water, which raises the ion activity product of calcite and thus enhances the potential for calcite precipitation. Gypsum dissolution is the most probable cause of the high concentrations of sulfate (relative to the conservative mixing model) found in some of the groundwater samples (fig. 42). These high sulfate concentrations substantiate the occurrence of gypsum dissolution; however, since the ground water has not reached equilibrium with respect to gypsum (fig. 52), gypsum equilibration is apparently kinetically limited from controlling groundwater composition in the mixing zone.

Pyrite

Pyrite oxidation is another process that can operate as a source of sulfate, as well as increase potential carbonate mineral dissolution. The reaction is written

$$FeS_2 + 4\tfrac{1}{2}O_2 + 2H_2O \rightarrow Fe(OH)_3 + H^{+} + 2SO_4^{=} \quad (43)$$

However, pyrite oxidation requires the presence of molecular oxygen in neutral solutions (Nordstrom, 1982). Several dissolved oxygen measurements on ground water in the mixing zone (table 7) suggest that this mechanism is unlikely to occur in the Upper Floridan aquifer. Although oxygen was detected in shallow ground-water samples from the overlying beds, it apparently is rapidly depleted during infiltration. Though the possibility of pyrite oxidation in the sediments cannot be eliminated, it appears unlikely that it is a significant process. For the purposes of the models presented here, pyrite oxidation was assumed to be insignificant.

Apatite

Malde (1959) presented chemical analyses of phosphatic rocks from the Oligocene and younger sediments in the area of Charleston, S.C., approximately 30 mi northeast of the study area. His data show that the phosphate minerals can be characterized as carbonate-fluorapatite, $Ca_{10}(PO_4, CO_3)_6F_{2-3}$, where PO_4 and CO_3 are apportioned approximately 5 to 1. The apatite minerals detected in the study area are in similar stratigraphic positions and are assumed to be compositionally similar.

Equilibrium constants for carbonate-fluorapatite are not available; however, the saturation index of the groundwater samples with respect to ideal fluorapatite has been determined (fig. 53). Figure 53 shows that all samples, as well as the conservative mixing model solutions, are significantly supersaturated. Fluoride was shown to behave nonconservatively (fig. 44); concentrations were high in samples with chloride concentrations below 100 mmol/kg, and low in samples with higher chlorides. The most likely explanation for this behavior is anion exchange on apatite, where fluoride and hydroxide ions exchange in the apatite lattice in a pH-dependent manner, as described by Zack

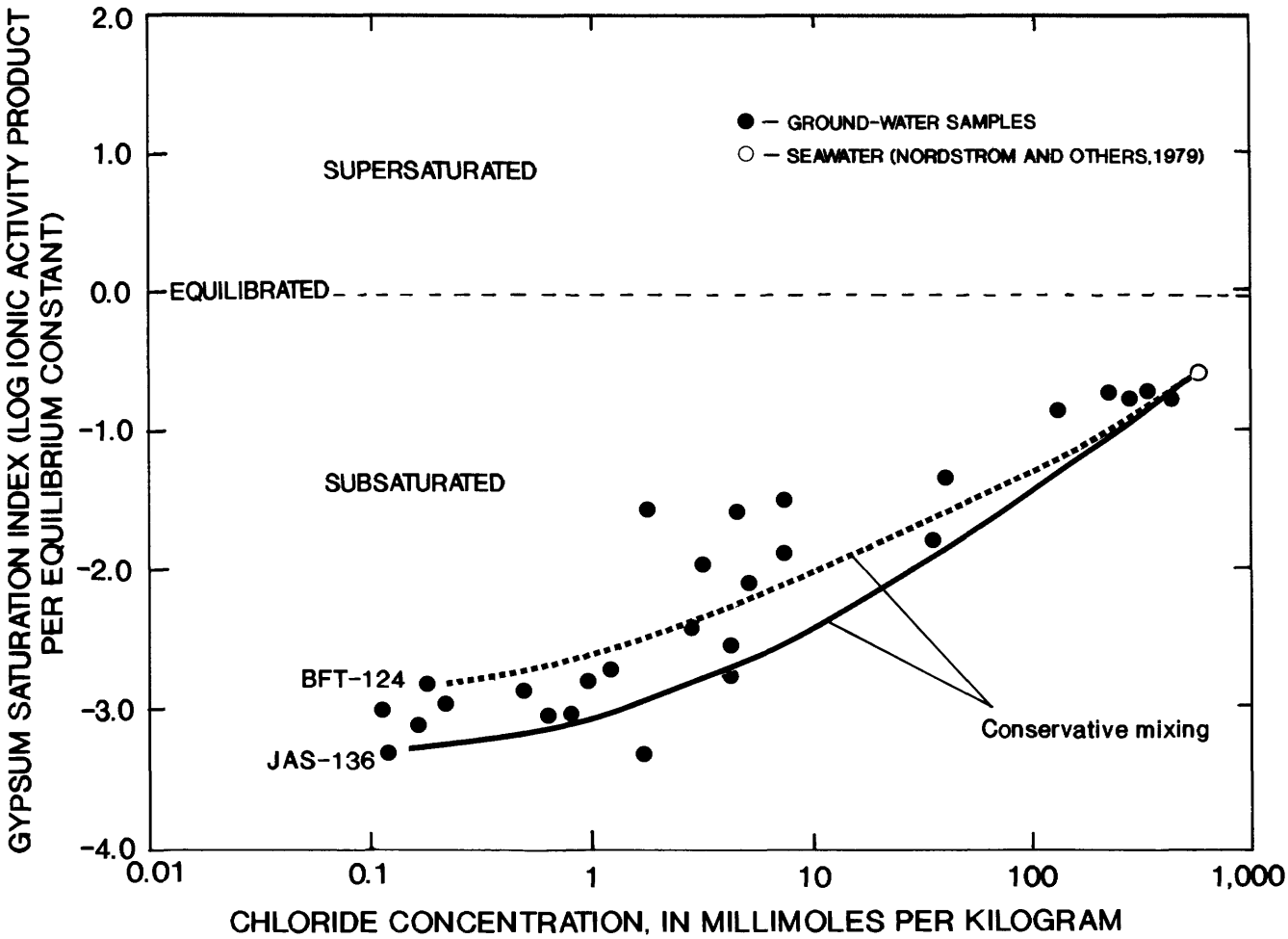

Figure 52. Saturation states with respect to gypsum of ground water compared to simulated values predicted by conservative mixing.

(1980). Ground-water samples in the mixing zone with high fluoride values have pH values somewhat higher than 7. Under these conditions, the hydroxide concentration is high enough to displace fluoride ions from the apatite lattice. In the higher-salinity, lower-pH samples, competition by hydroxide for exchange sites has decreased, allowing fluoride to replace hydroxide in the mineral and resulting in decreased fluoride concentrations.

Phosphate also shows nonconservative behavior (fig. 47) that could indicate reactions with apatite, but elevated phosphate concentrations are probably related to decomposition of organic matter rather than apatite dissolution. Anion exchange reactions on apatite minerals potentially affect the equilibrium state of ground water with respect to carbonate minerals. Acting as either a source or sink for hydroxide ions, the reaction could drive the equilibrium toward either supersaturation or subsaturation.

Organically Derived Compounds

A number of compounds could enter the ground-water system as the result of organic processes, which could occur in the root zone of shallow sediments as well as in deeper aquifers. Carbon dioxide is probably the most significant reactant that could be produced organically, but other compounds, such as hydrogen sulfide, ammonia, phosphate, and organic acids, also could be important. The implications of the production of these compounds in the ground water of the mixing zone are described in the following section.

Table 7.—Complete chemical and isotopic ground-water analyses

[°C, degrees Celsius; mmol/kg, millimoles per kilogram; mg/L, milligrams per liter; SMOW, Standard Mean Ocean Water; PDB, Chicago belemnitella americana standard from the Cretaceous Peedee Formation in South Carolina; dashes indicate no data]

Sample	Data source[1]	Aquifer[2]	Date	Sample interval (feet below land surface) Top	Bottom	Temperature (°C)	pH	Calcium (mmol/kg)	Magnesium (mmol/kg)	Sodium (mmol/kg)
1. JAS–136	a	uf	June 1985	200	245	21.1	8.24	0.32	0.45	0.40
2. HAM–122	a	uf	May 1986	82	174	20.7	7.55	1.2	.21	.24
3. BFT–1288	a	uf	Jan. 1985	60	115	19.8	7.51	1.4	.45	.57
4. BFT–441	a	uf	Jan. 1985	187	216	20.9	7.37	1.6	.66	1.3
5. BFT–795	a	uf	Jan. 1985	77	91	20.9	7.00	8.0	40	370
6. BFT–1689	a	uf	Jan. 1985	91	203	20.9	7.92	.67	.34	.48
7. BFT–566	a	uf	Feb. 1985	170	189	21.6	6.60	12	46	360
8. BFT–459	a	uf	Feb. 1985	85	100	20.5	7.12	6.7	1.3	26
9. BFT–121	a	uf	Feb. 1985	84	100	20.1	7.69	1.1	.09	.23
10. BFT–791	a	uf	March 1985	81	102	20.0	7.44	1.7	.49	.61
11. BFT–787	a	uf	April 1985	172	185	20.8	7.28	2.4	.32	1.5
12. BFT–210	a	uf	May 1985	130	160	20.8	8.17	.67	.41	.96
13. BFT–565	a	uf	May 1985	182	195	21.5	6.81	9.8	12	100
14. BFT–439	a	uf	July 1985	182	214	21.5	—	.80	.36	1.5
15. BFT–1672	a	uf	July 1984	[3]95	[3]107	20.8	7.74	1.2	.58	7.8
16. BFT–1672	a	uf	July 1984	[3]174	[3]211	22.1	7.01	8.5	27	206
17. BFT–1673	a	uf	Aug. 1984	[3]85	[3]101	21.5	7.43	1.4	1.0	3.6
18. BFT–1674	a	uf	Aug. 1984	[3]101	[3]113	23.0	7.33	1.7	.41	2.8
19. BFT–1674	a	uf	Aug. 1984	[3]170	[3]174	21.9	7.21	9.6	34	290
20. BFT–1675	a	uf	Aug. 1984	[3]89	[3]103	21.0	7.71	.90	.41	3.9
21. BFT–1675	a	uf	Aug. 1984	[3]186	[3]212	22.4	7.76	1.0	1.3	5.2
22. BFT–1676	a	uf	Aug. 1984	[3]97	[3]110	21.3	7.47	1.4	.26	1.7
23. BFT–1676	a	uf	Aug. 1984	[3]178	[3]182	22.0	7.32	4.0	1.3	11
24. BFT–1677	a	uf	Sept. 1984	[3]92	[3]99	21.0	7.40	3.3	3.1	27
25. BFT–1677	a	uf	Sept. 1984	[3]159	[3]176	21.7	7.11	8.3	18	172
26. BFT–1678	a	uf	Sept. 1984	[3]76	[3]86	20.8	7.54	1.0	.25	4.4
27. BFT–1678	a	uf	Sept. 1984	[3]151	[3]155	22.0	—	.25	.31	6.5
28. BFT–1679	a	uf	Sept. 1984	[3]108	[3]120	21.0	7.69	1.4	.91	8.3
29. BFT–1680	a	uf	Oct. 1984	[3]103	[3]117	20.9	6.99	12	19	161
30. BFT–1680	a	uf	Oct. 1984	[3]173	[3]218	21.7	6.92	6.5	17	190
31. BFT–1812	a	s	Jan. 1987	25	30	18.8	6.50	.63	.17	1.6
32. BFT–1816	a	s	Jan. 1987	23	30	19.6	7.94	.72	.10	.91
33. BFT–1842	a	h	Feb. 1987	49	62	19.8	6.70	2.3	.45	4.4
34. BFT–1843	a	s	Feb. 1987	10	29	19.3	6.13	1.5	.66	4.3
35. BFT–124	b	uf	April 1966	97	107	19.8	7.57	1.3	.053	.21
36. BFT–314	b	uf	April 1965	125	230	21.1	7.98	.57	.35	.65
37. BFT–287	b	uf	April 1966	90	195	20.6	7.34	1.6	.21	.87
38. BFT–317	b	uf	April 1966	86	196	20.1	7.61	1.0	.41	1.3
39. BFT–343	b	uf	April 1966	124	200	20.3	8.09	.52	.53	1.4
40. BFT–181	b	uf	April 1965	93	117	21.5	7.22	6.7	1.7	35
41. BFT–407	b	uf	April 1966	140	214	20.9	7.60	1.1	.45	4.3
42. HAM–73	c	uf	Feb. 1977	60	200	—	—	1.2	.11	.22
43. JAS–101	c	uf	Oct. 1956	190	450	—	—	1.1	.32	.43
44. BFT–206	d	uf	Nov. 1957	221	281	—	7.6	.50	.36	.57
45. JAS–1	d	uf	Aug. 1957	204	503	—	—	.55	.35	.39
46. CHT–19	d	uf	May 1955	—	603	—	7.6	.62	.36	.41
47. EFF–25	d	uf	Jan. 1941	—	425	—	—	.60	.38	.65
48. BRY–147	d	uf	June 1941	—	440	—	—	.55	.38	.61
49. CHT–296	d	uf	June 1941	—	367	—	—	.52	.49	.74
50. 25T001	e	uf	Aug. 1961	250	412	22.0	8.2	1.34	.32	.27

Table 7.—Complete chemical and isotopic ground-water analyses—Continued

Sample	Data source[1]	Aquifer[2]	Date	Sample interval (feet below land surface) Top	Bottom	Temperature (°C)	pH	Calcium (mmol/kg)	Magnesium (mmol/kg)	Sodium (mmol/kg)
51. 33U019	e	uf	Sept. 1963	270	290	—	7.2	1.00	.32	.17
52. 25U002	e	uf	March 1963	212	225	20.0	7.7	1.47	.11	.20
53. 31X017	e	uf	Sept. 1963	160	249	20.0	7.4	.77	.30	.27
54. HAM-36	e	uf	Jan. 1960	105	152	—	7.7	1.05	.21	.20
55. 33R021	e	uf	Sept. 1981	229	429	23.5	7.5	.72	.27	.35
56. 30S002	e	uf	Nov. 1963	440	480	—	7.9	.85	.33	.28
57. 27S001	e	uf	April 1967	370	432	22.0	7.8	.70	.32	.30
58. 33U009	e	uf	Sept. 1963	200	280	20.5	7.3	1.00	.32	.17
59. 27W001	e	uf	March 1966	123	132	—	7.2	1.15	.02	.083
60. 31W010	e	uf	March 1970	212	275	18.0	7.9	1.27	.28	.40

	Potasium (mmol/kg)	Chloride (mmol/kg)	Sulfate (mmol/kg)	Bicarbonate (mmol/kg)	Fluoride (mmol/kg)	Silica (mmol/kg)	Bromide (mmol/kg)	Sulfide (mmol/kg)	Ammonium (mmol/kg)	Nitrate (mmol/kg)
1.	0.059	0.12	0.070	1.79	0.018	0.88	0.00012	0.00	0.0022	0.001
2.	.049	.15	.034	2.83	.005	.45	<.002	.00	.0011	<.0006
3.	.050	.62	.37	3.65	.017	.57	.0011	.009	.026	<.0006
4.	.080	1.2	.076	3.94	.019	.60	—	.016	.071	<.0006
5.	9.5	430	20	6.36	.009	.27	.67	.42	.12	.01
6.	.074	.11	.072	2.31	.021	.60	.0005	.0003	.0033	<.0006
7.	7.2	430	17	10.0	.01	.42	.60	.74	—	<.006
8.	.15	34	.39	3.59	.011	.60	.05	.0082	—	<.006
9.	.017	.16	.033	2.28	.009	.20	<.0001	.0003	—	<.0006
10.	.041	.79	.033	3.93	.015	.58	.0005	.0003	—	<.0006
11.	—	1.8	—	4.50	.010	.47	.0013	.0003	.022	<.0006
12.	.041	.48	.096	2.25	.028	.72	.0006	.000	<.0006	<.0006
13.	1.4	130	5.9	5.55	.018	.50	.20	.097	.078	<.0006
14.	.082	.82	.18	2.28	.026	.75	.0006	.014	.0061	<.0006
15.	.16	7.4	.91	2.92	.037	.48	.011	.0044	.026	<.0006
16.	3.6	278	14	7.28	.027	.44	.42	.086	.19	<.0006
17.	.26	5.1	.43	3.13	.026	.57	.011	.012	.024	<.0006
18.	.10	2.8	.15	4.20	.016	.65	.0046	.002	.024	<.0006
19.	5.4	340	17	3.23	.016	.39	.56	.0093	.072	<.0006
20.	.12	3.1	.76	2.46	.037	.58	.0050	.0019	.013	<.0006
21.	.23	4.5	2.2	2.66	.058	.47	.0081	.0008	.021	<.0006
22.	.051	1.7	.020	3.48	.021	.71	.0025	.0006	.036	<.0006
23.	.21	21	.51	2.46	.021	.52	.031	.0008	.051	<.0006
24.	1.2	40	1.1	3.38	.053	.43	.048	.013	.071	<.0006
25.	2.9	211	7.6	5.01	.032	.46	.32	.032	.14	<.0006
26.	.15	4.2	.17	2.62	.037	.47	.0075	.0008	.002	<.0006
27.	.25	4.2	.47	3.30	.095	.32	.0066	—	.002	<.0006
28.	.31	7.3	2.1	2.74	.047	.43	.012	.012	.022	<.0006
29.	2.3	229	8.4	5.49	<.005	.32	.23	.040	.15	<.0006
30.	2.5	270	10	5.73	<.005	.35	.30	.025	.15	<.0006
31.	0.79	1.6	2.7	1.34	0.005	0.18	0.0018	<0.016	0.017	<0.0006
32.	.033	.54	.081	1.93	.021	.23	.0004	<.016	—	<.0006
33.	.12	5.1	1.0	3.15	.011	.18	.0070	<.016	.012	.051
34.	.61	6.2	.87	.80	.005	.12	.0054	<.016	.065	.0020
35.	.02	.18	.057	2.87	.005	.13	—	—	—	.0000
36.	.56	.21	.090	2.08	.02	.78	—	—	—	.0016
37.	.049	.87	.00	3.79	.01	.60	—	—	—	.0000
38.	.059	.93	.084	2.97	.03	.53	—	—	—	.0016
39.	.079	.96	.16	2.21	.03	.45	—	—	—	.13
40.	.19	44	1.3	3.90	.016	.63	—	—	—	.0016

Table 7.—Complete chemical and isotopic ground-water analyses—Continued

	Potasium (mmol/kg)	Chloride (mmol/kg)	Sulfate (mmol/kg)	Bicarbonate (mmol/kg)	Fluoride (mmol/kg)	Silica (mmol/kg)	Bromide (mmol/kg)	Sulfide (mmol/kg)	Ammonium (mmol/kg)	Nitrate (mmol/kg)
41.	0.13	3.2	0.66	2.75	0.03	0.42	—	—	—	0.006
42.	.061	.10	.046	2.62	.005	.40	—	—	—	.0005
43.	.056	.11	.037	3.08	.005	.55	—	—	—	—
44.	.069	.11	.062	2.10	.04	.70	—	—	—	.0000
45.	.051	.17	.068	1.97	.03	.83	—	—	—	.0002
46.	.049	.17	.068	2.13	.02	.78	—	—	—	.0000
47.	.059	.12	.054	2.39	.02	.65	—	—	—	.0000
48.	.061	.12	.059	2.26	.02	.73	—	—	—	.0000
49.	.087	.11	.18	2.31	.04	.58	—	—	—	.0000
50.	.056	.17	.046	3.44	.010	.45	—	—	—	.0015
51.	.051	.28	.046	2.62	.011	.52	—	—	—	.0000
52.	.036	.085	.017	3.28	.011	.48	—	—	—	.0000
53.	.11	.085	.087	2.30	.037	.70	—	—	—	.0000
54.	.056	.085	.036	2.46	.005	.50	—	—	—	.0015
55.	.064	.10	.055	2.13	.021	.85	0.00	—	<0.0006	—
56.	.028	.056	.037	2.46	.021	1.13	—	—	—	.0015
57.	.084	.11	.037	2.30	.016	.63	—	—	—	.005
58.	.051	.17	.046	2.62	.011	.57	—	—	—	.0000
59.	.0051	.11	.00	2.29	.005	.57	—	—	—	.053
60.	.056	.17	.017	3.27	.000	.72	—	—	—	.0000

	Phosphate (mmol/kg)	Total organic carbon (mg/L)	Dissolved organic carbon (mg/L)	Dissolved oxygen (mg/L)	Dissolved inorganic carbon[4] (mmol/kg)	Oxygen (per mil SMOW)	Deuterium (per mil SMOW)	Carbon-13 (per mil PDB)	Carbon-14 (percent modern carbon)
1.	—	0.30	—	0.0	1.78	−3.62	−16.8	−3.0	<1.5
2.	0.0016	1.6	—	.0	2.98	−3.41	−16.0	−10.5	37.2
3.	—	—	3.0	.1	3.88	−4.00	−22.4	−11.4	37.9
4.	<.0003	3.0	—	.2	4.27	−3.22	−18.9	−9.5	22.0
5.	.049	3.5	—	.8	6.69	.68	5.3	−8.2	64.8
6.	.0019	1.5	—	.5	2.35	−3.83	−17.8	−3.3	1.0
7.	.045	—	5.2	.7	12.6	−.2	3.5	−9.0	74.0
8.	.06	—	2.7	—	4.08	−3.1	−16.0	−13.9	54.7
9.	.0006	—	2.0	—	2.40	−4.0	−23.4	−12.1	49.0
10.	—	—	3.2	.0	4.22	−3.99	−22.2	−11.2	28.0
11.	.022	—	3.2	—	4.92	−3.2	−19.1	−12.2	39.5
12.	.006	—	1.3	.1	2.23	−3.90	−17.2	−1.8	2.3
13.	.0016	—	2.6	—	6.80	−2.53	−6.5	−9.6	13.0
14.	<.0003	—	3.9	.0	—	−3.84	−18.9	−1.6	<1.9
15.	.0063	—	.17	.0	3.00	−3.8	−21.6	−8.9	10.5
16.	.0010	—	.40	.1	8.12	−2.3	−11.3	−7.8	7.5
17.	.0016	—	.17	—	3.34	−3.9	−20.7	−7.4	10.6
18.	.0022	—	.19	.0	4.58	−3.6	−20.1	−12.0	—
19.	.0030	—	3.0	.1	3.43	−.5	.9	−9.0	18.2
20.	.0003	—	3.3	.0	2.54	−4.0	−21.6	−7.5	—
21.	<0.0003	—	1.8	.0	2.72	−3.7	−21.5	−3.4	2.3
22.	.0006	—	3.0	.0	3.71	−3.9	−22.5	−10.9	7.3
23.	<.0003	—	1.6	.9	2.67	−3.5	−19.8	−8.8	14.3
24.	.0013	—	1.9	.1	3.60	−3.2	−19.0	−7.2	5.0
25.	.0019	—	4.0	.5	5.51	−2.0	−13.3	−8.4	6.9

Table 7.—Complete chemical and isotopic ground-water analyses—Continued

	Phosphate (mmol/kg)	Total organic carbon (mg/L)	Dissolved organic carbon (mg/L)	Dissolved oxygen (mg/L)	Dissolved inorganic carbon[4] (mmol/kg)	Oxygen (per mil SMOW)	Deuterium (per mil SMOW)	Carbon-13 (per mil PDB)	Carbon-14 (percent modern carbon)
26.	.0013	—	1.1	.0	2.77	−3.7	−21.1	−3.1	—
27.	.0009	—	1.3	.0	—	−3.7	−21.5	−3.0	14.2
28.	.0003	—	2.2	.0	2.82	−3.8	−22.7	−6.6	—
29.	.002	—	5.2	.0	6.23	−2.2	−13.9	−11.6	6.0
30.	.002	—	5.0	.2	6.72	−1.9	−12.5	−10.1	19.8
31.	<.0003	—	3.8	4.18	2.31	—	—	−30.3	—
32.	.012	—	4.4	1.24	1.95	—	—	−13.	—
33.	.015	—	3.4	.00	4.46	−4.1	−21.	−12.2	87.3
34.	.0061	—	3.4	.14	2.07	−4.3	−23.	−19.9	124.0
35.	—	—	—	—	3.03	—	—	−12.1	50.0
36.	—	—	—	—	2.10	—	—	−9.0	2.3
37.	—	—	—	—	4.15	—	—	−12.9	40.0
38.	—	—	—	—	3.11	—	—	−8.7	18.7
39.	—	—	—	—	2.22	—	—	−5.1	1.4
40.	—	—	—	—	4.30	—	—	−13.9	25.7
41.	—	—	—	—	2.89	—	—	−13.7	11.3
42.	—	—	—	—	—	—	—	—	—
43.	—	—	—	—	—	—	—	—	—
44.	—	—	—	—	—	—	—	—	—
45.	—	—	—	—	—	—	—	—	—
46.	—	—	—	—	—	—	—	—	—
47.	—	—	—	—	—	—	—	—	—
48.	—	—	—	—	—	—	—	—	—
49.	—	—	—	—	—	—	—	—	—
50.	—	—	—	—	—	—	—	—	—
51.	—	—	—	—	—	—	—	—	—
52.	—	—	—	—	—	—	—	—	—
53.	—	—	—	—	—	—	—	—	—
54.	.00	—	—	—	—	—	—	—	—
55.	—	.20	—	—	—	−3.6	−22.0	−6.5	—
56.	—	—	—	—	—	—	—	—	—
57.	—	—	—	—	—	—	—	—	—
58.	—	—	—	—	—	—	—	—	—
59.	—	—	—	—	—	—	—	—	—
60.	—	—	—	—	—	—	—	—	—

[1] a, original data; b, Back and others (1970); c, Hayes (1979); d, Counts and Donsky (1963); and e, U.S. Geological Survey files.

[2] uf, Upper Floridan; h, Hawthorn; s, surficial.

[3] These wells were drilled offshore. The reference point for the depths is sea level.

[4] DIC was calculated from the complete chemical analyses using the computer program WATEQF (Plummer and others, 1976) to perform the equilibrium speciation calculations.

Input of carbon dioxide to ground water in the aquifer or in the overlying sediments can serve both as a source of inorganic carbon to the ground water as well as a mechanism for lowering the pH and driving the dissolution of calcite according to the following reactions:

$$CO_{2(aq)} + H_2O \leftrightarrow H_2CO_3 \leftrightarrow H^+ + HCO_3^- \quad (44)$$

$$H_2CO_3 + CaCO_3 \leftrightarrow Ca^{++} + 2HCO_3^- \quad (45)$$

The carbon dioxide in ground water may originate from different sources; it may be derived from plant respiration in the root zone or by oxidation of reduced carbon during decomposition of organic compounds in the sediments that constitute the aquifer and overlying beds. Also, atmospheric carbon dioxide gas may dissolve in surface water or rain before infiltration; however, atmospheric carbon dioxide ($P_{CO_2} = 10^{-3.5}$) generally contributes

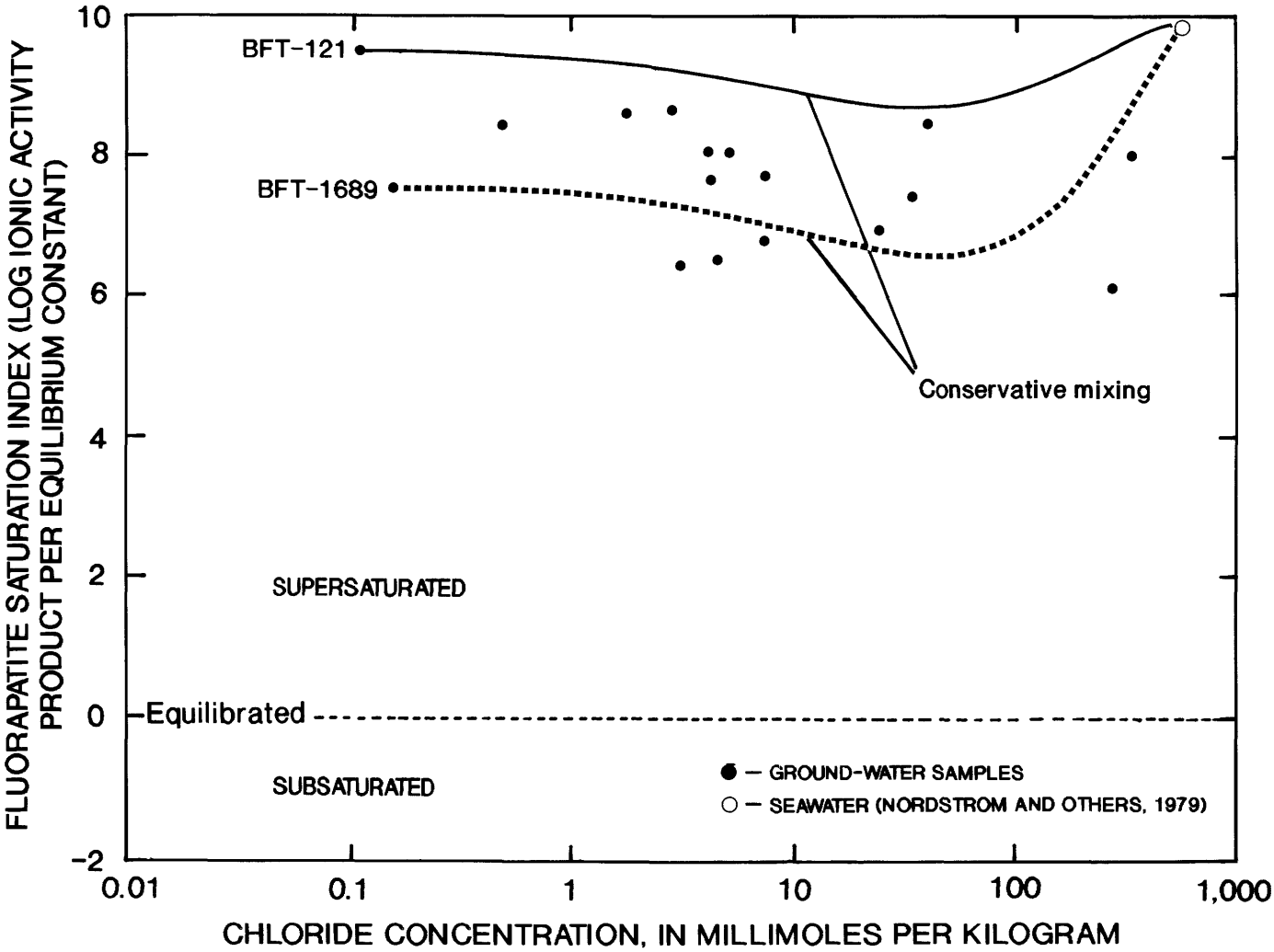

Figure 53. Saturation states with respect to fluorapatite of ground water compared to simulated values predicted by conservative mixing.

only a small amount of the dissolved carbon dioxide in ground water. Respiration and organic decomposition in the soil or root zone can contribute large amounts (P_{CO_2}= $10^{-1.0}$) of carbon dioxide to the ground water (Fontes, 1980). The degree of carbon dioxide contribution that occurs deeper in sediments is not well known.

The extent to which carbon dioxide in ground water causes dissolution of calcite is dependent on the mechanism of carbon dioxide input. Dissolved atmospheric or respired carbon dioxide can be represented by equations 44 and 45 and can be thought of as an injection of carbon dioxide gas into solution. The amount of calcite dissolved relative to the contribution of carbon dioxide is dependent on the solution pH and the equilibrium constants of the carbonate species. Within the pH range of the ground water in the zone of mixing (6.60–7.76), the reactions essentially cause the dissolution of one mole of calcite for every mole of contributed carbon dioxide, and result in two moles of bicarbonate.

The process of carbon dioxide generation by decomposition of organic compounds occurs by several different mechanisms, including oxygen reduction, nitrate reduction, sulfate reduction, and fermentation. The products of these reactions are dependent on the specific mechanism and could vary with regard to the microorganisms that mediate the process. The specific compounds that are decomposing and the valence of carbon in these compounds can also affect the resulting products. The reaction products may contain both acids and bases, and therefore could cause carbonate dissolution or precipitation, dependent on the proportion of acid to bases produced.

As an example, the decomposition of some simple compounds (formaldehyde and methane) by oxygen reduction can be represented by the following equations:

Carbon valence	Reaction	
0	$CH_2O+O_2 \rightarrow CO_2+H_2O$	(46)
−IV	$CH_4+2O_2 \rightarrow CO_2+2H_2O$	(47)

These reactions demonstrate the effect of differing carbon valence. The oxidation of methane (−IV) requires twice as much molecular oxygen as does oxidation of formaldehyde (0). The resulting products are the same, however, disregarding water. For both of these examples, the effect of organic compound decomposition is the same as that of atmospheric input or respiration.

The decomposition of organic compounds by nitrate and sulfate reduction has somewhat different effects from those of atmospheric contribution, respiration, and oxygen reduction, in that in addition to the generated carbon dioxide, the bases ammonia, hydroxide, and sulfide are produced. Under the anaerobic conditions required for these reactions, ammonia and sulfide are also generated by ammonification and desulfurization of decomposing organic compounds. These bases act as buffers, neutralizing the hydrogen ions that drive the dissolution of carbonate minerals. The valence of the carbon in decomposing organic compounds may control the amounts of the bases produced relative to carbon dioxide production, as in the following representative equations:

Carbon valence	Reaction	
	Nitrate reduction	
+II	$CO_2H_2+{}^{2/5}NO_3^- \rightarrow CO_2+{}^{1/5}N_2+{}^{4/5}H_2O+{}^{2/5}OH^-$	(48)
0	$COH_2+{}^{4/5}NO_3^- \rightarrow CO_2+{}^{2/5}N_2+{}^{3/5}H_2O+{}^{4/5}OH^-$	(49)
−IV	$CH_4+{}^{8/5}NO_3^- \rightarrow CO_2+{}^{4/5}N_2+{}^{6/5}H_2O+{}^{8/5}OH^-$	(50)
	Sulfate reduction	
+II	$CO_2H_2+1/4SO_4^= \rightarrow CO_2+1/4S^=+H_2O$	(51)
0	$COH_2+1/2SO_4^= \rightarrow CO_2+1/2S^=+2H_2O$	(52)
−IV	$CH_4+SO_4^= \rightarrow CO_2+S^=+2H_2O$	(53)

For low-valence carbon, that is -IV, in water with pH values similar to those measured in the zone of mixing (6.60–7.76), the buffer capacity of the generated bases may exceed the acidity of the generated carbonic acid.

The presence of sulfide in the ground-water samples, coupled with sulfate deficits observed in the mixing zone (fig. 42), indicates that sulfate reduction and desulfurization have occurred. The probable occurrence of nitrate reduction in the mixing zone during recharge is demonstrated by the difference in nitrate concentration of ground water from the Upper Floridan aquifer and ground water from the overlying Hawthorn aquifer. The concentration of nitrate from BFT-1842 (Hawthorn aquifer) was 0.051 mmol/kg, compared with concentrations that were below detection (0.006 and 0.0007, depending on analytical interferences) in the Upper Floridan aquifer. Additionally, significant concentrations of ammonia in the ground water indicate that ammonia breakdown products of amino compounds have been preserved.

The effect that these base-generating, organic decomposition reactions could have on carbonate mineral stability in solutions like those in the zone of mixing is illustrated in figure 54. Saturation indices predicted by the conservative mixing model (using equilibrium speciation calculations) are compared with saturation indices of the same solutions following simulated sulfate reduction with differing carbon valences. The magnitude of sulfate reduction used in the simulations (0.7 mmol/kg) is similar to that indicated in the zone of mixing by concentrations of dissolved sulfide. These plots show that, depending on the valence of carbon in the decomposing compounds, sulfate reduction could result in either increased or decreased levels of saturation as compared with the conservative mixing model. Under some conditions (low carbon valence), sulfate reduction could reverse the potential for dissolution to potential precipitation, and vice versa for high carbon valence. Nitrogen reduction would have similar effects, while ammonification and desulfurization would only have the effect of shifting the carbonate equilibrium toward supersaturation.

The examples of organic compound decomposition described above are written such that all of the carbon in the decomposing compounds is completely oxidized to carbon dioxide. This is not necessarily the case. Particularly under anaerobic conditions, the reaction products may include dissolved organic carbon (DOC) in the form of organic acids. The interstitial water of sediments generally tends toward low concentrations of DOC in oxygenated pore waters, where oxidation of carbon to carbon dioxide is nearly complete; however, substantially higher concentrations of DOC generally occur in anaerobic water, where oxidation processes are dominated by nitrate reduction, sulfate reduction, and fermentation (Thurman, 1985).

Krom and Sholkovitz (1977, 1978) found that the majority of DOC found in anaerobic pore waters from Loch Duich in Scotland was fulvic-acidlike material. The generation of organic acids during decomposition of other compounds will alter the ground-water equilibrium state with respect to carbonate minerals. The organic acids will tend to cause dissolution of the carbonates. The acidity of fulvic acids is approximately equal to 10 microequivalents per kilogram (μeq/kg) per milligram carbon (Oliver and others, 1983). The ground-water sample, from the mixing zone, found to contain the highest concentration of organic carbon was BFT–565 at 5.2 mg/L. Estimating that all of this carbon is in the form of fulvic acids, the organic acid contribution to the total acidity would be approximately 0.052 μeq/kg. This value is of the same order of magnitude as the alkalinity associated with ammonia and sulfide generated in the ground water. Organic acids may neutralize a significant amount of the alkalinity introduced by these bases.

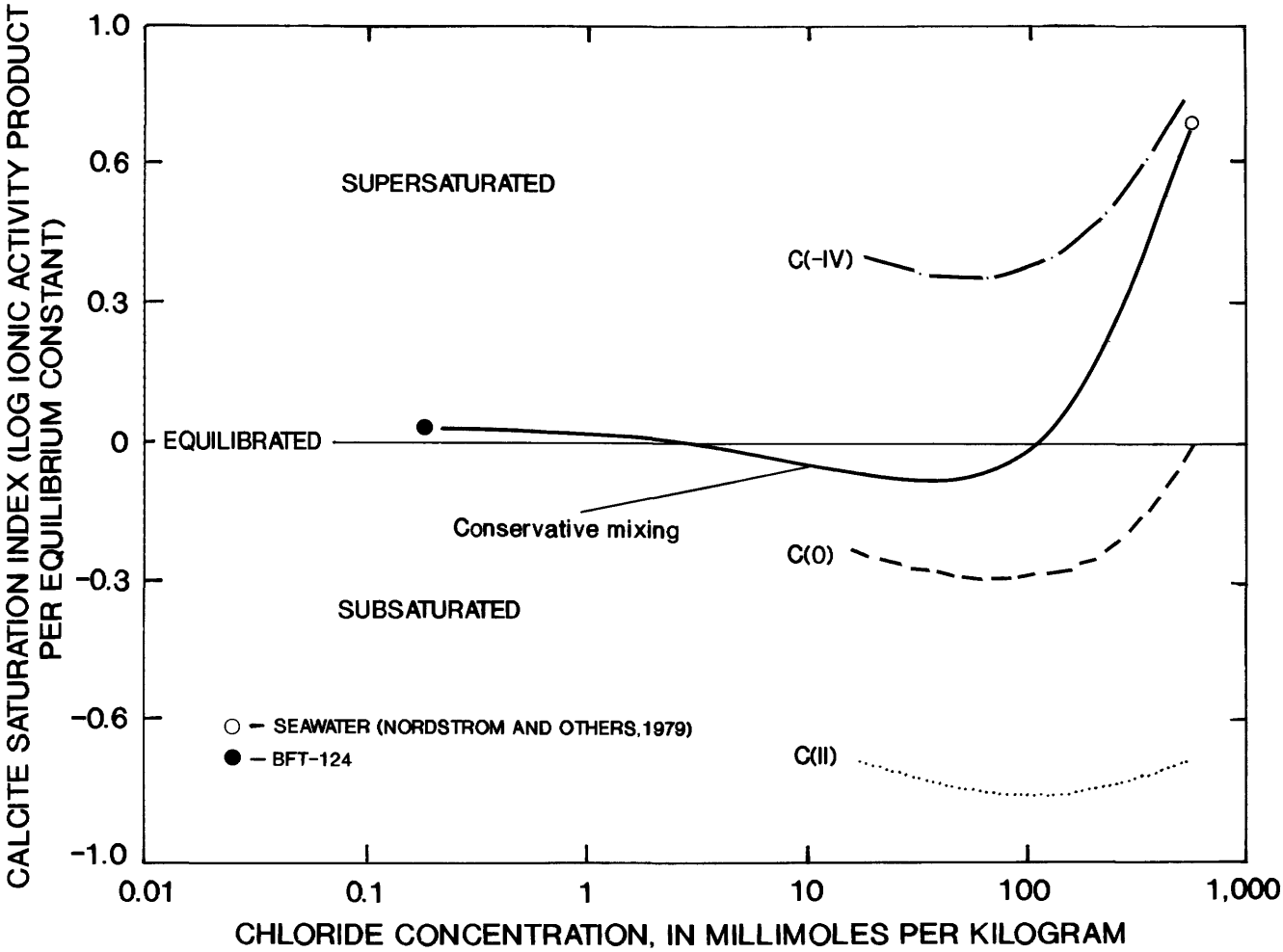

Figure 54. Saturation states with respect to calcite of simulated mixtures of seawater with ground-water sample from well BFT-124 under conditions of conservative mixing and of additional input of carbon dioxide in response to sulfate reduction.

Mass Balance Problem

The preceding section discussed the possibility for a number of hypothetical chemical processes to have participated in the chemical evolution of ground water in the zone of mixing. Several of these processes would have affected the chemical equilibrium in the ground water, increasing the potential for carbonate mineral precipitation, while others would have increased the potential for dissolution. The relative magnitudes of these opposing processes determines whether a net dissolution or a net precipitation of carbonate minerals has occurred in the aquifer and overlying sediments. A chemical mass balance has been formulated as part of this study to calculate reaction coefficients that quantify the effect of the various plausible chemical processes. A solution to the mass balance results in a conceptual model that estimates the net dissolution or precipitation of carbonate minerals that has occurred in the aquifer.

A mass balance solution for the chemical evolution of mixing ground water must explain the change between an initial composition and a final composition in terms of the hypothetical chemical reactions that represent each of the reacting mineral or gas phases. In this case, the initial compositions are those predicted by the conservative mixing model, while the final compositions are those of the corresponding ground-water samples. A unique algebraic solution to the mass balance problem requires that the number of chemical reactions, corresponding to unknown reaction coefficients, be equal to the number of ground-water constituents of known initial and final concentration included in the model. The significant ground-water constituents and the hypothetical chemical reactions are listed below:

Ground-water constituents

1. Calcium
2. Inorganic carbon
3. Sodium
4. Potassium

5. Magnesium
6. Ammonia
7. Sulfide
8. pH
9. Sulfate

Reactions

1. Calcite dissolution or precipitation
2. Calcium for sodium exchange
3. Calcium for potassium exchange
4. Calcium for magnesium exchange
5. Gypsum dissolution
6. Dolomite precipitation or dissolution
7. Carbon dioxide input (atmospheric, fermentation, respiration, oxygen reduction)
8. Ammonification
9. Sulfate reduction

The ground-water constituents are those that significantly deviated from the conservative mixing models. The nine reactions include the hypothesized mineral reactions that are feasible within the constraints of mineral saturation calculations, as well as ion exchange reactions and organic processes that are probable but that cannot be evaluated from saturation considerations. Reactions involving pyrite are considered to be negligible and have not been included for reasons discussed previously. Organic acid generation has not been included because the nature of these reactions is not well understood in this system. Desulfurization is assumed to be a minor process relative to sulfate reduction for generation of sulfide, as is typical of anaerobic, sulfate-rich sediments (Atlas, 1984), and has been omitted from the list of reactions. Also, nitrate reduction is not included because data on the nitrogen species are insufficient to properly describe the reaction. Anion exchange on apatite will be shown to be negligible and has also been deleted from the reaction set. The implications of these deletions will be discussed later.

A solution to the mass balance problem is complicated by the large errors associated with the deviations of sample compositions from the conservative mixing model. The errors reflect the difference between the boundaries of the conservative mixing models (figs. 35–47). A mass balance solution for the nine unknown reaction coefficients would require simultaneous solution of the nine reaction equations. The resulting combination of errors is too large for a meaningful interpretation. The total error can be reduced by combining several of the concentration terms into one unknown variable and adding another independent equation to allow for a solution. The requirement for another independent equation can be met by using a charge balance equation, to be discussed later. As a result, reaction coefficients for reactions corresponding to the combined variables cannot be calculated, but the errors are reduced sufficiently to allow for the solution of the reaction coefficient of primary interest, namely, that corresponding to carbonate mineral precipitation or dissolution.

The cation exchange reactions involving exchange of sodium, potassium, and magnesium for calcium can be combined as follows:

$$CaX+\Omega \leftrightarrow Ca^{++}+\Omega X \qquad (54)$$

where X is an exchange site and $\Omega = (2Na^{+}, 2K^{+}, Mg^{++})$. Gypsum dissolution can also be incorporated into equation 54 by recognizing the equivalence of the effect on charge in the solution of the sulfate anion, contributed to solution during gypsum dissolution, and the cations of sodium, potassium, and magnesium, removed from solution during an exchange reaction. Reaction 54 will be designated as the apparent exchange reaction in which sodium, potassium, magnesium, and sulfate have been combined to form a single variable Ω, where $\Omega = (2Na^{+}, 2K^{+}, Mg^{++}, -SO^{=}_{4})$. The error incurred by summing the components of Ω is eliminated by designating it as an unknown variable.

Dolomite reactions constitute another equation that can be eliminated from the mass balance problem by incorporation into other reactions. Dolomite is equivalent, in terms of mass balance, to pure calcite in which magnesium has been substituted for half the calcium, as in a cation exchange reaction. Dissolution of dolomite can, therefore, be represented in the mass balance problem as a combination of calcite dissolution and cation exchange as follows:

Calcite dissolution $2CaCO_3 \leftrightarrow 2Ca^{++}+2CO_3$ (55)

Cation exchange $MgX+Ca^{++} \leftrightarrow CaX+Mg^{++}$ (56)

Net reaction

$$2CaCO_3+MgX \leftrightarrow Ca^{++}+Mg^{++}+2CO^{=}_{3}+CaX \qquad (57)$$

where X is an exchange site.

The ionic components of the net products are equivalent to the products of dolomite dissolution. The reverse of these reactions is equivalent to dolomite precipitation. This relationship allows that specific consideration of dolomite reactions is not necessary for a mass balance solution. The same line of reasoning is valid for magnesium-substituted calcite. By writing reactions of magnesium-substituted calcite as a combination of pure calcite dissolution and cation exchange, these reactions need not be considered individually. The result in the mass balance problem will be that all carbonate minerals ranging in composition from pure calcite to dolomite will be represented by one dissolution/precipitation equation. The uncertainties about magnesium content of the carbonate minerals have been absorbed into the apparent exchange reaction.

By means of combination of variables and reactions, the number of unknowns to be solved has been reduced to five: the reaction coefficients for (1) carbonate mineral dissolution, (2) the apparent exchange reaction, (3) carbon dioxide input (atmospheric, fermentation, respiration, and oxygen reduction), (4) ammonification, and (5) sulfate reduction. The resulting reaction coefficient for carbonate dissolution will represent the net dissolution or precipitation of all carbonate minerals ranging between pure calcite and dolomite, since the dolomite and magnesium-substituted calcite reactions were incorporated with those of calcite. The reaction coefficient for the apparent exchange reaction will quantify the net change in calcium concentration. If reactions involving dolomite and high-magnesium calcite are significant, the reaction coefficient for apparent exchange becomes meaningless because it includes an artificial component representing the difference between the calcium concentration of dolomite or high-magnesium calcite and pure calcite. However, if carbonate reactions are dominated by pure or low-magnesium calcite, the artificial component would be insignificant, and the apparent exchange reaction would represent the change in calcium concentration due to cation exchange and gypsum dissolution.

A significant effect due to dolomite and high-magnesium calcite appears unlikely but cannot be ruled out. The reaction coefficient for carbon dioxide input (atmospheric, fermentation, respiration, oxygen reduction) represents the quantity of carbon dioxide contributed to ground water that cannot be accounted for by sulfate reduction. The reaction coefficient for sulfate reduction quantifies this process in terms of the amount of sulfate reduced. The corresponding amount of carbon dioxide contributed to the ground water by sulfate reduction is dependent on the average valence of the decomposing carbon compounds. Finally, the reaction coefficient for ammonification quantifies this process in terms of the amount of ammonia generated.

The reaction coefficients are derived by simultaneously solving five equations. Mass balance reactions can be written

Calcium	$[Ca_f^{++}]=[Ca_i^{++}]+AE+CDP$	(58)
Inorganic carbon	$[C_f]=[C_i]+CI+CDP+SR$	(59)
Sulfate reduction	$SR=[S_f]-[S_i]$	(60)
Ammonification	$AM=[NH_{3f}]-[NH_{3i}]$	(61)
Apparent exchange reaction	$AE=[\Omega_f]-[\Omega_i]$	(62)

where square brackets indicate species concentration and

AE reaction coefficient for the apparent exchange;
CDP reaction coefficient for carbon dissolution/precipitation;
CI reaction coefficient for carbon dioxide input (atmospheric, fermentation, respiration, oxygen reduction);
SR reaction coefficient for sulfate reduction; i and f initial and final concentrations, respectively;
z factor that varies according to the valence of the reduced carbon being oxidized by sulfate;
C total inorganic carbon species;
S total inorganic sulfide species;
NH_3 total inorganic ammonia species.

The term SR in equation 59 can be immediately solved by substituting the known values of initial and final sulfide concentration. The AM term in equation 61 can be similarly determined by substituting known values for ammonia concentrations. Because all terms in equation 62 are unknown, an additional equation is required to solve the mass balance. This equation is based on the charge balance of the reacting ions in the initial and final solutions. The charge balance equation, simplified by eliminating minor species, can be written

$$2[Ca_f^{++}]+2[\Omega_f^{++}]-[HCO_{3f}^-]-2[CO_{3f}^=]+[NH_{4f}^+]-2[S_f^=]-[HS_f^-]+[H_f^+]=$$
$$2[Ca_i^{++}]+2[\Omega_i^{++}]-[HCO_{3i}^-]-2[CO_{3i}^=]+[NH_{4i}^+]-2[S_i^=]-[HS_i^-]+[H_i^+]$$
$$-2[SO_{4r}^=]-[HSO_{4r}^-] \quad (63)$$

where subscripts i and f indicate initial and final solutions for bracketed ion concentrations, respectively, and subscript r indicates that the bracketed ion concentrations only include that part of the total concentration used in the reduction reactions. The $[HSO_{4r}]$ term is negligibly small and can be ignored; therefore, SR can be substituted in the charge balance equation for $[SO_{4r}]$. Then using the relationship in equation 62, equation 58 can be substituted into the charge balance, yielding

$$2[Ca_f^{++}]+2[Ca_f^{++}]-2[Ca_i^{++}]-2CDP-[HCO_{3f}^-]-2[CO_{3f}^=]+[NH_{4f}^+]-2[S_f^=]$$
$$-[HS_f^-]+[H_f^+]=$$
$$2[Ca_i^{++}]+[HCO_{3i}^-]-2[CO_{3i}^=]+[NH_{4f}^+]-2[S_i^=]-[HS_i^-]+[H_i^+]-2SR \quad (64)$$

The charge balance equation can now be solved to give the reaction coefficient for calcite dissolution/precipitation, CDP. Substituting back into equation 58, a value can be determined for AE, the reaction coefficient for apparent exchange.

Substitution of the calculated value for CDP into equation 59 still leaves two unknowns, CI and z. The value of z, which varies according to the valence of carbon in the decomposing compounds, cannot be determined from the available data. Therefore, the reaction coefficient for CI cannot be determined. However, by combining CI and zSR into one term, the problem can be solved for the total carbon dioxide flux, which represents the net input of carbon dioxide to the ground water by all sources, including sulfate reduction.

In order to solve the problem as presented above, it was necessary to estimate the speciation of the ions. This

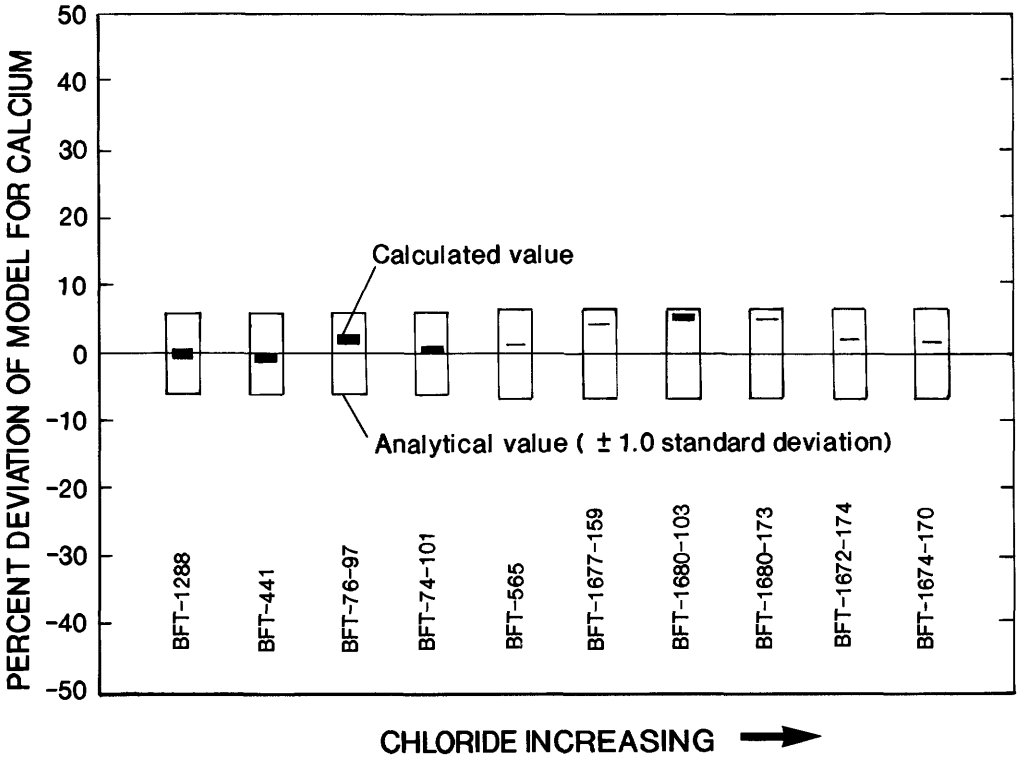

Figure 55. Deviation of the calcium concentrations resulting from the mass balance calculations, as compared to the measured values. Analytical precision is indicated as ±1.0 standard deviation.

was done using equilibrium speciation calculations. Temperature effects were estimated with the van't Hoff relationship, and the thermodynamic data are from Parkhurst and others (1980). Ion activities were estimated from concentrations by using the relationships of Davies (Parkhurst and others, 1980). The calculations for speciation, mass balance, and charge balance were done using the computer program PHREEQE (Parkhurst and others, 1980) with an aqueous model designed for this problem, allowing a more rigorous list of aqueous species to be used than is shown in equation 63.

The mass balance problem was solved for 10 samples that were compositionally different from the conservative mixing model with regard to all of the significant constituents. The use of the aqueous model to estimate speciation of the ions and solve the mass balance and charge balance resulted in small errors, as shown by the deviations of the calculated concentrations of calcium and DIC from the actual sample values in figures 55 and 56. The dark bars represent the range of error for the calculated values that occurred due to the differences between the boundaries of each conservative mixing model that served as the basis for the initial solutions in the mass balance problem. The open bars represent the precision (±1.0 standard deviation) of the sample analyses. For all cases except one, the model values do fall well within the limits of analytical error.

The purpose of the mass balance exercise was to estimate reaction coefficients for the hypothetical chemical reactions. The method was successful in describing the magnitude of two of these processes, carbonate mineral dissolution and carbon dioxide influx. Cumulative errors precluded a meaningful solution for the other coefficients. The results are shown in figures 57 and 58. Clearly, a net dissolution of carbonate minerals has occurred in every sample tested. All the samples have been affected by an influx of carbon dioxide from the possible combined effects of atmospheric input, respiration, and decomposition of organic compounds. Reaction coefficients for the apparent exchange reactions (fig. 59) show considerable variation among the samples; however, interpretation of these data is limited by the assumptions inherent in the apparent exchange reactions.

The effects on the ground water of organic acid generation from decomposition of organic compounds were not considered in the mass balance problem due to insufficient data on the nature of organic reactions. The possible error introduced by this deletion is considered here. The obvious result of introducing acidic compounds to the ground water would be to shift the equilibrium toward subsaturation with respect to the carbonate minerals. The value estimated previously for the maximum acidity contributed by organic acids in the ground water samples was 0.052 μeq/kg for sample BFT–565. This is a very small contribution of acid relative to the acidity contributions associated with the indicated carbon dioxide fluxes (0.84–7.72 μeq/kg). The deletion of this process from the

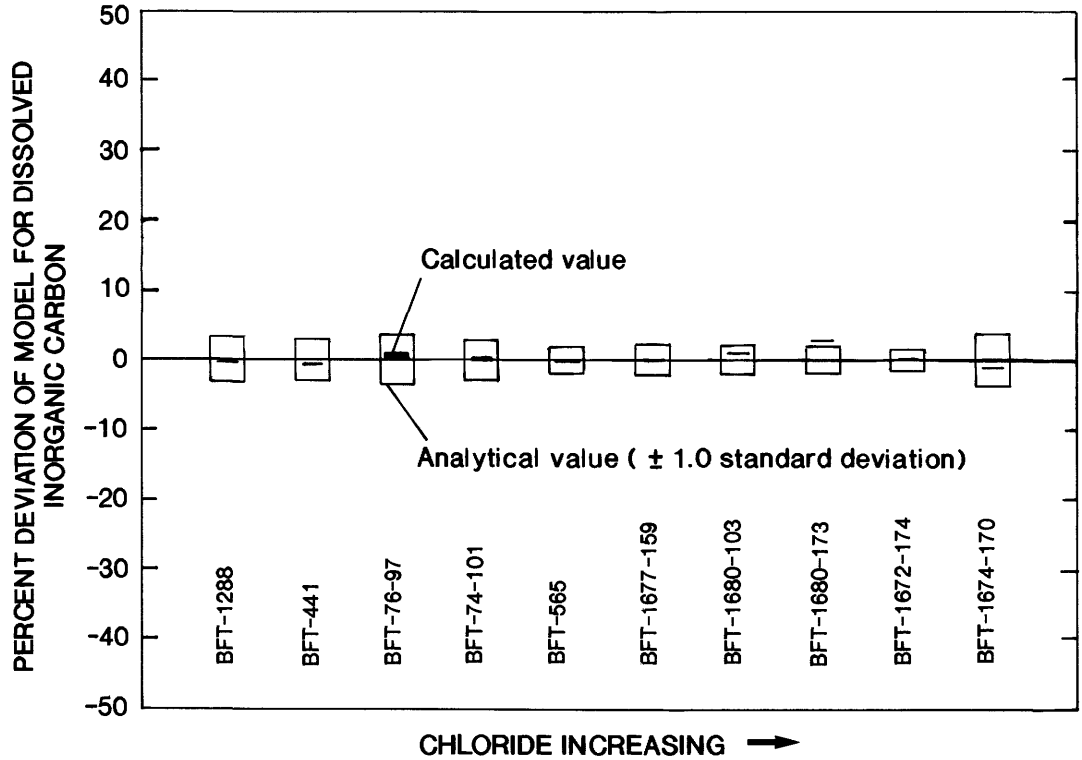

Figure 56. Deviation of the dissolved inorganic carbon concentrations resulting from the mass balance calculations, as compared to the measured values. Analytical precision is indicated as ±1.0 standard deviation.

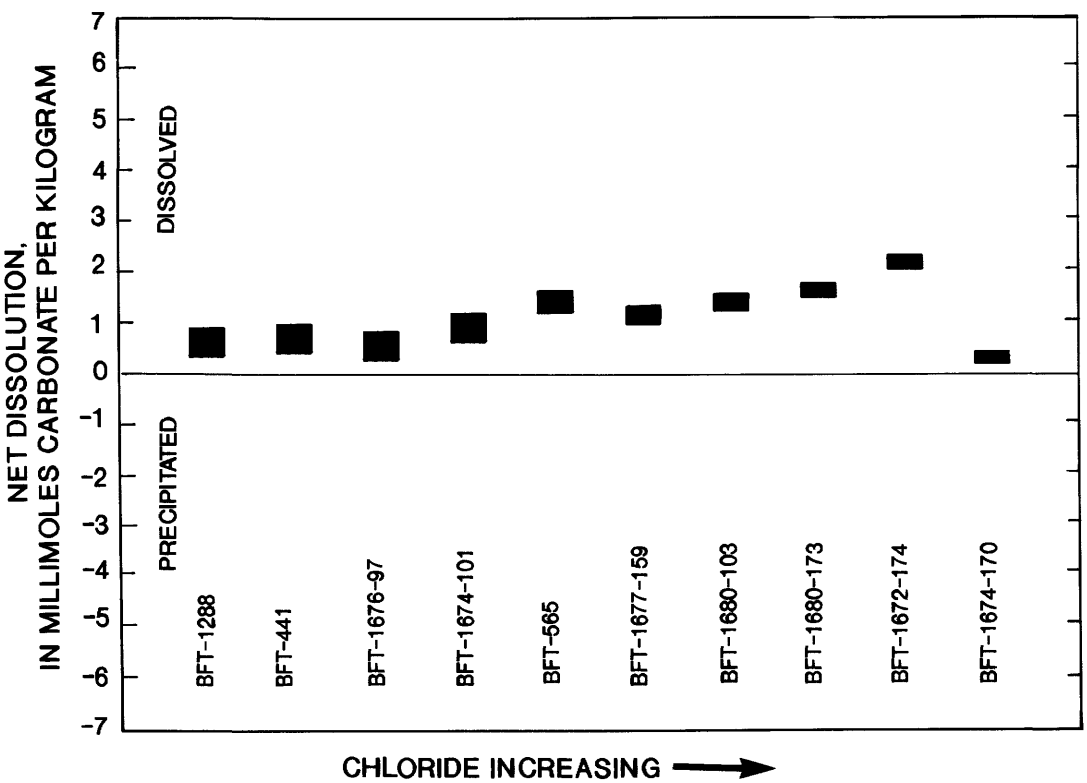

Figure 57. Net carbonate mineral dissolution in ground water of the mixing zone.

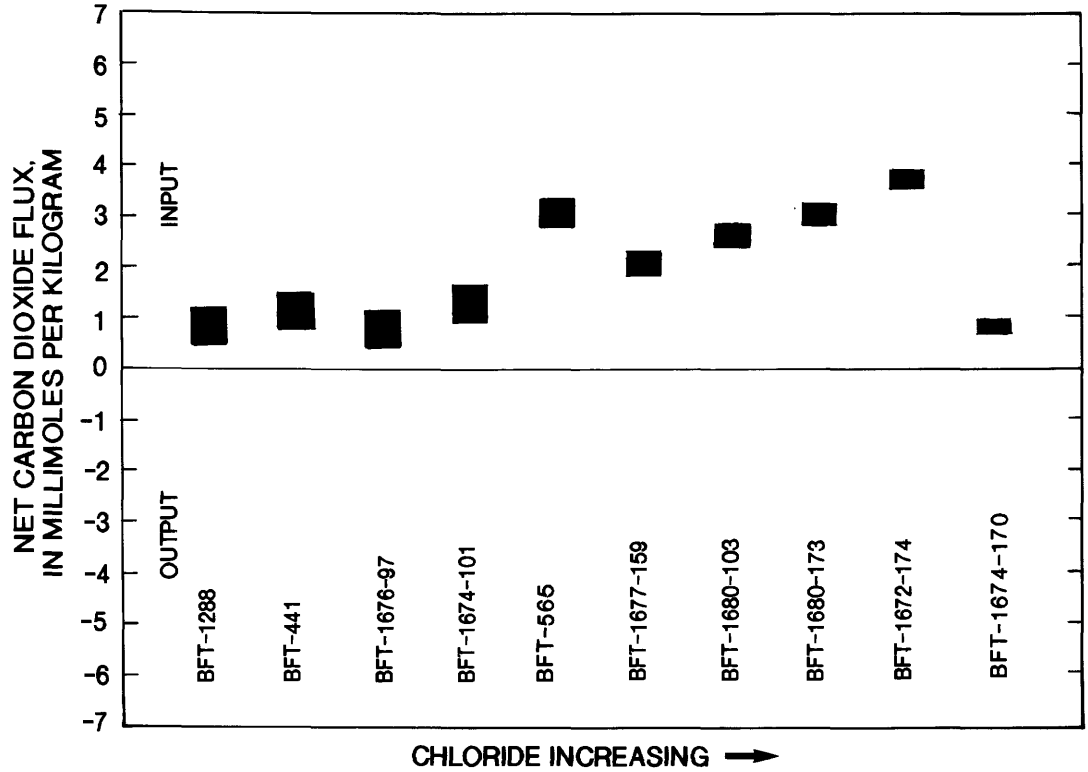

Figure 58. Net carbon dioxide flux into ground water of the mixing zone.

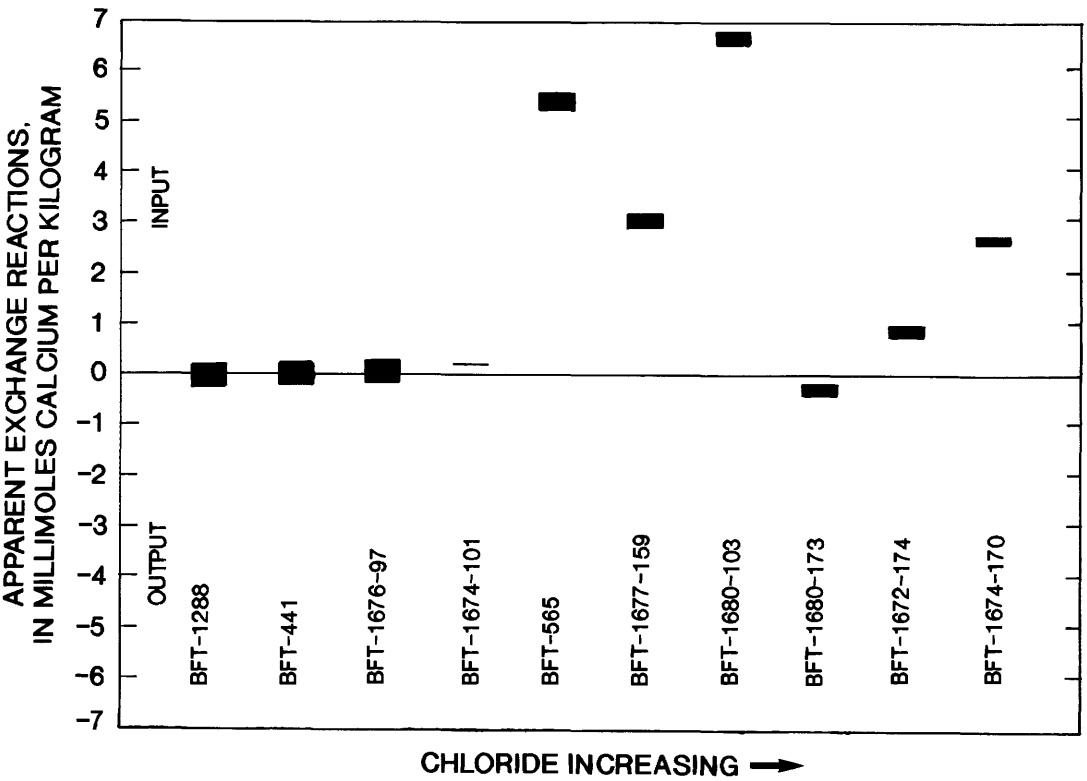

Figure 59. Net apparent exchange in ground water of the mixing zone.

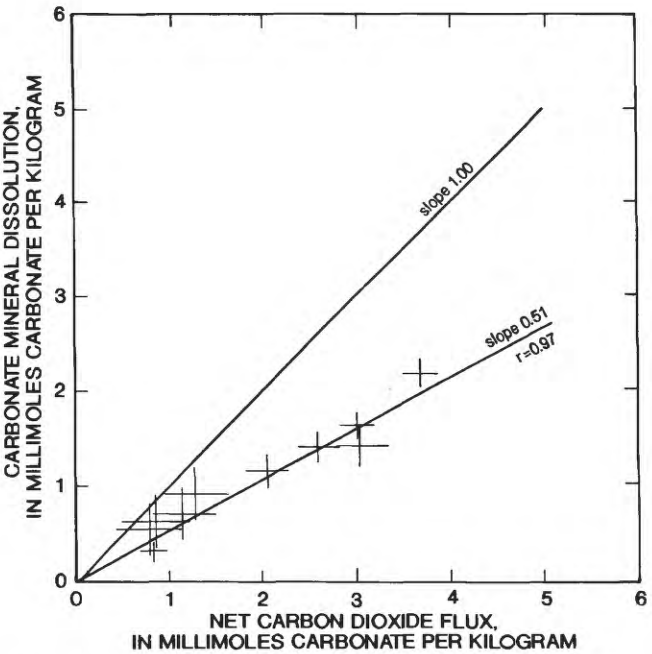

Figure 60. Relation between net carbonate mineral dissolution and net carbon dioxide flux in ground water of the mixing zone.

mass balance model has resulted in a negligible underestimation of the amount of carbonate dissolution and an equally minor overestimation of the carbon dioxide influx.

The effects of hydroxide generation, in the course of nitrate reduction, on the ground water also were not considered in the mass balance problem due to insufficient nitrate data. The error introduced by this deletion can also be shown to be negligible for the samples used in this study. Generation of hydroxide in the ground water would shift the equilibrium toward supersaturation with respect to the carbonate minerals. The maximum nitrate concentration measured in any of the water samples was 0.051 mmol/kg in BFT–1842 from the Hawthorn Formation. According to the stoichiometry of equation 48, the maximum amount of hydroxide generated by the complete reduction of this nitrate to nitrogen gas would be 0.051 mmol/kg. This amount is minor relative to the acidity generated in the form of carbon dioxide and has resulted in a negligible overestimation of the amount of carbonate dissolution and a negligible underestimation of carbon dioxide influx.

Another reaction that was neglected in the mass balance problem was anion exchange on apatite. The maximum exchange in the samples was indicated by a contribution to solution of 0.09 mmol/kg (BFT–1678) of fluoride, which would result in an equivalent removal of hydroxide from the ground water. Again, the magnitude of this process is negligible relative to the acidity introduced by carbon dioxide influx.

The relation between the magnitudes of carbonate dissolution and of carbon dioxide flux as determined from the mass balance solution is shown in figure 60. These values exhibit a good positive correlation (least squares regression r=0.94). If carbonate dissolution in the samples had occurred only in response to carbon dioxide influx, the plotted points would be expected to fall approximately on a line passing through the origin with a slope equal to one. This is because within the pH range of ground water in the mixing zone, the reaction would closely approximate the stoichiometry of equations 44 and 45. All points in figure 60 fall significantly below a line of slope equal to one, indicating that other processes besides carbon dioxide influx have had a significant effect on the ground-water chemistry. Thus there has been a shift in the chemical equilibrium, and only about one-half of the carbonate dissolution expected from the carbon dioxide influx has occurred. This result illustrates the significance of processes other than carbon dioxide influx on the geochemical evolution of the ground water and the diagenesis of carbonate aquifer minerals. The plausible processes, which have had the combined effect of minimizing carbonate mineral dissolution by carbon dioxide, include cation exchange, gypsum dissolution, generation of bases by sulfate and nitrate reduction, ammonification, and desulfurization and equilibration of supersaturated seawater with carbonate minerals.

Diagenesis

The diagenetic features of the carbonate rocks in the Upper Floridan aquifer reflect a history of both dissolution and precipitation of calcite. This is consistent with the processes described by the geochemical models formulated in this study, and it is likely that these processes have had a considerable impact on the diagenesis of the aquifer rocks.

Low-Salinity Zone

The processes described by the conceptual model of the chemical evolution of the ground water in the low-salinity zone have significant implications for the development of porosity and permeability in the aquifer. The contribution of calcium to the ground water, as a result of incongruent dissolution of oligoclase, cation exchange, and gypsum dissolution, supersaturates the ground water with respect to calcite, causing a net precipitation of calcite cements. Clays are formed during the incongruent dissolution of feldspars. Both of these processes result in redistribution of porosity and probable restriction of permeability. The dissolution and reprecipitation of calcites due to compositional variation probably contributes to the recrystallization of micrite, skeletal fragments, and cements and to the transformation of high-magnesium calcite to low-magnesium calcite, as observed in the aquifer.

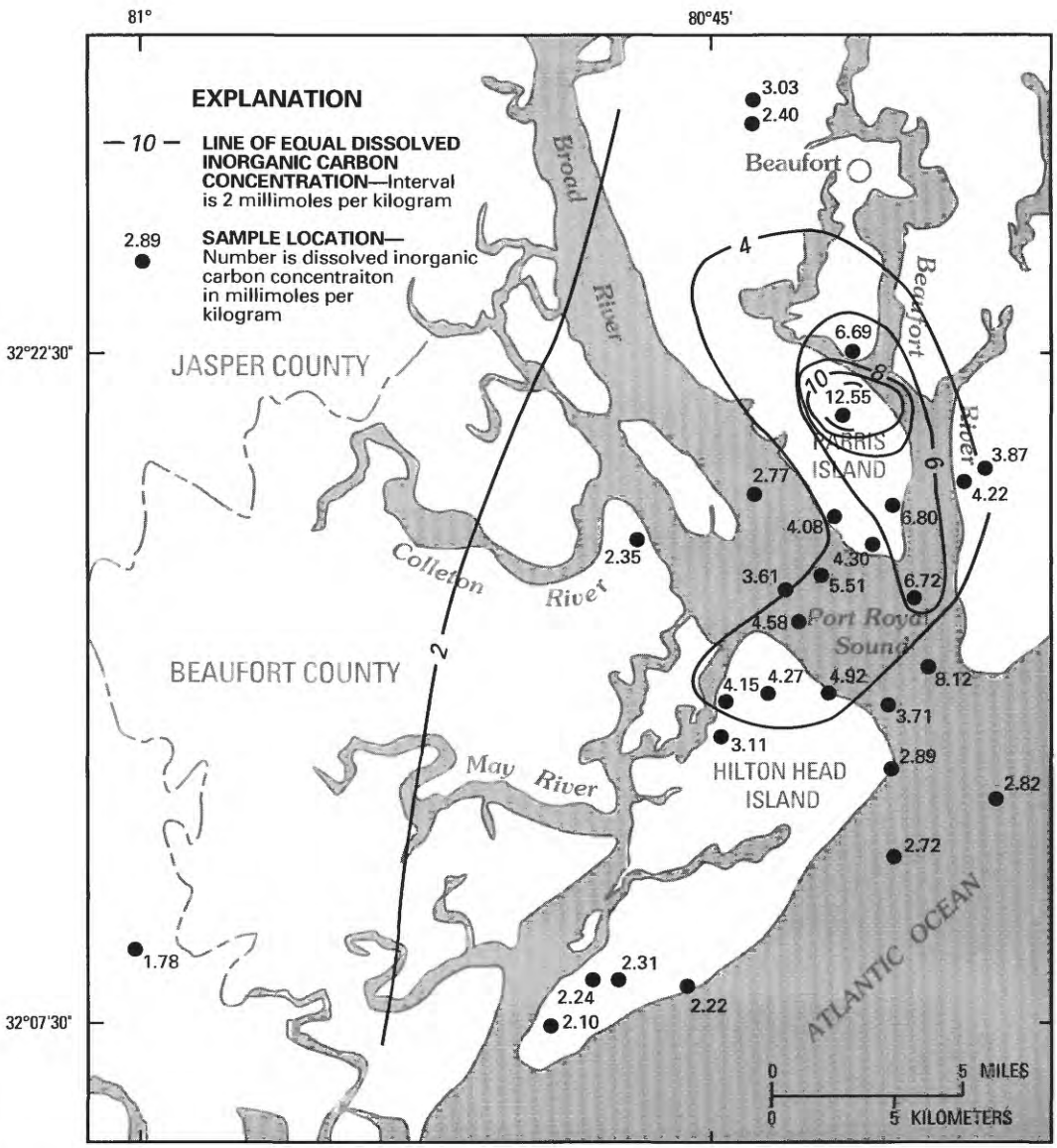

Figure 61. Concentration of dissolved inorganic carbon in the Upper Floridan aquifer.

Mixing Zone

The conceptual geochemical model formulated for the mixing zone described the ground-water composition as the product of nonconservative processes as well as mixing of low-salinity water with seawater. The mass balance exercise showed that processes that shift the chemical equilibrium of the ground water toward subsaturation with respect to the carbonate minerals have dominated the reactions, so that a net dissolution of carbonate minerals has occurred. The relation between carbon dioxide influx and carbonate dissolution shown in figure 60 suggests that carbon dioxide influx is directly related to the magnitude of dissolution of the carbonates in the aquifer and overlying sediments.

The areal distribution of dissolved inorganic carbon in ground water in the Upper Floridan aquifer is shown in figure 61. High values of DIC are indicative of high carbon dioxide influx. A comparison of the dissolved inorganic carbon distribution with the distribution of carbon-14 activity of dissolved inorganic carbon (fig. 17) shows a similarity in the patterns. The highest values for both inorganic carbon and carbon-14 activity occur beneath Parris Island and the northern tip of Hilton Head Island. The similarity of the distributions of total inorganic carbon and carbon-14 activity suggests that carbon dioxide influx and, therefore, carbonate mineral dissolution, is most prevalent where recharge has occurred. An exception to this correlation is in the area of recharge north of Parris Island sampled by wells BFT–121 and BFT–124. These samples have high

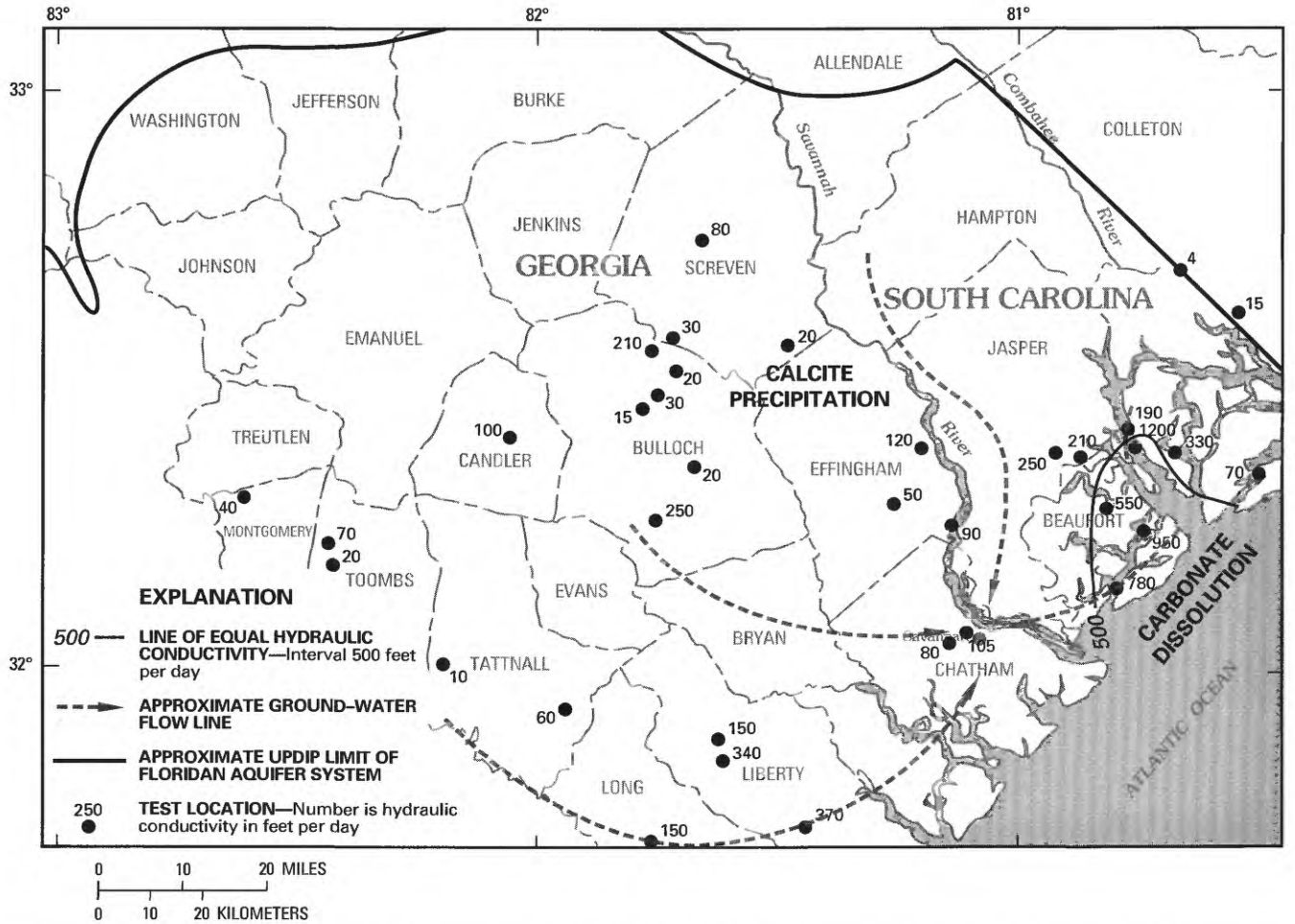

Figure 62. Major carbonate diagenetic zones and distribution of hydraulic conductivity in the Upper Floridan aquifer (modified from Krause, 1982).

carbon-14 activities but moderately low concentrations of dissolved inorganic carbon. The relation between dissolved inorganic carbon and chloride (fig. 37) provides an explanation. The highest concentrations of dissolved inorganic carbon are shown to be associated with high-chloride waters, indicating that the highest carbon dioxide fluxes are related to recharged seawater. The dissolved inorganic carbon concentrations in the high-chloride waters are higher than would be expected from atmospheric contribution and probably reflect carbon dioxide influx by respiration or decomposition of organic material. Positive correlations between chloride and both sulfide (fig. 45) and ammonia (fig. 46) show that these mechanisms of organic matter decomposition are most active in the high-chloride waters. These processes would be expected to occur as seawater infiltrates marsh or creek bed sediments, which contain large amounts of organic matter. Low-salinity water, recharging in the area near wells BFT–121 and BFT–124, apparently contacts sediments that are less prolific at carbon dioxide generation.

The contribution of carbon dioxide to recharging ground water at Port Royal Sound and the surrounding area probably has had a significant influence on the evolution of porosity and permeability of the Upper Floridan aquifer. The conceptual model presented above showed that in the zone of mixing, recharge-associated carbon dioxide influx, combined with other processes, has resulted in a net dissolution of carbonate minerals. This result is in contrast with net calcite precipitation that has occurred in the aquifer updip of the zone of mixing. Comparison of the areal distribution of these contrasting diagenetic zones (fig. 62) with the areal distribution of hydraulic conductivity in the aquifer (modified from Krause, 1982) shows a striking relation between the area of recharge, associated with high carbon dioxide and chloride, and the area of high hydraulic conductivity. Thus, the diagenetic processes identified in this study could be reflected in the distribution of hydraulic conductivity in the aquifer.

SUMMARY AND CONCLUSIONS

The ground water in the Upper Floridan aquifer in the coastal areas around Port Royal Sound and Hilton Head Island, S.C., is characterized by variable concentrations of

chloride, ranging from 0.11 to 430 mmol/kg. The variation is the result of seawater mixing with fresh ground water. An old component of freshwater originates inland at recharge areas near the aquifer outcrop. Prior to extensive development of the aquifer, ground-water flow lines emanated from the recharge areas and converged near Port Royal from the north and west. An old component of seawater in the aquifer is apparently the landward extension of seawater from the offshore parts of the aquifer. The distribution of carbon-14 activity in the ground water shows that local recharge of both freshwater and seawater in the area surrounding Port Royal Sound supplies younger components of water to the aquifer.

The purpose of this study was to formulate conceptual geochemical models of the reactions that have affected the chemical evolution of the ground water, and to demonstrate the probable effect these reactions have had on diagenesis of the aquifer, particularly concerning the net dissolution or precipitation of the carbonate minerals that compose the bulk of the aquifer. The study area was divided into two parts: a zone of mixing that includes all ground water influenced by seawater mixing, and a low-salinity zone that includes only ground water outside of the influence of seawater mixing. Geochemical reaction models were formulated to describe the geochemical processes reflected by the ground water compositions in both zones.

The chemistry of the ground water in the Upper Floridan aquifer, in the low-salinity zone, changes as it flows downgradient. This chemical evolution of the ground water is qualitatively similar, regardless of which specific flow line is traced. Upgradient ground water is predominantly of the calcium bicarbonate type, reflecting dissolution of the calcite aquifer matrix. The pH of the ground water and concentrations of silica, magnesium, sodium, potassium, fluoride, and sulfur increase downgradient, while concentrations of calcium and DIC decrease.

The consistency of the evolutionary pattern across the study area suggests that the ground-water chemistry along each flow line is controlled by similar chemical processes. A quantitative model was formulated to describe the processes based on the compositional difference between two points on a single flow path. The observed chemical evolution can be explained as the product of seven chemical processes as follows:

1. Dissolution of calcite,
2. Precipitation of calcite,
3. Incongruent dissolution of alkali feldspar to form clay minerals,
4. Incongruent dissolution of oligoclase to form clay minerals,
5. Cation exchange of sodium for calcium on clays,
6. Anion exchange of fluoride for hydroxide on apatite, and
7. Dissolution of gypsum.

The plausibility of these reactions was evaluated, and the relative influence of each reaction was quantified in terms of reaction coefficients in the model by applying three types of constraints:

1. Saturation limits of minerals found to exist in the aquifer,
2. Chemical mass balance of the ground-water constituents, and
3. Mass transfer of carbon isotopes.

The resulting model shows that the simultaneous dissolution and precipitation of calcite is responsible for the contribution of magnesium to the ground water and provides a sink for calcium as well. The Upper Floridan aquifer consists primarily of calcite in the form of skeletal fragments, micrite, and sparry cements. Calcites from the low-salinity zone of the aquifer were found to contain between two and six percent magnesium carbonate. The compositional variations of the calcites result in a range of stabilities for these minerals. Unstable, higher magnesium calcite dissolves, causing supersaturation and precipitation of stable, lower-magnesium calcite.

The identification of incongruent dissolution of feldspars is particularly notable because it demonstrates the significant influence that small amounts of some silicate minerals in a carbonate aquifer can exert on diagenesis of the carbonate minerals and the chemical evolution of the ground water. Traces of alkali and plagioclase feldspars are present in the aquifer. Dissolution of these minerals is accompanied by precipitation of clay minerals and a resulting pH increase and contribution of silica, calcium, sodium, and potassium to the ground water. The increase in pH and contribution of calcium to the aqueous solution causes calcite supersaturation, resulting in a net precipitation of calcite cements.

Cation exchange, anion exchange, and gypsum dissolution are responsible for less significant changes in the ground-water chemistry. Sodium-for-calcium exchange on clays may contribute minor amounts of calcium to the ground water and provide a minor sink for sodium. The small increase in concentration of fluoride along flow paths is explained by hydroxyl for fluoride exchange on apatite minerals found in trace amounts in the aquifer. Dissolution of gypsum (or possibly oxidation of pyrite), also a trace mineral, explains minor increases in sulfate along flow paths and is a minor source of calcium.

This conceptual model, while applicable qualitatively to the entire study area, was formulated for a designated segment of a single flow line bounded by two wells from which high-quality data were available. The model is therefore only quantitatively applicable to the restricted segment of flow line for which it was developed. Also, the fact that a model as described can be formulated within the constraints of mineral saturation, mass balance, and isotope

mass transfer is not proof that the model is a unique solution to the problem of explaining the observed spatial variations in the ground-water chemistry.

A possible alternative to this model is an eighth process, carbon dioxide input. The plausible sources of carbon input into the ground water along the flow line cannot necessarily be restricted to calcite dissolution, as was assumed in the initial flow-line model. Carbon dioxide may also have contributed to the total carbon input. The maximum limit of these contributions was established from mass balance of carbon and magnesium and mass transfer of carbon-13. Nonmethanogenic carbon dioxide input is limited to less than 22 percent of the total carbon input, while methanogenic carbon dioxide is limited to less than 67 percent. While carbon dioxide contributions of this magnitude would result in substantial changes in the reaction coefficients determined in the original model, the proposed list of chemical reactions used in the model would not change. Due to carbon dioxide input, proportionately less dissolution of calcite would be required as a source of carbon. However, the total carbon input must increase as the carbon dioxide input increases, resulting in an increase in actual calcite dissolution. In response to the increase in calcite dissolution, calcite precipitation must also increase to maintain the magnesium and carbon mass balances. The precipitation of calcite must be driven by increasing pH and calcium contribution from incongruent dissolution of oligoclase and alkali feldspar, cation exchange, and gypsum dissolution.

In the mixing zone, geochemical reaction models were formulated based on deviations of sample compositions from those expected from conservative mixing. Assuming that chloride is conservative in the mixing zone, a conservative mixing model was constructed for each of several major and minor constituents of the ground water. The models describe the concentration range that would be expected for each of the constituents if the waters mix conservatively. Comparison of sample compositions from the mixing zone with those predicted by the model showed that bromide and silica appear to behave conservatively, while nonconservative behavior is exhibited by calcium, DIC, magnesium, sodium, potassium, sulfate, fluoride, ammonia, sulfide, phosphate, and pH.

The conservative behavior of bromide substantiates the assumption of a seawater source, as opposed to a brine, in the mixing zone. The nonconservative constituents indicate that the ground-water composition cannot be explained on the basis of mixing only, but must have evolved by a combination of mixing and chemical reactions. Plausible reactions were hypothesized from minerals in the sediments, thermodynamic potential for those minerals to dissolve or precipitate, and possible input of organically derived compounds such as carbon dioxide. The plausible reactions that could have substantially affected the ground-water composition are dissolution and precipitation of calcite and dolomite, dissolution of gypsum, cation exchange, ammonification, and carbon dioxide contribution by such mechanisms as atmospheric influx, respiration, fermentation, oxygen reduction, nitrate reduction, and sulfate reduction.

All of the ground water in the Upper Floridan aquifer, in the zone of mixing, was close to equilibrium with respect to calcite, suggesting that equilibration with calcite is a kinetically dominating reaction. In contrast, simulated conservative mixtures were shown to deviate from calcite equilibrium, resulting in potentially precipitating or dissolving solutions, depending on the degree of mixing.

The relative influence of the chemical processes in the model on ground-water evolution and carbonate mineral diagenesis was determined by solving a chemical mass balance problem based on the plausible chemical reactions and the observed deviations in ground-water composition from the simulated conservative mixtures. In order to derive a meaningful solution, it was necessary to combine several of the reactions and variables, resulting in an additional unknown. The modified mass balance problem was then solved by including a charge balance equation. Solution of the mass balance problem resulted in reaction coefficient values that describe the magnitude of the chemical reactions that have occurred. For all samples to which the mass balance approach could be applied, a net dissolution of carbonate minerals was found to have occurred. A net influx of carbon dioxide had also occurred in all samples. Only about one-half the amount (that would have been expected) of carbonate minerals had dissolved from the reaction of the influxed carbon dioxide, indicating that the other hypothetical reactions had a significant buffering influence on the influx of carbon dioxide and its effect on carbonate diagenesis.

Comparison of the areal distribution of dissolved inorganic carbon with that of the carbon-14 activity of DIC shows a correlation between local recharge around Port Royal Sound and high values of inorganic carbon. Dissolved inorganic carbon concentration also directly correlates with chloride concentration. These relations, coupled with the mass balance results, suggest that locally recharging water is transporting high concentrations of carbon dioxide, and the result is in a net dissolution of the carbonate minerals. The highest concentrations of carbon dioxide are associated with recharging seawater. Dissolution of the carbonate aquifer, in this area of high carbon dioxide influx due to recharge, has probably been an important factor in the evolution of hydraulic conductivity in the aquifer. The areal distribution of hydraulic conductivity supports this conclusion through the high values (>500 ft/d) in the Port Royal Sound area, which are surrounded by significantly lower values corresponding to the parts of the aquifer where calcite precipitation is occurring.

REFERENCES CITED

Atlas, R.M., 1984, Microbiology—Fundamentals and applications: New York, Macmillan Publishing, 879 p.

Back, William; Hanshaw, B.B.; Plummer, L.N.; Rahn, P.H.; Rightmire, C.T.; and Rubin, M., 1983, Process and rate of dedolomitization: Mass transfer and ^{14}C dating in a regional carbonate aquifer: Geological Society of America Bulletin, v. 94, p. 1415–1429.

Back, William; Hanshaw, B.B.; Pyler, T.E.; Plummer, L.N.; and Weidie, A.E., 1979, Geochemical significance of groundwater discharge in Caleta Xel Ha, Quintana Roo, Mexico: Water Resources Research, v. 15, no. 6, p. 1521–1535.

Back, William; Hanshaw, B.B.; and Rubin, M., 1970, Carbon-14 ages related to occurrence of salt water: American Society of Civil Engineers Proceedings, Journal of the Hydraulics Division, no. 1970.

Badiozamani, K., 1973, The Dorag dolomitization model—Application to the Middle Ordovician of Wisconsin: Journal of Sedimentary Petrology, v. 43, p. 965–984.

Barnes, Ivan, 1964, Field measurement of alkalinity and pH: U.S. Geological Survey Water-Supply Paper 1535-H, p. 17.

Bogli, A., 1964, Mischungskorrosion: ein Beitrag zum Verkarstungs problem: Erdkunde, v. 18, p. 83–92.

Burt, R.A.; Belval, D.L.; Crouch, M.; and Hughes, W.B., 1987, Geohydrologic data from Port Royal Sound, Beaufort County, South Carolina: U.S. Geological Survey Open-File Report 86–497, 69 p.

Busby, J.F.; Lee, R.W.; and Hanshaw, B.B., 1983, Major geochemical processes related to the hydrology of the Madison Aquifer System and associated rocks in parts of Montana, South Dakota, and Wyoming: U.S. Geological Survey Open-File Report 83–4093, 171 p.

Bush, P.W., and Johnston, R.H., 1988, Ground-water hydraulics, regional flow, and ground-water development of the Floridan aquifer system in Florida, and in parts of Georgia, South Carolina, and Alabama: U.S. Geological Survey Professional Paper 1403–C.

Callahan, J.T., 1964, The yield of sedimentary aquifers of the coastal plain southeast river basins: U.S. Geological Survey Water-Supply Paper 1669–W, 56 p.

Chapelle, F.H., and Knobel, L.L., 1985, Stable carbon isotopes of HCO_3 in the Aquia aquifer, Maryland: Evidence for an isotopically heavy source of CO_2: Ground Water, v. 23, no. 5, p. 592–599.

Clark, J.S.; Longsworth, S.A.; McFadden, K.W.; and Peck, M.F., 1985, Ground-water data for Georgia, 1984: U.S. Geological Survey Open-File Report 85–331, 105 p.

Claypool, G.E., and Kaplan, I.R., 1974, The origin and distribution of methane in marine sediments, *In* I.R. Kaplan, ed., Natural gases in marine sediments: New York, Plenum Press, p. 99–139.

Colquhoun, D.J.; Heron, S.D., Jr.; Johnson, H.S., Jr.; Pooser, W.K.; and Siple, G.E., 1969, Up-dip Paleocene-Eocene stratigraphy of South Carolina reviewed: Columbia, S.C., South Carolina Geological Survey, Geologic Notes, v. 13, no. 1, p. 1–25.

Comer, C.D., 1973, Upper Tertiary stratigraphy of the lower coastal plain of South Carolina: Columbia, S.C., University South Carolina, Department of Geology, M.S. thesis, 19 p.

Cooke, C.W., 1936, Geology of the coastal plain of South Carolina: U.S. Geological Survey Bulletin 867, 196 p.

Cooke, C.W., and MacNeil, F.S., 1952, Tertiary stratigraphy of South Carolina: U.S. Geological Survey Professional Paper 243–B, p. 19–29.

Cooper, H.H.; Kohout, F.A.; Henry, H.R.; and Glover, R.E., 1964, Seawater in coastal aquifers: U.S. Geological Survey Water-Supply Paper 1613–C, 85 p.

Counts, H.B., 1958, The quality of ground water in the Hilton Head Island area, Beaufort County, South Carolina: Atlanta, Ga., Georgia Department of Mines, Mining and Geology, Georgia Mineral Newsletter, v. 11, no. 2, p. 50–51.

Counts, H.B., and Donsky, Ellis, 1963, Salt-water encroachment geology and ground-water resources of Savannah area Georgia and South Carolina: U.S. Geological Survey Water-Supply Paper 1611.

Duncan, D.A., 1972, High resolution seismic study, *in* Port Royal Sound Environmental Study: Columbia, S.C., South Carolina Water Resources Commission, p. 85–106.

Dunham, R.J., 1962, Classification of carbonate rocks according to depositional texture: American Association of Petroleum Geologists Memoir 1, p. 108–121.

Fontes, J.Ch., 1980, Environmental isotopes in groundwater hydrology: *in* P. Fritz and J.Ch. Fontes, eds., Handbook of environmental isotopes, v. 2, The terrestrial environment: New York, Elsevier, p. 75–140.

Hanshaw, B.B.; Back, W.; and Deike, R.G., 1971, A geochemical hypothesis for dolomitization by ground water: Economic Geology, v. 66, p. 710–724.

Hayes, L.R., 1979, The ground-water resources of Beaufort, Colleton, Hampton and Jasper Counties, South Carolina: South Carolina Water Resources Commission Report 9.

Hazen, Richard, and Sawyer, A.W., 1956, Water supply in the vicinity of Beaufort, South Carolina: Engineering report to the Bureau of Yards and Docks, Department of the Navy, contract NBY–4440, 40 p.

———1957, Supplementary report on water supply in the vicinity of Beaufort, South Carolina: Engineering report to the Bureau of Yards and Docks, Department of the Navy, contract NBY–4440, 32 p.

Hubbert, M.K., 1940, The theory of ground-water motion: Journal of Geology, v. 48, no. 8, part 1, p. 786–944.

Karaka, Y.K., and Barnes, I., 1973, SOLMNEQ: Solution-mineral equilibrium computations: National Technical Information Service P.B. 215899, 81 p.

Krause, R.E., 1982, Digital model evaluation of the predevelopment flow system of the Tertiary limestone aquifer, southeast Georgia, northeast Florida, and southern South Carolina: U.S. Geological Survey Water-Resources Investigations 82–173, 27 p.

Krom, M.D., and Sholkovitz, E.R., 1977, Nature and reactions of dissolved organic matter in the interstitial waters of marine sediments: Geochimica et Cosmochimica Acta, v. 41, p. 1565–1573.

———1978, On the association of iron and manganese with organic matter in anoxic marine pore waters: Geochimica et Cosmochimica Acta, v. 42, p. 607–611.

Land, L.S., 1973a, Holocene meteoric dolomitization of Pleistocene limestones, North Jamaica: Sedimentology, v. 20, p. 411–424.

———1973b, Contemporaneous dolomitization of middle Pleistocene reefs by meteoric water, North Jamaica: Bulletin of Marine Science, v. 23, p. 64–92.

Langmuir, D., 1971, The geochemistry of carbonate ground waters in central Pennsylvania: Geochimica et Cosmochimica Acta, v. 35, p. 1023–1046.

Malde, H.E., 1959, Geology of the Charleston phosphate area, South Carolina: U.S. Geological Survey Bulletin 1079, 105 p.

McCollum, M.J., and Counts, H.B., 1964, Relations of saltwater encroachment to the major aquifer zones, Savannah area, Georgia and South Carolina: U.S. Geological Survey Water-Supply Paper 1613–D, 26 p.

Mercado, A., 1985, The use of hydrogeochemical patterns in carbonate sand and sandstone aquifers to identify intrusion and flushing of saline water: Ground Water, v. 23, no. 5, p. 635–645.

Miller, J.A., 1986, Hydrogeologic framework of the Floridan aquifer system in Florida and in parts of Georgia, Alabama, and South Carolina: U.S. Geological Survey Professional Paper 1403–B, 91 p.

Mundorff, M.J., 1944, Ground water in the Beaufort area, South Carolina: U.S. Geological Survey, Report to the U.S. Navy Department.

Nordstrom, D.K., 1982, Aqueous pyrite oxidation and the consequent formation of secondary iron minerals, *in* Acid sulfate weathering: Madison, Wisc., Soil Science Society of America, p. 37–63.

Nordstrom, D.K.; Plummer, L.N.; Wigley, T.M.; Wolery, T.J.; Ball, J.W.; Jenne, E.A.; Bassett, R.L.; Crerar, D.A.; Florence, T.M.; Fritz, B.; Hoffman, M.; Holdren, G.R., Jr.; Lafon, G.M.; Mattigod, S.V.; McDuff, R.E.; Morel, F.; Reddy, M.M.; Sposito, G.; and Thrailkill, J., 1979, A comparison of computerized chemical models for equilibrium calculations in aqueous systems, *in* Jenne, E.A., ed., Chemical modeling in aqueous systems, speciation, sorption, solubility, and kinetrics, Series 93: Washington, D.C., American Chemical Society, p. 857–892.

Nuzman, C.E., 1970, BASF Corporation aquifer test Port Victoria, South Carolina: Kansas City, Mo., Layne-Western Company, Inc., Engineering report, 71 p.

———1972, Water-supply study, Hilton Head Island, South Carolina: Kansas City, Mo., Layne-Western Company, Inc., Engineering report, 40 p.

Oliver, B.G.; Thurman, E.M.; and Malcolm, R.L., 1983, The contribution of humic substances to the acidity of colored natural waters: Geochimica et Cosmochimica Acta, v. 47, p. 2031–2035.

Parkhurst, D.L.; Thorstenson, D.C.; and Plummer, L.N., 1980, PHREEQE—A computer program for geochemical calculations: U.S. Geological Survey Water-Resources Investigations 80–86, 210 p.

Plummer, L.N., 1975, Mixing of sea water with calcium carbonate ground water, *in* Whitten, E.H.T., ed., Quantitative studies in the geological sciences: Geological Society of America Memoir 142, p. 219–238.

Plummer, L.N., and Back, William, 1980, The mass balance approach: Application to interpreting the chemical evolution of hydrologic systems: American Journal of Science, v. 280, p. 130–142.

Plummer, L.N.; Jones, B.F.; and Truesdell, A.H., 1976, WATEQF—A FORTRAN IV version of WATEQ, a computer program for calculating chemical equilibrium of natural waters: U.S. Geological Survey Water Resources Investigations 76–13, 61 p.

Plummer, L.N., and MacKensie, F.T., 1974, Predicting mineral solubility from rate data, Application to the dissolution of magnesian calcites: American Journal of Science, v. 274, p. 61–83.

Plummer, L.N.; Parkhurst, D.L.; and Thorstenson, D.C., 1983, Development of reaction models for ground-water systems: Geochimica et Cosmochimica Acta, v. 47, p. 665–686.

Runnels, D.D., 1969, Diagenesis, chemical sediments, and mixing of natural waters: Journal of Sedimentary Petrology, v. 39, p. 1188–1201.

Scholle, P.A., 1978, Carbonate rock constituents, textures, cements, and porosities: American Association of Petroleum Geologists Memoir 27, 241 p.

Siple, G.E., 1956, Memorandum on the geology and groundwater resources of the Parris Island area, South Carolina: U.S. Geological Survey Open-File Report, 29 p.

———1960, Geology and ground-water conditions in the Beaufort area, South Carolina: U.S. Geological Survey Open-File Report, 124 p.

———1967, Salt-water encroachment in coastal South Carolina: Columbia, S.C., South Carolina Geological Survey, Geologic Notes, v. 11, no. 2, p. 21–36.

———1969, Saltwater encroachment of Tertiary limestone along coastal South Carolina: Columbia, S.C., South Carolina Geological Survey, Geologic Notes, v. 13, no. 2, p. 51–65.

Skougstand, M.W.; Fishman, M.J.; Friedman, L.C.; Erdmann, D.E.; and Duncan, S.S., 1979, Methods for the analyses of inorganic substances in water and fluvial sediment: Techniques of Water-Resources Investigations of the U.S. Geological Survey, book 5, chap. A, 626 p.

Smith, B.S., 1988, Ground-water flow and saltwater encroachment in the Upper Floridan aquifer, Beaufort and Jasper Counties, South Carolina: U.S. Geological Survey Water Resources Investigation 87–4285, 61 p.

———1993, Saltwater movement in the Upper Floridan aquifer beneath Port Royal Sound, South Carolina: U.S. Geological Survey Open-File Report 91–483, 64 p.

South Carolina Water Resources Commission, 1972, Port Royal Sound environmental study: Columbia, S.C., The State Printing Co., 555 p.

Spiker, E.C., and Hatcher, P.G., 1984, Carbon isotope fractionation of sapropelic organic matter during early diagenesis: Organic Geochemistry, v. 5, no. 4, p. 283–290.

Sprinkle, C.L., 1982, Chloride concentration in water from the upper permeable zone of the Tertiary limestone aquifer system, southeastern United States: U.S. Geological Survey Water Resources Investigations Open-File Report 81–1103, 1 plate.

Stringfield, V.T., 1966, Artesian water in Tertiary limestone in the southeastern states: U.S. Geological Survey Professional Paper 517, 226 p.

Thrailkill, J., 1968, Chemical and hydrologic factors in the excavation of limestone caves: Geological Society of American Bulletin, v. 79, p. 19–46.

Thurman, E.M., 1985, Organic geochemistry of natural waters: Dordrecht, The Netherlands, Martinus Nijhoff/Dr. W. Junk Publishers, 497 p.

Truesdell, A.H., and Jones, B.F., 1974, WATEQ, a computer program for calculating chemical equilibria in natural waters: U.S. Geological Survey Journal of Research, v. 2, p. 233–248.

Ward, W.C., and Halley, R.B., 1985, Dolomitization in a mixing zone of near-seawater composition, Late Pleistocene, northeastern Yucatan Peninsula: Journal of Sedimentary Petrology, v. 55, p. 407–420.

Warren, M.S., 1944, Artesian water in southeastern Georgia, with special reference to the coastal area: Atlanta, Ga., Georgia Geological Survey Bulletin 49, 40 p.

Whiticar, M.J.; Faber, E.; and Schoell, M., 1986, Biogenic methane formation in marine and freshwater environments: CO_2 reduction vs. acetate fermentation—Isotope evidence: Geochimica et Cosmochimica Acta, v. 50, p. 693–709.

Wigley, T.M.L., and Plummer, L.N., 1976, Mixing of carbonate waters: Geochimica et Cosmochimica Acta, v. 40, p. 989–995.

Wigley, T.M.L.; Plummer, L.N.; and Pearson, F.J., 1978, Mass transfer and carbon isotope evolution in natural water systems: Geochimica et Cosmochimica Acta, v. 42, p. 1117–1139.

Zack, A.L., 1980, Geochemistry of fluoride in the Black Creek aquifer system of Horry and Georgetown Counties, South Carolina—and its physiological implications: U.S. Geological Survey Water-Supply Paper 2067, 40 p.

APPENDIX: SATURATION INDEX CALCULATIONS

The saturation indices (SI) for oligoclase and alkali feldspar (high and low) were estimated from thermodynamic data for the end-member feldspars of albite, anorthite, sanadine, and microcline, assuming ideal mixing in the solid solutions as follows.

Oligoclase, of the average composition found in the Upper Floridan aquifer ($Ca_{0.28}Na_{0.72}Al_{1.28}Si_{2.72}O_8$), is a solid solution composed of 72 percent albite ($NaAlSi_3O_8$) and 28 percent anorthite ($CaAl_2Si_2O_8$). Approximating that the properties of oligoclase approach those of an ideal solid solution, the equilibrium constant $K_{oligoclase}$ can be calculated from the values reported for albite (log $K_{albite}=-18.002$) and anorthite (log $K_{anorthite}=-19.424$) (Truesdell and Jones, 1974) by the relation

$$0.28(\log K_{anorthite})+0.72(\log K_{albite})=\log K_{oligoclase}$$

resulting in log $K_{oligoclase}=-18.400$.

Based on equilibrium speciation calculations performed using the program WATEQF, the ion activity product (IAP) can be calculated for oligoclase using the relation

$$IAP=a_{Ca^{2+}}^{0.28}a_{Na^+}^{0.72}a_{Al(OH_4)}^{1.28}-a_{H_4SiO_4}^{2.72}$$

where a is activity, in accordance with the reaction

$$Ca_{0.28}Na_{0.72}Al_{1.28}Si_{2.72}O_8+8H_2O=0.28Ca^{2+}0.72Na^+ +1.28Al(OH)_4^-+2.72H_4SiO_4$$

The calculations were made for aqueous solutions from wells HAM–122 and BFT–1689, resulting in log $IAP_{HAM-122}=-20.881$ and log $IAP_{BFT-1689}=-19.996$. SI was then calculated for each aqueous solution according to

$$SI=\log\frac{IAP}{K}$$

resulting in $SI_{oligoclase}=-2.48$ for HAM–122 and $SI_{oligoclase}=-1.59$ for BFT–1689.

Similarly, the alkali feldspar of average composition found in the Upper Floridan aquifer ($K_{0.74}Na_{0.26}AlSi_3O_8$) can be approximated as an ideal solid solution of high albite ($NaAlSi_3O_8$) and sanadine ($KAlSi_3O_8$) in its high-temperature and -pressure form, or of low albite and microcline in its low-temperature and -pressure form. The equilibrium constants for the end-member feldspars are log $K_{albite(high)}=5.00$, log $K_{albite(low)}=3.94$, log $K_{sanadine}=1.51$, and log $K_{microcline}=1.29$ (Karaka and Barnes, 1973). Following the same procedure as above, the equilibrium constants for the alkali feldspar can be calculated for both the high and low forms, corresponding to the equation

$K_{0.74}Na_{0.26}AlSi_3O_8+4H^+ +4H_2O\leftrightarrow 0.74K+0.26Na+Al^{3+}+3H_4SiO_4$, resulting in log $K_{(high)}=2.42$ and log $K_{(low)}=1.98$. The IAP values for HAM–122 and BFT–1689 were calculated from the relation

$$IAP=\frac{a_{K^+}^{0.74}a_{Na^+}^{0.26}a_{Al^{3+}}a_{H_4SiO_4}}{a_{H^+}^4}$$

resulting in log $IAP_{HAM-122}=2.736$ and log $IAP_{BFT-1689}=3.617$. The corresponding SI values are $SI_{alk\ feld\ (high)}=0.32$ and $SI_{alk\ feld\ (low)}=0.76$ for HAM–122, and $SI_{alk\ feld\ (high)}=1.20$ and $SI_{alk\ feld\ (low)}=1.64$ for BFT–1689.